

THE INFLUENCE OF PVAP ON THE STABILITY OF  
AMORPHOUS SOLID DISPERSIONS OF  
ITRACONAZOLE PRODUCED USING  
HOT MELT EXTRUSION  
TECHNOLOGY

---

A Dissertation  
Submitted to  
the Temple University Graduate Board

---

In Partial Fulfillment  
of the Requirements for the Degree  
DOCTOR OF PHILOSOPHY

---

By  
Cara Young  
January 2014

Examining Committee Members:

Reza Fassihi, Ph.D., Doctoral Advisory Chair, Department of Pharmaceutical Sciences  
Daniel Canney, Ph.D., Doctoral Examining Chair, Department of Medicinal Chemistry  
David Lebo, Ph.D., Committee Member, Department of Pharmaceutical Sciences  
Ho-Lun Wong, Ph.D., Committee Member, Department of Pharmaceutical Sciences  
Stephanie Wunder, Ph.D., External Committee Member, Department of Chemistry

## ABSTRACT

The purpose of this study was to improve the melt extrusion processability of polyvinyl acetate phthalate (PVAP) and investigate its use as a stabilizing polymer for supersaturated solutions of itraconazole (ITZ) in neutral pH aqueous media and in the solid-state during storage over time. Polyvinyl pyrrolidone vinyl acetate (PVPVA) was incorporated into PVAP as a carrier matrix with the aim of lowering the melt viscosity and increasing the plasticity of PVAP while maintaining its high glass transition temperature ( $T_g$ ). Amorphous solid dispersions of ITZ (40% w/w) in a 30:70% w/w PVAP:PVPVA mixture were produced by melt extrusion. Solid-state analyses of the composition were performed using differential scanning calorimetry and X-ray diffraction. Dissolution analysis was conducted using a pH-change method. Solid-state analyses demonstrated that the extruded composition was entirely amorphous and ITZ was largely distributed in PVAP- and PVPVA-rich portions of the ternary dispersion. Dissolution analysis revealed that PVAP functioned to prolong the release of supersaturated levels of ITZ from the dispersion following an acidic-to-neutral pH transition. In the solid state, ITZ remained in its amorphous form throughout 6 months of storage. The results of this study suggest that substantial improvements in melt extrusion with PVAP can be achieved by incorporating PVPVA and that the PVAP-PVPVA polymer combination can stabilize amorphous ITZ.

To my husband, Phil

## **ACKNOWLEDGMENTS**

The contributions of the many friends, mentors, collaborators, and students with whom I have worked are gratefully acknowledged. In particular, Professors Reza Fassihi, Daniel Canney, David Lebo and Ho-Lun Wong and their students from Temple University. I am particularly grateful for the expertise of Dr. Stephanie Wunder.

## **PREFACE**

The majority of marketed drugs have been isolated and delivered to the body in their crystalline state. In most instances, this state represents the lowest energy form of the drug with the greatest physical and chemical stability. The approach described herein is a shift away from the crystalline state and instead focuses on producing pharmaceutically acceptable, high-energy, amorphous forms of drugs. Amorphous drug delivery provides opportunities for significant increases in aqueous solubility and bioavailability of active pharmaceutical ingredients.

# TABLE OF CONTENTS

	Page
<b>ABSTRACT</b> .....	<b>ii</b>
<b>ACKNOWLEDGMENTS</b> .....	<b>iv</b>
<b>PREFACE</b> .....	<b>v</b>
<b>LIST OF TABLES</b> .....	<b>xi</b>
<b>LIST OF FIGURES</b> .....	<b>xiii</b>
 <b>CHAPTER</b>	
<b>1. INTRODUCTION</b> .....	<b>1</b>
Increasing Number of Poorly Water-Soluble Drugs.....	<b>2</b>
Defining a Drug as Poorly Soluble.....	<b>4</b>
Biopharmaceutics Classification System.....	<b>6</b>
Factors Affecting the Dissolution Rate of Drugs.....	<b>7</b>
Formulation Strategies for Poorly Water-Soluble Drugs.....	<b>8</b>
Salt Formation.....	<b>9</b>
Crystal Modification.....	<b>9</b>
pH Modification.....	<b>10</b>
Cyclodextrin Complexation.....	<b>10</b>
Self-Emulsification.....	<b>11</b>
Particle Size Reduction.....	<b>12</b>
Amorphization.....	<b>12</b>
Solid Dispersions.....	<b>19</b>
Marketed Products Based on Solid Dispersion Technology.....	<b>24</b>
Methods of Preparing Solid Dispersions.....	<b>24</b>
Spray Drying.....	<b>25</b>

Precipitation .....	25
Melt Extrusion .....	26
Extrusion Technology.....	29
Background.....	29
Melt Extrusion for Pharmaceutical Dosage Forms.....	30
Marketed and In-Development Products Based on HME.....	31
Polymer Selection .....	33
HME Equipment Overview .....	35
HME Process Overview.....	39
Manufacturability.....	48
Stability.....	52
Hygroscopicity of the Polymer .....	55
Drug and Polymer Interactions .....	57
2. PROBLEM AND OBJECTIVES .....	58
Statement of the Problem.....	58
Overall Objective .....	59
Supporting Objectives.....	59
3. MATERIALS AND METHODS.....	61
Polyvinyl Acetate Phthalate (PVAP).....	61
Salts.....	62
Vinylpyrrolidone Vinyl Acetate (PVPVA).....	62
Itraconazole (ITZ).....	63
Food Effect in BCS Class II Drugs.....	65
Biopharmaceutics of Itraconazole.....	67
Thermogravimetric Analysis (TGA).....	69
Thermal Decomposition of PVAP .....	70
Isothermal TGA Analysis of PVAP.....	70
Thermal Decomposition of PVPVA .....	70
Glass Transition Temperature (Tg).....	70
Tg of PVAP.....	71
Tg of PVPVA and Itraconazole .....	75
Tg of ITZ-PVPVA and ITZ-Polymer Blends .....	76

Tg of Extruded ITZ-Polymer Blend .....	76
Melt Viscosity of PVAP, PVPVA, PVAP-Plasticizer and PVAP-PVPVA Blends .....	77
Hygroscopicity of PVAP and PVPVA .....	78
Sample Preparation to Evaluate the Water Affinity of PVAP and PVPVA .....	78
TGA Analysis of PVAP After Exposure to Various Relative Humidities.....	78
Loss on Drying After Exposure to Various Relative Humidities for PVAP and PVPVA .....	79
DSC Analysis of PVAP After Exposure to Various Relative Humidities.....	79
Solubility Parameter for PVAP, Plasticizers, Polymers and Other Excipients .....	80
Miscibility Studies for PVAP, PVPVA and Itraconazole.....	83
HME Processing .....	84
Motor Load .....	84
Preparation of PVAP-PVPVA-ITZ Solid Dispersions .....	84
Analysis of PVAP Content .....	85
Analysis of ITZ Content .....	85
X-Ray Powder Diffraction (XRPD).....	85
Dissolution .....	86
Sink Conditions.....	87
Non-Sink Conditions (Supersaturated).....	87
Area Under the Supersaturated Dissolution Curves .....	91
Stability.....	91
4. RESULTS AND DISCUSSION .....	93
Thermal Decomposition of PVAP .....	93
Isothermal TGA of PVAP.....	95
Glass Transition Temperature (Tg) of PVAP .....	96
Conventional Differential Scanning Calorimetry (DSC).....	96
Modulated DSC (MDSC) .....	97
Thermomechanical Analysis (TMA) .....	98
Dynamic Mechanical Analysis (DMA) .....	99

Thermal Analysis Summary .....	100
Melt Viscosity of PVAP .....	101
Hygroscopicity of PVAP .....	102
TGA and Loss on Drying of PVAP After Exposure to Various Relative Humidities .....	102
DSC Analysis of PVAP After Exposure to Various Relative Humidities.....	103
Water-Solid Interactions .....	104
Moisture Uptake Summary .....	106
Solubility Parameter.....	106
Method of Hoftyzer and Van Krevelen .....	106
Method of Hoy.....	108
Solubility Parameter Summary .....	109
Solubility Parameters for Plasticizers, Polymers and Other Excipients.....	110
Melt Viscosity of PVAP and Plasticizers .....	113
PVPVA as an Alternative to Plasticizers .....	117
Characterization of PVPVA.....	118
MDSC of PVPVA.....	118
TGA of PVPVA.....	119
Melt Viscosity of PVPVA .....	120
Moisture Uptake of PVPVA .....	121
PVPVA Characterization Summary .....	122
Miscibility of PVAP-PVPVA Polymer Blends .....	123
Processability of the Polymer Blends .....	124
Analysis of PVAP Content .....	125
Melt Viscosity of the Polymer Blend.....	126
Itraconazole.....	128
Tg and Tm of ITZ .....	128
Miscibility of PVAP-PVPVA-ITZ Blends .....	130
Processability of ITZ-Polymer Blends.....	135
Analysis of ITZ Content .....	137
Miscibility of ITZ-PVAP-PVPVA Extrudate.....	137

X-Ray Diffraction (XRD) .....	138
Dissolution .....	139
Sink Conditions .....	139
Non-Sink Conditions (Supersaturated) .....	142
Area Under the Curve .....	146
Stability .....	148
X-Ray Diffraction (XRD) .....	148
USP Enteric Test Method A .....	149
ITZ Miscibility in Polymers .....	151
Targeting Supersaturated Drug Delivery .....	152
Influence of PVAP on Amorphous Solid Dispersions of ITZ .....	154
5. CONCLUSIONS .....	157
Future Direction .....	157
<b>BIBLIOGRAPHY .....</b>	<b>158</b>

## LIST OF TABLES

Table	Page
1. Approximate Solubility Terms as Described in Pharmaceutical Compendia.....	5
2. Classification of Drug Substances According to the BCS.....	6
3. Methods of Manufacturing Amorphous Materials .....	13
4. Factors Found to Influence the Physical Stability of Amorphous Drugs .....	18
5. Types of Solid Dispersions .....	20
6. Polymers Commonly used in Preparing Solid Dispersions .....	23
7. Marketed Drug Products Formulated as Solid Dispersions.....	24
8. Advantages and Disadvantages of Different Processing Technologies.....	28
9. Advantages of HME in Formulation Development .....	31
10. Marketed and In-Development Drug Products Based on HME .....	32
11. Commonly Used Polymers for Melt Extrusion .....	34
12. Basic Requirements for Polymers Used in Melt Extrusion .....	35
13. Bioavailability of Itraconazole Solid Dispersions in Rat Models.....	64
14. Pharmacokinetics of Itraconazole in Healthy Males With and Without a Meal.....	67
15. ICH Guidelines for Stability Testing Conditions.....	92
16. Thermal Analysis Summary of PVAP.....	101
17. Group Contributions for PVAP (Method of Hoftyzer/Van Krevelen) .....	107
18. Hansen Solubility Parameters for PVAP (Method of Hoftyzer/Van Krevelen) ....	107
19. Group Contributions for PVAP (Method of Hoy) .....	108
20. Hansen Solubility Parameters for PVAP (Method of Hoy).....	108
21. Total Solubility Parameter for PVAP .....	110
22. Difference in Solubility Parameter ( $\Delta\delta$ ) of PVAP and Various Plasticizers .....	111

23.	Difference in Solubility Parameter ( $\Delta\delta$ ) of PVAP and Various Polymers .....	112
24.	Difference in Solubility Parameter ( $\Delta\delta$ ) of PVAP and Various Excipients .....	113
25.	Partial and Total Solubility Parameters for PVAP, PVA, and PEG .....	117
26.	Partial and Total Solubility Parameters for PVAP, PVPVA, and Itraconazole.....	118
27.	PVAP Content as a Function of Temperature.....	126
28.	Polymer Combinations Tested for Processability by Melt Extrusion.....	128
29.	Assay Results for ITZ in the Ternary Solid Dispersions .....	137
30.	Equilibrium Solubility of Pure ITZ, Concentrations of ITZ in Acid and Buffer Phases from Supersaturated Dissolution Testing, and ITZ Saturation Solubility in DMSO.....	146
31.	Area Under the Supersaturated Dissolution Curve for the Acid Phase, Neutral Phase, and Total Dissolution Test.....	145

## LIST OF FIGURES

Figure	Page
1. Publications from 1998 to 2012 Pertaining to Poorly Soluble Drugs.....	3
2. Lattice Structure of a Crystalline Solid and Amorphous Structure of a Glassy Solid .....	14
3. Illustration of the Variation of Enthalpy Versus Temperature .....	15
4. Lower Energy Crystal Configuration and Higher Energy Amorphous States.....	16
5. Solid Dispersions Based on Amorphous Carriers.....	21
6. Melt Extrusion Process for Pharmaceutical Dosage Forms.....	30
7. Melt Extrusion Equipment with Downstream Calendering Device .....	36
8. Pelletizer and Strands of Extrudate Cut into Small Pieces .....	36
9. Single Screw and Twin Screw Extruders.....	37
10. Examples of Rod and Ribbon Dies.....	37
11. Component Parts of an Extruder.....	38
12. Modular Screw Elements, Barrels, and Assembled Screw Elements .....	38
13. Geometry of an Extruder Screw .....	41
14. Illustration of Dispersive and Distributive Mixing.....	47
15. Effect of Varying Feed Rate, Screw Speed, and Temperature on Residence Time and Torque .....	50
16. Chemical Repeat Units of PVAP .....	61
17. Chemical Repeat Units of PVPVA.....	62
18. Chemical Structure of Itraconazole .....	65
19. Intestinal Transport and Metabolism of Itraconazole .....	68
20. TGA Analysis of PVAP, Chemical Structure of PVAP, and Visual Observations of PVAP Heated to Various Temperatures .....	94

21.	TGA Analysis of PVAP Compared to PVA.....	95
22.	Isothermal TGA Analysis of PVAP at 120°C, 130°C, 140°C, and 150°C.....	96
23.	Conventional DSC Thermograms of PVAP at 10°C/min., 15°C/min., and 30°C/min. ....	97
24.	MDSC Heat-Cool-Heat Cycles for PVAP.....	98
25.	TMA Analysis of PVAP.....	99
26.	Storage and Loss Modulus versus Temperature by DMA for PVAP.....	100
27.	Melt Viscosity of PVAP.....	102
28.	Moisture Uptake for PVAP as a Function of Humidity.....	103
29.	The Tg of PVAP with Increasing Humidity as Measured by MDSC in the Reversing Heat Flow Signal.....	104
30.	Chemical Repeat Units of PVAP.....	107
31.	PVAP Mixtures Containing 30%, 40% and 50% w/w TEC and Heated to 100°C, 120°C, 140°C and 160°C.....	115
32.	PVAP Mixtures Containing 30%, 40% and 50% w/w Triacetin and Heated to 100°C, 120°C, 140°C and 160°C.....	116
33.	PVAP Mixtures Containing 50% PEG 400 or PEG 3350 and Heated to 100°C, 120°C, 140°C and 160°C.....	116
34.	MDSC Heat, Cool, Heat Cycle for PVPVA.....	119
35.	Weight Loss as a Function of Temperature by TGA for PVPVA.....	120
36.	Melt Viscosity of PVPVA and PVAP.....	121
37.	Moisture Uptake for PVPVA by LOD as a Function of Humidity.....	122
38.	MDSC Analysis of PVAP-PVPVA Polymer Blends.....	124
39.	Torque Generated from Different Polymer Ratios as a Function of Extrusion Time.....	125
40.	Melt Viscosities for Pure PVAP, Pure PVPVA, and 30:70% PVAP:PVPVA Polymer Blend.....	127
41.	MDSC Analysis for ITZ.....	130

42.	MDSC Analysis of ITZ:Polymer (1:2 PVAP:PVPVA) Powder Blends .....	134
43.	MDSC Analysis of ITZ:PVPVA Powder Blends .....	134
44.	Torque Generated from Different Polymer Blends Versus ITZ-Polymer Blends as a Function of Extrusion Time.....	136
45.	Extrudate Containing ITZ-PVPVA and ITZ-PVAP-PVPVA .....	136
46.	MDSC Analysis of Extruded 40:60% ITZ:Polymer Blend (1:2 PVAP:PVPVA) .....	138
47.	X-Ray Diffraction Profiles for the Melt Extruded Powder Blend Containing 40:60% ITZ:Polymer Blend (1:2 PVAP:PVPVA).....	139
48.	Sink Dissolution Profiles of Melt Extruded Powders Containing Binary and Ternary Mixtures of ITZ in SGF.....	140
49.	Dissolution Results for Sporanox Capsules using FDA Test Method in SGF ...	143
50.	Supersaturated Dissolution Profiles of Melt Extruded Powders Containing Binary and Ternary Mixtures of ITZ in 0.1N HCl for 2 hours followed by pH 6.8 Buffer .....	145
51.	X-Ray Diffraction Profiles for Melt Extruded Powder Blend Containing 40:60% ITZ:Polymer Blend (1:2 PVAP:PVPVA) After 1, 3, and 6 Months of Storage at 30°C/65% RH .....	148
52.	Supersaturated Dissolution Profiles of Melt Extruded Powders Containing 40:20:40% ITZ:PVAP:PVPVA in 0.1N HCl for 2 hours followed by pH 6.8 Buffer Before and After 6 Months of Storage at 30°C/65%RH .....	149
53.	Extruded ITZ-PVAP-PVPVA and ITZ-PVPVA Solid Dispersions After 6 Months of Storage at 30°C/65%RH .....	150

## **CHAPTER 1**

### **INTRODUCTION**

Drugs are administered to the body in several ways. Patients and clinicians prefer the oral route because it is convenient and painless, both of which promote therapeutic compliance (1). Pharmaceutical companies are also attracted to oral drug delivery because of the variety of dosage forms they can produce at comparatively low cost (1). Generally, solid oral dosage forms such as tablets and capsules are favored because they provide accurate dosing and a high degree of drug stability (1). However, oral delivery of poorly water-soluble drugs commonly results in low absorption (1).

For a solid dosage form to be successful after oral administration, the drug must first dissolve in the gastrointestinal (GI) fluids, then be absorbed across the intestinal mucosa and pass through the liver to reach the systemic circulation and exert its pharmacological effect (2). Poor water solubility hinders dissolution and therefore limits drug concentrations at the target site, which reduces absorption and therapeutic effects (3). The physiology of the GI tract, with its high intestinal surface area and rich blood supply, offers the potential for excellent drug absorption and consequently high bioavailability (4,2). However, oral bioavailability is often low and variable because the process of drug absorption from the GI tract is complex and influenced by numerous physiological factors including GI motility, pH, efflux transporters, and pre-systemic

metabolism (5,6,2). In addition, several extrinsic factors such as food intake, formulation design, and physicochemical properties of the drug affect bioavailability (5,6,2).

The unpredictable nature of GI absorption suggests drug molecules must possess optimal biopharmaceutical properties to achieve drug concentrations that are therapeutically effective upon oral administration. Some ideal properties of an orally administered drug would be: 1) aqueous solubility sufficient to allow a single dose to dissolve in 100 to 400 ml of water; 2) apparent partition coefficient (Log P) value of about 2; 3) minimal first pass metabolism; and 4) elimination half-life appropriate for the dosing schedule (7,8). Unfortunately, few drug molecules have ideal biopharmaceutical properties and, in fact, the number of molecules with insufficient or poor aqueous solubility has steadily grown (9).

### **Increasing Number of Poorly Water-Soluble Drugs**

One indication of the growth in the number of compounds that are poorly soluble is the increase in the number of publications per year dealing with poorly soluble drugs (1). Figure 1 shows a marked increase in the number of these publications from 1998 to 2012 (10,1). An increase in poorly water-soluble drugs is especially noteworthy because compounds with insufficient solubility typically have higher risks of attrition and higher costs in drug development (11). The increase in the number of poorly soluble compounds has been associated with two main factors: the increase in molecules synthesized for screening and a shift in therapeutic targets.

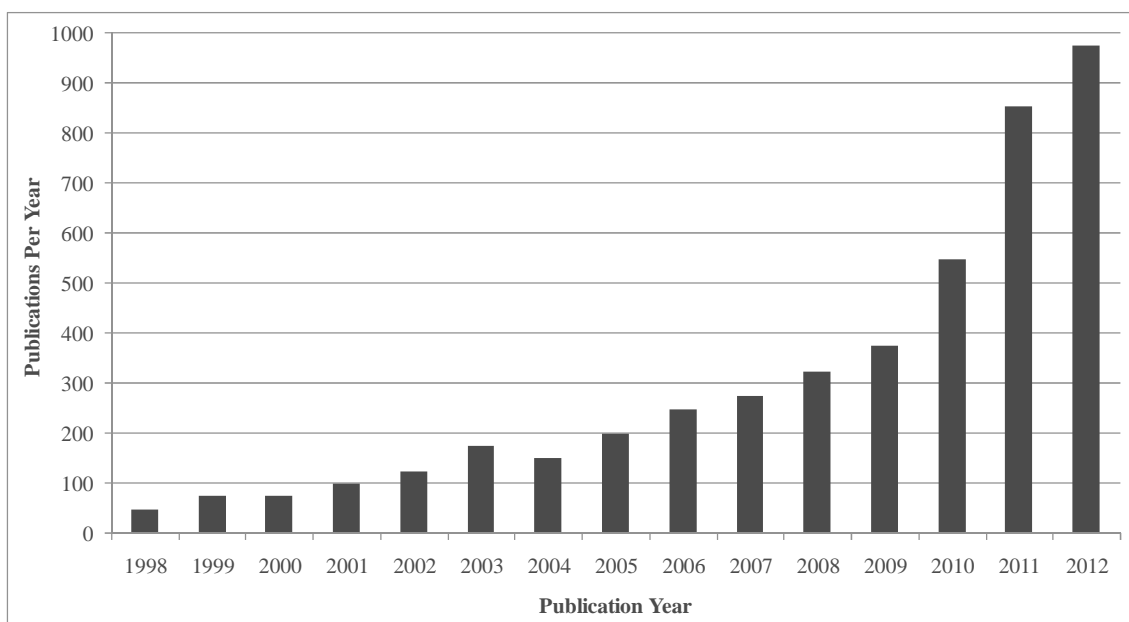


Figure 1. Publications from 1998 to 2012 Pertaining to Poorly Soluble Drugs. Adapted from Buckley 2012.

First, there has been a significant increase in the total number of compounds overall in drug discovery programs based on advances in combinatorial chemistry and high-throughput screening (HTS) (11). Many lead compounds of drug discovery programs are routinely obtained through HTS of compound collections. These collections typically consist of legacy compounds from previous projects, file enrichment activities, and compound library purchases (11). File enrichment activities and compound library purchases have both been used to increase the size and diversity of collections; yet the chemistry of these compounds and their purification methods tends to produce a bias toward low solubility (11). Similarly, lead candidates identified through HTS of compound collections often have high molecular weight and lipophilicity, and consequently poor water solubility (9,12,11). During lead optimization, further decreases in solubility can occur when more lipophilic substituents are added to improve potency and selectivity (11).

Second, the increase in the number of poorly soluble compounds has been attributed to shifts in biological therapeutic targets (13). For example, a shift of therapeutic targets from aminergic G-protein-coupled receptors and enzymes to more challenging targets such as kinases, ion channels, nuclear receptors and protein-protein interactions often leads to compounds with lower solubility (11,9,12,14,15). The latter type of target classes frequently requires more lipophilic compounds for binding affinity or produces compounds with strong intermolecular interactions, such as wide aromatic regions and/or intermolecular hydrogen bonds (16). The pursuit of novel compounds that have specific interactions with more modern therapeutic targets has produced new chemical entities (NCEs) with challenging physicochemical properties (13,17). Specifically, more poorly water-soluble compounds have emerged. This has become a major obstacle in drug discovery and development (11). It has been estimated that up to 40 percent of NCEs under development are categorized as poorly soluble (18,1).

### **Defining a Drug as Poorly Soluble**

Adequate aqueous solubility of NCEs is one of the primary properties required for successful product development of a solid oral dosage form (2). Solubility is generally defined as the amount of a substance that dissolves in a given amount of solvent (19). The solubility of a drug may be expressed in a number of different ways. Certain pharmaceutical compendia list the solubility of drugs as the number of milliliters of solvent in which one gram of solute will dissolve (19). For substances whose solubilities are not definitely known, the values are described using certain general terms, as given in Table 1 (20,19). Currently, about 40 percent of marketed, immediate release oral drugs

are categorized as practically insoluble (21,22). The term practically insoluble applies to drugs that are almost totally water-insoluble or are at least poorly water-soluble (23), the latter term typically referring to drugs with an aqueous solubility less than 100 µg/ml (24).

Table 1. *Approximate Solubility Terms as Described in Pharmaceutical Compendia*

Term	Parts of Solvent Required to Dissolve 1 Part of Solute
Very soluble	Less than 1 part
Freely soluble	1 to 10 parts
Soluble	10 to 30 parts
Sparingly soluble	30 to 100 parts
Slightly soluble	100 to 1000 parts
Very slightly soluble	1000 to 10,000 parts
Practically insoluble or insoluble	More than 10,000 parts

The term poorly soluble can also be applied to any drug that has a dose (mg) to aqueous solubility (mg/ml) ratio greater than 100 ml, where the drug solubility is based on its neutral form (for example, free base or free acid) in unbuffered water (23,24). The dose:solubility ratio represents the volume of gastrointestinal (GI) fluids necessary to dissolve an administered dose of the drug (24). When this volume exceeds the volume of fluid available in the GI tract (typically estimated at 250 ml), incomplete bioavailability from solid oral dosage forms is anticipated because drugs must be in solution prior to absorption (24,25,26).

Lastly, a drug can be described as poorly soluble based on its dissolution rate (24). The aqueous solubility of a drug influences its dissolution rate, which in turn determines its concentration in solution, and can affect the driving force for its diffusion across intestinal membranes (27). A drug is described as poorly soluble when its

dissolution rate is so slow that dissolution takes longer than the transit time past its absorption site (24). In general, drugs with very low solubility and slow dissolution rates will exhibit dissolution-limited oral absorption and thus poor bioavailability (27).

### *Biopharmaceutics Classification System*

The two key properties for potential drug candidates that define the extent of oral bioavailability are aqueous solubility and intestinal permeability (2). Based on these two critical parameters, the Biopharmaceutics Classification System (BCS) assigns drugs to one of four categories (25,1). Table 2 shows the classification system according to the BCS (26).

Table 2. *Classification of Drug Substances According to the BCS*

Class	Solubility	Permeability
1	High	High
2	Low	High
3	High	Low
4	Low	Low

Traditionally, the BCS is used to justify biowaivers for Class 1 drug substances (26), but more recently, the concept of BCS has been used to indicate the level of difficulty expected to progress drug candidates through development, and to identify formulation development strategies (21,28,29). For example, BCS Class 1 drugs have no rate-limiting step for absorption so conventional tablet or capsule formulations are typically designed to ensure rapid dissolution in the GI tract (21). In contrast, the bioavailability of BCS Class 3 and Class 4 drugs is rate-limited by membrane permeability in the GI tract (21). Permeability may be improved, although success has been limited, by adding permeation enhancers to the formulation, such as fatty acids, bile

salts, surfactants and polysaccharides (21,30,31,24). Lastly, for BCS Class 2 drugs, which are characterized as having low solubility and high permeability, the bioavailability of the drug is rate-limited by its solubility (21). Drug concentration in the GI tract is a function of both solubility and dissolution rate, so increasing the solubility and/or dissolution rate of the drug can increase bioavailability (32). Formulation approaches for BCS Class 2 and Class 4 compounds are similar, though the absorption of Class 4 drugs still may be limited by their poor permeability after dissolution in the GI tract (21).

An ideal drug substance has high aqueous solubility and high permeability (BCS Class 1), but only about 5% of NCEs meet these criteria, while approximately 90% are considered poorly soluble in combination with either high or low permeability (BCS Class 2 or 4) (3). The combination of low solubility and low permeability often prevents BCS Class 4 compounds from being developed and marketed. On the other hand, many BCS Class 2 compounds have advanced from discovery into development, and several have become successful, marketed drugs (13,33,34,2). Studies estimate that Class 2 molecules account for over 75 percent of drug candidates (35,11), 60 percent of NCEs (36,37), and 90 percent of marketed drugs (37,36). Their commercial success has been attributed to various formulation technologies capable of increasing the dissolution rate of the drug (13,21).

### **Factors Affecting the Dissolution Rate of Drugs**

There are several physicochemical factors that affect the dissolution rate of drugs (21). From the following modification of the Noyes-Whitney equation (Eq. 1), where

$\frac{dX}{dt}$  is the rate of drug dissolution at time (t), the important factors to the kinetics of drug

dissolution are as follows:

$$\frac{dX}{dt} = \frac{AD}{h} \left( C_s - \frac{X_d}{V} \right) \quad \text{Eq. 1}$$

surface area available for dissolution (A), diffusion coefficient of the drug (D), thickness of the boundary layer adjacent to the dissolving drug surface (h), saturation solubility of the drug (Cs), amount of dissolved drug (Xd), and volume of dissolution media (V) (24,21). In principle, variation of any of these factors will cause a change in the rate of dissolution. Horter et al. discussed in detail the many physicochemical and physiological aspects that influence each factor (24). In practice, however, only the solubility and surface area of the drug are actually controllable parameters (21). The diffusion layer thickness is a function of the hydrodynamics of the system and therefore, difficult to control (24). Likewise, the diffusion coefficient cannot be manipulated, except perhaps by slight changes in the viscosity of the dissolution medium (24). Thus, these factors are regarded as uncontrollable in dosage form development (21). Conversely, several formulation methods can be used to alter the solubility or surface area parameters and thereby, the dissolution behavior of drugs (21).

### **Formulation Strategies for Poorly Water-Soluble Drugs**

Some formulation approaches considered effective for increasing the saturation solubility and surface area of a drug include: salt formation, crystal modification, pH modification, cyclodextrin complexation, self-emulsification, particle size reduction, and amorphization (21,24). A brief review of these techniques follows.

### *Salt Formation*

Salt formation is the most common method of increasing solubility and dissolution rate of acidic and basic drugs (38). Salts are formed from chemical reactions involving a proton transfer from an acid to a base (21). Drugs that are either acidic or basic, therefore, can potentially form a wide range of salts (39). In practice, hydrochloride salts of basic drugs and sodium salts of acidic drugs are most common (39). The aqueous solubility of an acidic or basic drug as a function of pH dictates whether the compound will form suitable salts and what some of their physicochemical properties might be (38,40). In some cases, salt formation may not be feasible due to physical and chemical properties of the drug (38). In other cases, though salts can be synthesized, they may not provide the desirable properties of enhanced dissolution rate and bioavailability (38). Some factors limiting the use of salts in dosage forms include low aqueous solubility, conversion of free acid or base form, and poor stability (38).

### *Crystal Modification*

Many drugs are able to crystallize into multiple metastable forms known as polymorphs (24). Common methods of producing different polymorphic forms of a drug include recrystallizing from different solvents, melting, or rapid cooling (24). Each polymorph has a different energy and thereby differs in physicochemical properties such as melting point, solubility and stability (24). Appropriate polymorph selection, therefore, can be a viable approach to enhancing the dissolution rate of poorly soluble drugs (24,41). However, the more soluble, higher energy metastable polymorphic forms eventually convert to a less soluble, lower energy form (24,42). This conversion, which

is possible during manufacturing and storage, has limited the more widespread commercialization of polymorphs (24,42).

### *pH Modification*

pH modification is a common strategy to enhance the dissolution rate of weakly acidic or basic drugs because the solubility of the drug is pH dependent (43). A particular pH change can increase the solubility of the drug by triggering its dissociation (43). To produce a pH change, pH modifiers are incorporated into the formulation. These modifiers can alter the microenvironmental pH surrounding a dissolving solid to an optimal pH for enhanced solubility (43,44,45,46). The microenvironmental pH can be defined as the pH of the saturated solution immediately surrounding the drug particle (43,47). Deliberate modifications to the microenvironmental pH have reportedly improved solubility, dissolution rate, and chemical stability of drug substances in a predictable manner (21,43,47,48). For example, tartaric acid enhanced the dissolution rate of a weakly basic drug with poor intrinsic solubility when incorporated into a tablet formulation (48).

### *Cyclodextrin Complexation*

Cyclodextrins and their derivatives are oligomers of glucose that can form water-soluble inclusion complexes with small hydrophobic molecules and portions of large compounds (49). Their ability to form inclusion complexes is due to the typical torus or doughnut-ring arrangement of the constituent glucose units (24,49). The interior of the cavity is relatively hydrophobic and thus can accommodate drug molecules to form

inclusion complexes while the exterior of the cyclodextrin structure remains sufficiently hydrophilic to impart water solubility to the complex (49). Cyclodextrin complexation, therefore, is a technique that can be used to improve the apparent solubility and dissolution rates of poorly soluble drugs. Drawbacks associated with some forms of cyclodextrins include internal cavity diameters not large enough to accommodate drugs, increases or decreases in the reactivity of the drug, low aqueous solubility, toxicity, and incomplete dissociation of the complex that compromises permeability (24,49).

### *Self-Emulsification*

Self-emulsification drug delivery systems (SEDDS) have been used to enhance the oral bioavailability of poorly soluble drugs and, particularly, highly lipophilic drugs (21). Self-emulsification formulations are typically isotropic mixtures comprising oil, surfactant, co-solvent, and solubilized drug (50). These formulations can rapidly form oil-in-water emulsions when dispersed in an aqueous phase (50). The rapid emulsification of these formulations in the GI tract can provide improved oral bioavailability and reproducible plasma concentration profiles (50). SEDDS can be further classified into self-microemulsification drug delivery systems (SMEDDS) and self-nanoemulsification drug delivery system (SNEDDS), according to the size range of their oil droplets (51). Smaller droplet size has been shown to increase the extent of absorption of orally administered drugs (21). Lipid formulations tend to be more suitable for drug substances with relatively high intrinsic lipophilicity to ensure their solubility and stability in limited amounts of oil (21).

### *Particle Size Reduction*

The particle size of the drug influences its dissolution rate. Specifically, dissolution accelerates with increasing surface area, which in turn increases with decreasing particle size (24,21). Reducing the particle size of the drug using micronization techniques is often a successful strategy for enhancing the dissolution rate of a drug (21). However, reducing particle size can also promote agglomeration of drug particles, which may decrease the effective surface area available for dissolution (21). In such cases, a surfactant may be required to improve the wettability and increase the effective surface area of the drug particles (21).

### *Amorphization*

Amorphous forms of active pharmaceutical ingredients (APIs) can be desirable for solubility enhancement because they have the potential to produce solution concentrations many times greater than their crystalline forms (52). Studies have shown that amorphous solids can produce 1.1 to 1000-fold increases in solubility compared to the same drug in its crystalline form (21,53,54). For comparison, the expected differences in aqueous solubility between two crystalline polymorphs of the same drug substance are typically only two-fold, and hydrated versus non-hydrated forms of small molecule drug substances range from two to ten-fold (55,56,57).

Amorphous drugs are formed either by preventing crystal lattice before it forms or by disrupting existing crystal structure (58). Common techniques used for preparing amorphous solids are outlined in Table 3 (2,59,60). With the exception of crystal disruption, most techniques begin by solubilizing or melting the drug substance, followed

by solvent removal or melt quenching, respectively, at rates that kinetically avoid crystallization (2).

Table 3. *Methods of Manufacturing Amorphous Materials. Adapted from Hancock 2012*

From	Method	Examples
Crystal	Disruption of existing crystal structure Energy Input	Milling or grinding Compression or decompression Dehydration or desolvation Irradiation Reaction
Solution	Solvent removal	Spray-drying Freeze-drying Precipitation Polymerization Reaction
Liquid	Rapid cooling Energy removal	Melt quenching / rapid cooling Melt extrusion Nucleation suppression Polymerization Reaction
Vapor	Rapid cooling Energy removal	Sublimation Reaction

The control of amorphous solids in the development of pharmaceutical products begins with an understanding of the amorphous state relative to the crystalline state. Crystal structure forms by repeating a three-dimensional pattern of atoms, ions or molecules; the repetition of the structural units over long atomic distances is referred to as long-range order (61). Amorphous solids (e.g., glasses) do not have long-range order but instead have a limited, localized order close to their structural units (61). Figure 2 illustrates the structural differences between crystalline and amorphous states (62).

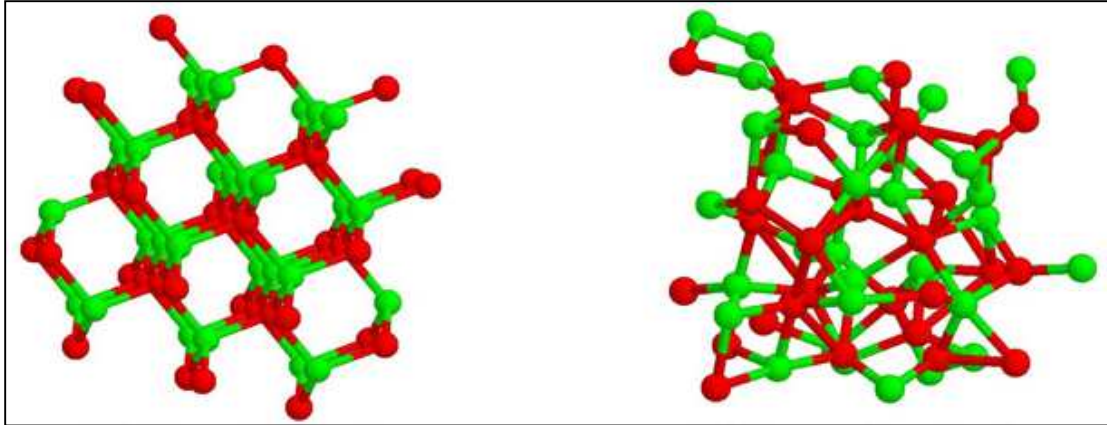


Figure 2. Lattice Structure of a Crystalline Solid (left) and Amorphous Structure of a Glassy Solid (right)

The irregular arrangement of molecules in an amorphous state usually causes the molecules to be spaced further apart than in a crystal and, consequently, the specific volume is greater and the density lower than that of the crystal (59). Figure 3 depicts the variation in enthalpy or specific volume with temperature (63). From Figure 3 it can be seen that while the melt usually crystallizes at  $T_m$ , if the cooling rate is too fast to permit crystallization, enthalpy and volume may follow the equilibrium line of the liquid beyond  $T_m$  into the supercooled liquid region without showing any discontinuity in enthalpy and volume (59,64). As the viscosity of the material increases upon cooling, there is a reduction in molecular motion until the molecules move so slowly that they have no time to organize themselves before the temperature is lowered further (64). This results in a change in slope, usually seen at a characteristic temperature known as the glass transition temperature ( $T_g$ ) (59). The properties of the glassy material at  $T_g$  deviate from those of the equilibrium supercooled liquid to give a nonequilibrium state having even higher enthalpy and volume than the supercooled liquid, as shown in Figure 3 (59,64).

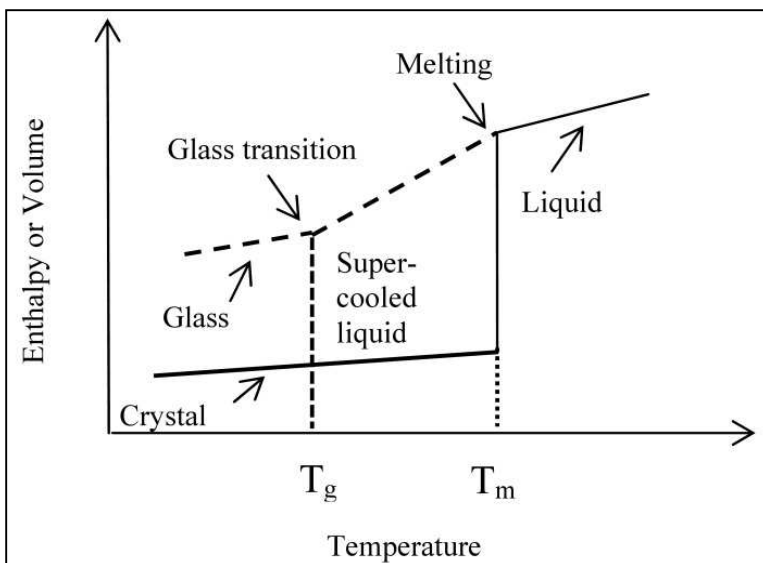


Figure 3. Illustration of the Variation of Enthalpy (or Volume) Versus Temperature

Since amorphous solids possess considerably lower packing energy compared to crystalline solids by virtue of their disordered structure, amorphous solids exhibit decreases in intermolecular interactions and corresponding increases in both enthalpy and entropy (13,52,65). The increase in enthalpy is never completely compensated for by the increase in entropy, however, and the Gibbs free energy, which reflects the balance between them, actually increases (19). The Gibbs free energy of an amorphous substance at a given temperature, therefore, is always higher than the Gibbs free energy of that same substance in its crystalline state (61). This means that amorphous drug formation affects the molecular interactions in the solid, which in turn influence the solubility and dissolution properties of the drug. Generally, the solubility of a solid in a solvent depends on the competition of solute:solvent interactions and solid:solid interactions (58). In an amorphous solid, therefore, decreased solute:solute interactions increase the escaping tendency of the molecules, and thus more molecules dissolve in a given solvent relative to the crystalline form under the same set of conditions (58).

The higher free energy of an amorphous material, shown in Figure 4, leads to higher apparent solubility and dissolution rate, but also produces higher chemical reactivity and a tendency to spontaneously crystallize over time (59,66,64). The amorphous state, therefore, is thermodynamically unstable, or metastable, relative to the crystalline state (59). Crystallization of an amorphous material over time effectively negates any solubility enhancement, so an understanding of the critical factors associated with crystallization is crucial to stabilizing amorphous drugs.

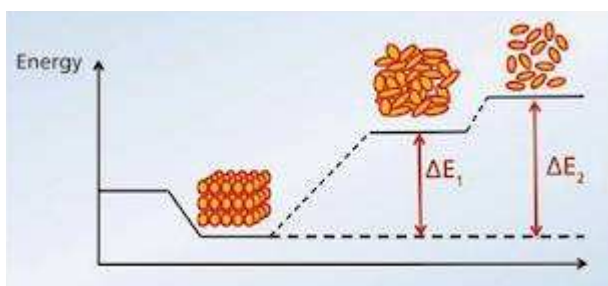


Figure 4. Lower Energy Crystal Configuration and Higher Energy Amorphous States. Adapted from Kolter 2010

The crystallization process is governed by both kinetic and thermodynamic factors and depends on two successive but independent processes: nucleation and crystal growth (64). For nucleation or crystal growth to begin, clusters of ions or molecules called nuclei must exceed a critical size before they become stable and capable of growing into crystals (64). The temperature dependence of the kinetic factors and the thermodynamic driving force for nucleation have opposite signs; kinetics and greater molecular mobility favor nucleation at higher temperatures, whereas thermodynamics and increased viscosity favor nucleation at low temperatures (64). Therefore, nucleation occurs in the balance of these two factors and the maximum rate of crystallization occurs somewhere between the melting temperature ( $T_m$ ) and glass transition temperature ( $T_g$ ), which are illustrated in Figure 3 (64). The  $T_g$  is considered to be a key parameter for

stabilization because it delineates a temperature range between high and low molecular mobility (67,68). Molecular mobility and the corresponding risk of crystallization are reduced by storing amorphous materials below their T<sub>g</sub>, i.e., in their glass state (64). However, molecular mobility below T<sub>g</sub> still occurs, though it is over a longer time period than above T<sub>g</sub>, and can be sufficient to result in crystallization during typical pharmaceutical storage times (64).

The factors affecting crystallization of an amorphous solid have been categorized as thermodynamic (entropy, enthalpy, Gibbs free energy) (64,69,70), kinetic (molecular mobility) (64,71,72), or molecular (e.g., hydrogen bonding interactions) (64,73,74,75). In addition, parameters such as moisture content and the methods and conditions used to generate the amorphous form have been reported to influence crystallization (64,76,77,78). Each factor is presented in more detail in Table 4 (64). In short, amorphous compounds with high T<sub>g</sub>, high configurational entropy barrier, and low molecular mobility are expected to show the greatest stability (64,60).

Table 4. *Factors Found to Influence the Physical Stability of Amorphous Drugs.*  
*Adapted from Laitinen 2012*

Factors on the molecular level			
Factor	Indicator	Observed impact on stability	Ref.
Molecular mobility	Glass transition temperature (Tg)	Molecular mobility is higher above Tg. Lower molecular mobility below Tg slows crystallization, but storage below Tg alone cannot ensure stability.	(79,70, 80)
	Structural relaxation ( $\alpha$ relaxation)	$\alpha$ relaxations require a cooperative motion of multiple molecules and thus, are associated with a large energy barrier. Above Tg, short relaxation times contribute to significant rates of crystallization.	(81,71, 72)
	Local mobility ( $\beta$ relaxation)	Local non-cooperative motion has a smaller energy barrier and continues to occur over long timeframes below Tg. These secondary motions are the precursors to $\alpha$ relaxation.	(59,82, 83,80)
Entropic barrier for crystallization	Configurational entropy	Compounds with high entropy barriers and low mobility show greater physical stability. In contrast, molecules with low entropies require less mobility for spontaneous crystallization.	(70,81, 84)
Enthalpic driving force	Configurational enthalpy	Reported to be a relatively poor predictor of crystallization. Higher configurational enthalpy may have contributed to increased nucleation rates of nifedipine.	(70,69)
Overall thermodynamic driving force	Gibbs free energy	Reported to be a relatively poor predictor of crystallization	(70)
Hydrogen bonding	-	Given similar Tg values, compounds with strong intermolecular hydrogen bonding showed greater stability than those without.	(73,75, 69,74)

Table 4. (continued)

Factors independent of the molecule			
Factor	Indicator	Observed impact on stability	Ref.
Environmental stress	Temperature and humidity during handling & storage	Molecular mobility increases with temperature, particularly near T <sub>g</sub> . Plasticizing effects of water can lower T <sub>g</sub> , which results in enhanced molecular mobility and crystallization rates.	(59,82, 85)
Preparation methods	Solvent evaporation, quench cooling, and mechanical activation methods	Different preparation methods may result in different mechanical stresses and thermal histories, producing different degrees of relaxation. The stability of amorphous indomethacin varied by method: quench cooled > cryo-milled > spray dried > ball milled, which correlated with the relaxation time values for the samples.	(82,76, 86,77,78,87)
Preparation conditions	Evaporation rates, cooling rates, processing temperatures, and processing times	Increased cooling rates improved melt-quenched indomethacin stability by reducing the number of nuclei. Different inlet temperatures used during spray drying of cefditoren pivoxil altered particle morphology and improved stability.	(82,77, 88)

### *Solid Dispersions*

It is difficult to achieve a physically stable amorphous state of a drug alone (13). To prevent crystallization of an amorphous drug in a formulation, one or more polymers are often incorporated as stabilizers (89,90). Typically, the amorphous drug is dispersed throughout the polymer, forming a solid dispersion (90). Newman et al. reported the outcomes from the past fifteen years in the field of solid dispersions (91). The authors found that in about 80% of all cases, solid dispersions led to improved bioavailability; No improvements were found in 10% of the cases, and in another 10%, solid dispersions reduced bioavailability (91). In the past decade, broad application of solid dispersions as

an enabling formulation technology has contributed significantly to successful clinical evaluations and commercialization of poorly soluble compounds (13,52,65).

The term solid dispersion refers to a group of solid products typically consisting of at least two different components: generally a hydrophilic carrier and a hydrophobic drug (92). In a solid dispersion, the carrier can be either crystalline or amorphous and the drug can be dispersed molecularly, in clusters of amorphous particles, or in crystalline particles.

Table 5 shows six different types of solid dispersions (93). The latter three types can be further classified as crystalline glass suspensions, amorphous glass suspensions and solid glass solutions, respectively (93). Figure 5 illustrates their compositions.

Table 5. *Types of Solid Dispersions. Adapted from Dhirendra 2009*

	Type of Solid Dispersion	Carrier	Drug	Phases
I.	Eutectics	Crystalline	Crystalline	2
II.	Amorphous precipitations in crystalline carrier	Crystalline	Amorphous	2
III.	Solid solutions	Crystalline	Molecularly dispersed	-
	Continuous vs. discontinuous	Crystalline	Molecularly dispersed	1 or 2
	Substitutional vs. interstitial	Crystalline	Molecularly dispersed	1 or 2
IV.	Glass suspensions	Amorphous	Crystalline	2
V.	Glass suspensions	Amorphous	Amorphous	2
VI.	Glass solutions	Amorphous	Molecularly dispersed	1

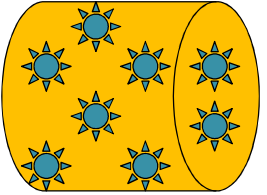
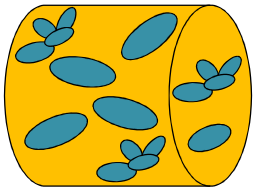
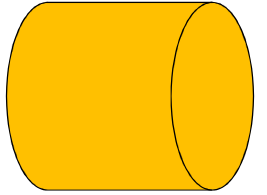
Type of Solid Dispersion			
	IV	V	VI
	Glass suspensions		Glass solution
Carrier phase	Amorphous	Amorphous	Amorphous
Drug phase	Crystalline	Amorphous	Molecularly dispersed
DSC analysis	T <sub>g</sub> + T <sub>m</sub>	2 x T <sub>g</sub>	1 x T <sub>g</sub>
System stability	Very stable	Kinetically stable (oversaturated)	Stable (drug below saturation solubility)

Figure 5. Solid Dispersions Based on Amorphous Carriers

Ideally, in a solid dispersion, the drug is combined with a water-soluble carrier to produce a single-phase amorphous mixture of drug and carrier (13). When this occurs, the drug remains dissolved in the carrier at room temperature and upon aging (94). In a thermogram obtained by differential scanning calorimetry (DSC), a single-phase system shows only one glass transition temperature (92). These miscible, glassy drug-carrier systems (Figure 5, type VI) are commonly termed solid solutions (93). In general, the stability of a molecularly dispersed drug depends upon its interactions with the carrier, such as hydrogen bonding and hydrophobic interactions (92). Therefore, to obtain a stable solid solution, the total interaction forces between the drug and carrier should be stronger than the self-association forces among the drug molecules themselves (92).

Alternatively, the combined drug-carrier system can produce a two-phase mixture of drug and carrier. In a two-phase system, the drug primarily exists in either the crystalline or amorphous state (93). When the drug exists as crystals in the carrier (Figure 5, type IV), DSC analysis detects both the melt of the crystalline drug and the glass transition of the amorphous carrier (92). This is the most stable type of solid dispersion because the drug remains in its favored crystalline state (92). In the other two-

phase system, there is amorphous drug or amorphous drug clusters incorporated in the carrier, but they are not molecularly dispersed (Figure 5, type V). The concentration of drug is in excess of its saturation solubility at room temperature and the excess drug separates as a solid amorphous phase dispersed in a carrier (94). In this case, DSC analysis shows two glass transition temperatures: one from the amorphous carrier and the other from the amorphous drug (92). These amorphous solid dispersions are usually metastable. That is, the presence of the amorphous drug clusters in the solid dispersion may lead to nuclei formation and crystal growth (93). One way to kinetically discourage an amorphous drug from recrystallizing is to immobilize the drug in a supersaturated state in a highly viscous polymer (92).

In general, polymers are preferred as carriers over small molecule excipients because they typically possess two desirable characteristics: 1) high glass transition temperatures ( $T_g$ ), which minimize drug mobility in the solid state, and 2) a broad range of non-covalent interactions between the drug and functional groups on the polymer (13). The drug-polymer interactions are critical to achieve physical and chemical stability of the drug in a solid dispersion (13). Most of the polymers used in the pharmaceutical industry to prepare solid dispersions are either water soluble at all pH conditions or are pH dependent with dissolution properties of enteric coating systems under more alkaline conditions (93). Polymers commonly used to prepare solid dispersion-based formulations are listed in Table 6 with their corresponding  $T_g$  and soluble pH range (95).

Table 6. *Polymers Commonly used in Preparing Solid Dispersions. Adapted from Shah 2012*

Polymer	Synonyms	Tg (or Tm) (°C)	Soluble pH Range
<i>Cellulose based</i>			
Hypromellose (HPMC)	Methocel	168-209	1-10
Hypromellose phthalate (HPMCP)	HP 50, 55	133-137 (150)	> 5.0
Hypromellose acetate succinate (HPMCAS)	Aqoat	113-120	> 5.5
Cellulose acetate (CA)	N/A	170-190 (250)	Insoluble
Cellulose acetate phthalate (CAP)	Aquacoat	160-170 (192)	> 6.0
Ethyl cellulose (EC)	Ethocel	129-133	Insoluble
Hydroxypropyl cellulose (HPC)	Klucel	100-150	1-10
<i>Vinyl based</i>			
Polyvinyl pyrrolidone vinyl acetate (PVPVA)	Copovidone, Kollidon, Plasdone	101-106	1-10
Polyvinyl pyrrolidone (PVP)	Povidone, Kollidon, Plasdone	120-174	1-10
Polyvinyl caprolactam polyvinyl acetate polyethylene glycol	Soluplus	60	1-10
<i>Methacrylate based</i>			
Methacrylic acid copolymer Type A, NF Methacrylic acid:methyl methacrylate (1:1)	Eudragit L100	> 150	> 6.0
Methacrylic acid copolymer Type B, NF Methacrylic acid:methyl methacrylate (1:2)	Eudragit S100	> 150	7.0
Methacrylic acid copolymer Type C, NF Methacrylic acid:ethyl acrylate (1:1)	Eudragit L100-55	110	> 5.5
<i>PEG or Polyol copolymer based</i>			
Polyethylene glycol (PEG)	Carbowax	55-66	1-10
Polyoxyethylene-polyoxypropylene (Poloxamer)	Pluronic	(55)	1-10

## Marketed Products Based on Solid Dispersion Technology

Examples of recently marketed drug products formulated as solid dispersions are listed in Table 7. Their recent commercialization demonstrates the acceptance and utility of amorphous solid dispersion (ASD) technology in the pharmaceutical industry.

Table 7. *Marketed Drug Products Formulated as Solid Dispersions. Adapted from Smithey 2013*

Brand name (Drug name)	Indication	Manufacturer	Primary ASD Polymer	Method of Manufacture
Zelboraf (Vermurafenib)	Metastatic melanoma	Roche	HPMCAS	Precipitation
Incivek (Telaprevir)	Hepatitis C	Vertex Pharmaceuticals	HPMCAS	Spray drying
Tibotec (Etravirine)	HIV	Janssen Therapeutics	HPMC	Spray drying
Cesamet (Nabilone)	Antiemetic	Meda; Valeant	PVP	Melt extrusion
Kaletra (lopinavir/ritonavir)	HIV	Abbott	PVPVA	Melt extrusion

## Methods of Preparing Solid Dispersions

After selecting some promising polymers, selection of the best processing technology is essential. Choosing the most appropriate process for manufacturing a solid dispersion depends on the physicochemical properties of the drug and the polymer, e.g., solubility, melting point, T<sub>g</sub>, and stability (95). In addition, availability of the equipment, robustness of the manufacturing process, and intellectual property rights should be considered (95). There are several technologies that can be used to produce amorphous solid dispersions, including: spray granulation, fluid bed layering, co-grinding, ultra-rapid freezing, and supercritical fluid processing (95). However, these methods have had limited success due to slow evaporation rates, solvent solubility, and/or incomplete conversion of the drug to an amorphous form (95). At present, the favored technologies

for manufacturing solid dispersions are spray drying, precipitation, and melt extrusion (95). Each of these processes has been used to manufacture marketed drugs. The following section briefly discusses these technologies and a summary highlighting the advantages and disadvantages of each is listed in Table 8 (95).

### *Spray Drying*

Spray drying is a well-established technology in the industry for transforming solutions, emulsions or suspensions into a dry powdered form (95). In this process, drug and polymer or other excipients are dissolved in a common solvent and sprayed into a drying chamber of heated gas, e.g., air or nitrogen, that causes the solvent to rapidly evaporate from the droplets (13). The dried particles, which are normally less than 100 microns, are then collected using a cyclone and baghouse filter system (13). Challenges associated with spray drying include: organic solvent solubility, residual solvent removal, environmental, health, and safety concerns surrounding flammable organic solvents, and handling small particles with low bulk density and poor flowability (13,95). The advantages of spray drying are rapid solvent removal (10-100 milliseconds), which results in good uniformity of molecular dispersions, and small particle size, which leads to rapid dissolution (13,95).

### *Precipitation*

Amorphous solid dispersions can be produced when the drug and polymer or other excipients are precipitated together by changing the solubility conditions, either by adding an anti-solvent or by evaporating the solvent (95). Typically, drug and polymer

are dissolved in a solvent first and then water is added to cause rapid co-precipitated (13). The solvent-controlled precipitation is conducted under either acidic or basic conditions based on the ionic natures of the drug and polymer used in the process (95). Challenges for co-precipitation methods include the need to use solvents during processing, identification of suitable anti-solvents for both drug and polymer, and control strategies for reproducibility and homogeneous mixture formation (13,95). One advantage of this approach relative to spray drying is the expanded solvent choice; many compounds have poor solubility in solvents appropriate for spray drying, but are soluble in dimethylsulfoxide (DMSO) or similar solvents that are ideal for precipitation processes (13,95).

#### *Melt Extrusion*

Melt extrusion uses high-shear-induced transient heating to form a solid dispersion (13). Typically, crystalline drug and amorphous polymer are continuously fed into a twin-screw extruder that conveys the material down a barrel where it is exposed to shear (13). Extruders generate energy by friction to overcome the crystal lattice energy of the drug and simultaneously soften the polymer (95). The applied shear stress transforms the drug into its amorphous form (95). In a melt extrusion process, the heat is produced primarily in a high shear zone, followed by relatively rapid cooling that prevents thermal degradation of the drug and polymer (13). Challenges to the melt extrusion process include its limited applicability to heat sensitive materials and, in some instances, the need to include plasticizers to improve the processability of a drug-polymer system (13,95). Benefits of this approach are the avoidance of volatile organic solvents

during the process, the ability to form various physical forms using calendering devices, and the small equipment footprint (13). Melt extrusion is also more cost-efficient and less complex than other processing techniques (95).

Table 8. *Advantages and Disadvantages of Different Processing Technologies. Adapted from Shah 2012*

Technology	Advantages	Disadvantages
Spray drying	Rapid removal of solvent Relatively low temperature processing for highly volatile solvents or thermal labile drugs Continuous processing	Use of organic solvents Identifying common solvent for drug and polymer Removing solvent, may require secondary drying step High manufacturing costs Very fine particles, low bulk density, poor flow properties
Precipitation	Suitable for drugs that cannot be spray dried due to low solubility in common organic solvents Use of ionic polymers may provide high degree of supersaturation pH dependent solubility may result in high exposure and prolonged plasma profiles	Requires polymers with different solubility in solvent vs. antisolvent Weak bases (and acid) drugs show significant solubility in acidic (and basic) solvents For extraction purposes, adequate solubility in water miscible solvents may require multiple washing steps to remove solvents
Melt extrusion	Short residence times limit the exposure to processing temperature Non-solvent processing eliminates the need for solution preparation and solvent removal Customizable process, extruder components are modular Eliminates effects from humidity and oxygen Robust processing control and easy commercial scale-up Broad selection of polymers and excipients with different physicochemical properties Continuous process Easy downstream processing	High energy related to shear forces High melt viscosity causes torque limitations High density and low porosity of thermoplastic extrudates reduces compaction properties of the material

In recent years, interest in melt extrusion techniques for pharmaceutical applications has grown steadily (96). Compared to other pharmaceutical technologies such as tableting, melt extrusion is still an emerging technology and its potential has not been fully explored (96). The following section is a review of extrusion technology.

## **Extrusion Technology**

### *Background*

Extrusion technology has become well known in many diverse industrial fields over the last century (97). Extrusion is the process of converting a raw material into a product of uniform shape and density by forcing it through a die under controlled conditions (98). Joseph Brama invented the extrusion process at the end of the eighteenth century to manufacture lead pipes (99). In the early 1930's, extensive industrial use of extruders in the polymer industry began with the extrusion of thermoplastic materials (100). In 1935, the food industry manufactured pasta products using extrusion technology (97). Currently, extrusion technology is one of the most widely applied processing technologies in the plastic, rubber, and food industries; more than half of all plastic products, such as plastic bags, sheets, and pipes are manufactured by this process (101).

Melt extrusion or hot melt extrusion (HME) was introduced in the mid-nineteenth century when it was used in a wire insulation polymer coating process (99). In the 1980s, BASF SE was the first to apply the HME process based on polymers with high glass transition temperatures, e.g., polyvinylpyrrolidones, to pharmaceuticals (102). Later, Soliqs, the drug delivery business unit of Abbott GmbH & Co. KG, commercialized the

technology and subsequently launched several drug products (102,103). A number of research groups since then have demonstrated HME processes as being a viable technique for the preparation of pharmaceutical drug delivery systems (104)

### *Melt Extrusion for Pharmaceutical Dosage Forms*

HME refers to the processing of polymeric materials at temperatures above their glass transition temperature ( $T_g$ ) in order to affect molecular-level mixing of active compounds and thermoplastic polymers (105). Figure 6 shows an overview of the HME process for pharmaceutical dosage forms.

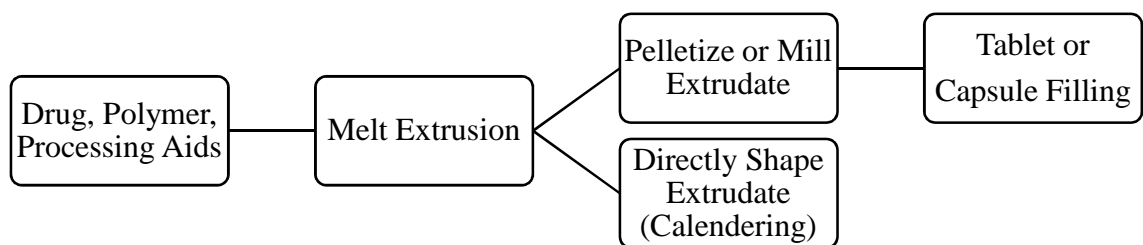


Figure 6. Melt Extrusion Process for Pharmaceutical Dosage Forms

In the pharmaceutical industry, HME has been shown to be a viable technology for the preparation of granules, sustained release tablets, transmucosal and transdermal drug delivery systems, and implantable devices (99,106). Moreover, for pharmaceutical applications, HME offers many advantages over traditional processing techniques. Some advantages of HME are summarized in Table 9 and include: 1) solvent-free process, 2) mixing, melting, and compounding in a single device, 3) no compressibility requirements, 4) simple, continuous, and efficient processing, 5) dispersive and distributive mixing increases dissolution rates, and 6) molecularly dispersed drug substances improve bioavailability (99,104,105,102).

Table 9. *Advantages of HME in Formulation Development*

Challenge	Solution by HME
Poor API stability during processing caused by hydrolysis	Solvent-free alternative to aqueous or hydroalcoholic granulation processes
Environmental, health and safety-related concerns	Organic solvent-free process alternative No residual solvents testing on products
Multiple manufacturing unit operations	Eliminates separate unit operations and increases manufacturing efficiency
Excipient and/or drug compressibility	No requirements on compressibility; poorly compactable materials can be incorporated into an extruded dosage form
Scale-up	Small and large-scale equipment exists; Geometrically similar extruder designs and scale factors for throughput and specific energy input make scale-up easier
Poor bioavailability due to inadequate drug solubility	Prepare solid solution or solid dispersion for enhanced dissolution rates
Multiple dosing regimens	High extrudate density can reduce dosing regimens
Dust	Extrudate is dust free and ideal for high potency compounds

*Marketed and In-Development Products Based on HME*

While perceived by many to be a recent development for pharmaceuticals, the first melt extruded drug product was marketed in 1981 (96). Subsequent products have been developed periodically over the last thirty years (96). Table 10 lists drug products made using melt extrusion technology that are currently marketed and under development (96). Once developed, melt extruded dosage forms are reliable and robust, offering many benefits in cost efficiency (96). Compared to other processes for the production of solid dispersions, HME is less complex since the manufacturing of the dosage form requires only a few steps and avoids the use of organic solvents (96).

Table 10. *Marketed and In-Development Drug Products Based on HME. Adapted from DiNunzio 2012*

Product	Indication	Company	Approval Stage
Lacrisert (HPC rod)	Dry eye syndrome	Merck	Marketed
Zoladex (Goserelin Acetate Implant)	Prostate cancer	AstraZeneca	Marketed
Implanon (Etonogestrel)	Contraceptive	Organon	Marketed
Gris-PEG (Griseofulvin)	Anti-fungal	Pedinol Pharmacal	Marketed
Rezulin (Troglitazone)	Diabetes	Wyeth	Withdrawn, API toxicity
Palladone TM (Hydromorphone)	Pain	Purdue Pharma	Withdrawn, alcohol dose dumping
NuvaRing (Etonogestrel, Ethinyl Estradiol)	Contraceptive	Merck	Marketed
Norvir (Ritonavir)	Anti-viral (HIV)	Abbott	Marketed
Kaleatra (Ritonavir/Lopinavir)	Anti-viral (HIV)	Abbott	Marketed
Eucreas (Vildagliptin/Metformin HCl)	Diabetes	Novartis	Marketed
Zithromax (Azythromycin)	Antibiotic	Pfizer	Marketed
Orzurdex (Dexamethasone)	Macular edema	Allergan	Marketed
Posaconazole	Anti-fungal	Merck	In development
Anancetrapib	Cardiovascular disease	Merck	In development
Dapivirine, Maraviroc, BMS793, CMPD167	Anti-viral	Particle Sciences	In development

### *Polymer Selection*

Several polymeric materials are currently used for the production of melt-extruded solid dispersions, including nonionic and ionic polymers (96). In most cases, these materials were designed for other pharmaceutical technologies and have been applied to melt extrusion (96). For example, polymethacrylate polymers are commonly used in enteric coatings and vinylpyrrolidones are traditionally used in granulation and compression applications (96). Based on the pH dependent solubility of the polymer, immediate or delayed i.e., enteric release systems can be developed (102). The selection of the polymer strongly influences the release rate of the drug. In most cases, immediate-release systems have been developed and commercialized thus far (102). The most commonly used polymers for melt extrusion are listed in Table 11.

Polymers used in melt extrusion should exhibit thermoplastic characteristics, becoming soft and pliable when heated and hardening when cooled (103). Moreover, they should demonstrate thixotropic behavior, becoming less viscous with increasing shear stress (103). Polymers should also have suitable glass transition ( $T_g$ ) and thermal degradation ( $T_{deg}$ ) temperatures that reportedly range from 50°C to 180°C (102), although extrusion processing temperatures are more commonly in the narrow range from 90°C to 140°C (96). As a general rule, extrusion is performed at temperatures from 20°C to 40°C above the material's  $T_g$  (96). Ideally, the difference between the processing temperature ( $T_g$  plus 20°C to 40°C) and  $T_{deg}$  is large enough to avoid the risks of thermal degradation, though thermal stress within the extruder lasts for only 0.5 min. to 5 min., short enough to prevent degradation of some thermal-sensitive polymers and drugs (102). Polymers with a high solubilization capacity are also preferred if larger amounts of drug need to be

dissolved in the polymer (102). Some basic requirements for high solubilization capacity include lipophilicity, hydrogen bond acceptors or donors, and amide groups (107). Lastly, solubility parameter can be used to predict the miscibility of drug-polymer systems and therefore, their stability over time (108,109). Table 12 lists the basic requirements for polymers used in HME.

Table 11. *Commonly Used Polymers for Melt Extrusion. Adapted from DiNunzio 2012*

Polymer	Tg (°C)	Grades	Comments
Hypromellose	170-180	Methocel E5	Non-thermoplastic API must plasticizer polymer Good nucleation inhibition Difficult to mill extrudate
Vinylpyrrolidone	168	Povidone K30	API must plasticize polymer Potential for hydrogen bonding Hygroscopicity can limit stability Residual peroxides Extrudate mills easily
Vinylpyrrolidone-vinylacetate copolymer	106	Kollidon VA 64	Easily extruded No API plasticization required Hygroscopicity can limit stability More hydrophobic than vinylpyrrolidone Processed around 130°C
Polyethylene glycol, vinyl acetate, vinyl caprolactam graft copolymer	70	Soluplus	Newest polymer for melt extrusion Easily extruded Low Tg can limit stability No compendial status
Polymethacrylates	130	Eudragit L100-55, L100	Not easily extruded without plasticizer Degradation onset is 155°C Ionic polymer soluble above pH 5.5
Hypromellose acetate succinate	120-135	Aqoat L, M, H	Easily extruded Processed at temperatures above 140°C Ionic polymer soluble above pH 5.5 Excellent solubility enhancing polymer Stable to 190°C depending on processing conditions
Amino methacrylate copolymer	56	Eudragit E PO	Processed at about 100°C Degradation onset is above 200°C Low Tg can limit stability

Table 12. *Basic Requirements for Polymers Used in Melt Extrusion. Adapted from Kolter 2010*

Polymer Property	Requirement for HME
Thermoplastic behavior	Deformability is essential upon heating Most polymers also exhibit thixotropic behavior
Glass transition temperature (T <sub>g</sub> )	50°C to 180°C, higher temperatures provide better stability Extrusion temperatures typically range from 90°C to 140°C
Thermal stability (T <sub>deg</sub> )	50°C to 180°C, higher temperatures provide better stability Thermal stress lasts about 0.5 min. to 5.0 min. Extrusion temperatures typically range from 90°C to 140°C
Hygroscopicity	Low hygroscopicity prevents crystallization
Toxicity	No to very low as application amounts are large; the polymer serves as a matrix
Solubilization capacity	High capacity allows large quantities of drug to be dissolved; lipophilicity, hydrogen bonding acceptors or donors, and amide groups improve solubilization capacity
Solubility parameter	Molecularly dispersed systems are more stable

#### *HME Equipment Overview*

Hot melt extrusion equipment consists of an extruder, auxiliary equipment for the extruder, downstream processing equipment, and monitoring devices used to evaluate the extrusion process (101). The extruder is typically composed of a motor, hopper, barrel, screws, and die, as shown in Figure 7. The auxiliary equipment for the extruder consists of a heating and cooling manifold used to heat or cool the barrel, and a conveyer belt equipped with air nozzles that cool the molten material while it is being transported away from the die (104). Downstream processing equipment includes such things as pelletizers and calendering devices (104). A pelletizer, shown in Figure 8, is used to cut long, continuous, solid, cylindrical strands of extrudate into several smaller rod-shaped pieces that can be filled into capsules or milled and blended for tableting (104). Calendering devices are used for directly shaping the extrudate into its final dosage form (Figure 7).

Monitoring devices on the equipment consist of temperature gauges along the barrel and die, a screw speed controller, an extrusion torque monitor, and pressure gauges (99).

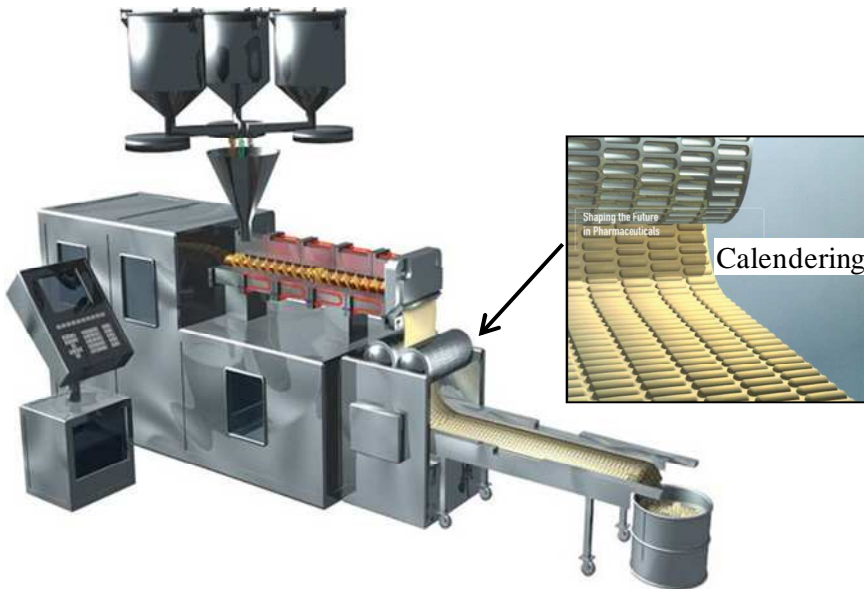


Figure 7. Melt Extrusion Equipment with Downstream Calendaring Device

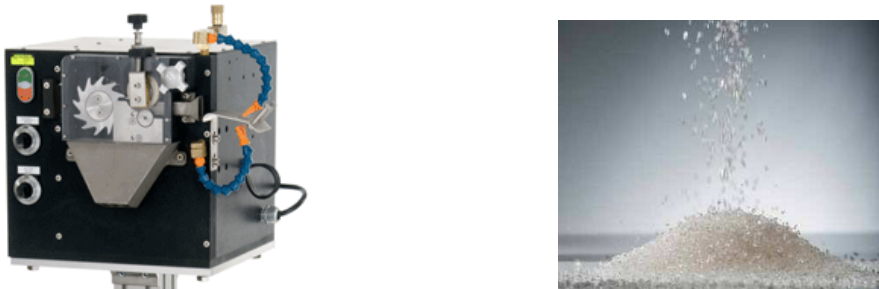


Figure 8. Pelletizer and Strands of Extrudate Cut into Small Pieces

Generally, the extruder consists of one (single) or two (twin) rotating screws inside a stationary cylindrical barrel (Figure 9). A motor, connected to one end of the barrel, continuously rotates the screws. The die, connected to the opposite end of the barrel, determines the shape of the extruded product. Rod dies, for example, produce solid cylindrical strands, where ribbon dies creates flat films or sheets. Pictures of rod and ribbon dies are shown in Figure 10.

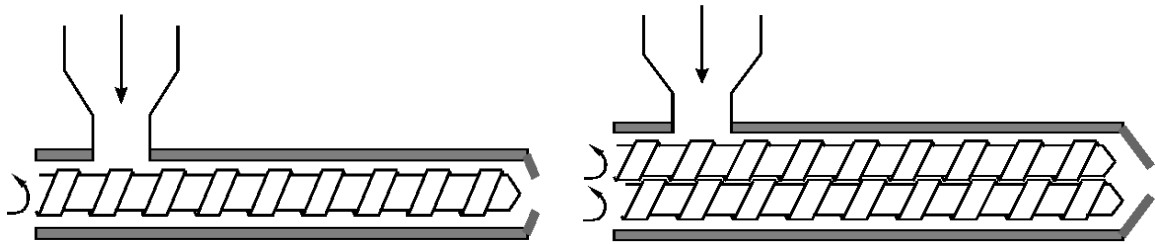


Figure 9. Single Screw (Left) and Twin Screw (Right) Extruders



Figure 10. Examples of Rod (Right) and Ribbon (Left) Dies

The heat required to melt the material is supplied by the combination of the barrel heater and the heat generated by friction as the material is sheared between the rotating screw(s) and the wall of the barrel (110). The space between the screw diameter and the width of the barrel is normally in the range of 0.1 mm to 0.2 mm (110). The extrusion channel is conventionally divided into three sections: solids-conveying or feed, transition or compression, and metering sections, as shown in Figure 11.

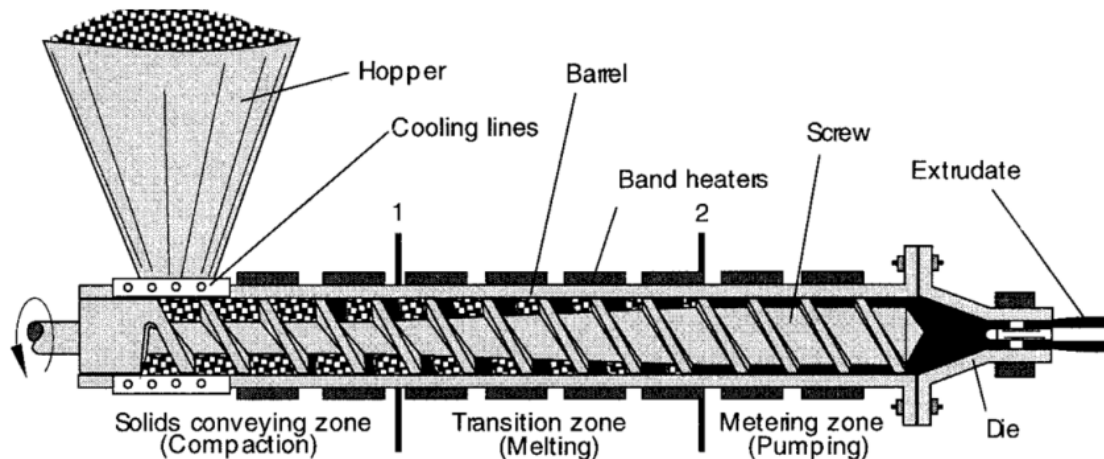


Figure 11. Component Parts of an Extruder

Most commercial extruder barrels and screws are modular, providing a choice of screw elements or interchangeable barrel sections that can alter the configuration of the feed, transition, and metering sections (104). Figure 12 shows individual screw elements and barrel modules that can be assembled into various configurations to perform a sequence of unit operations.

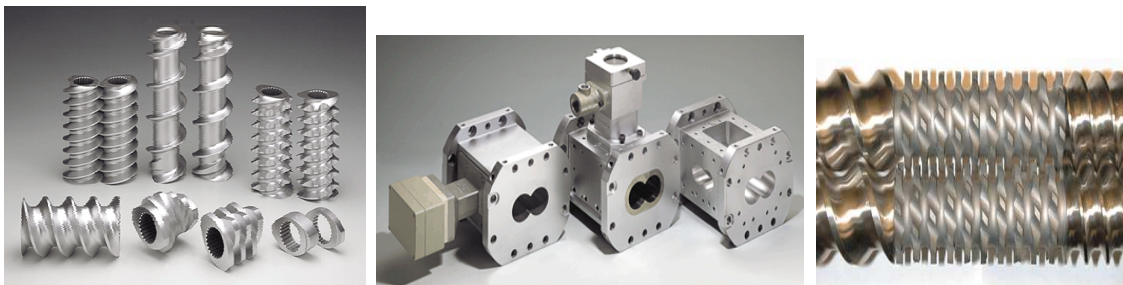


Figure 12. Modular Screw Elements, Barrels, and Assembled Screw Elements

Extruders are defined by the barrel or screw diameter, and length, referred to as the L/D or length divided by diameter ratio (111,112). This ratio is the length of the barrel, from the feed hopper to the die, divided by the inside barrel diameter (111) or the length of the screw divided by the screw diameter (112). Typically, extrusion process lengths range from 24/1 to 50/1 (112). Single screw extruders are generally 36/1 or

shorter and twin screw extruders are generally configured from 60/1 to 100/1 (112). A certain processing length is required for each unit operation (feeding, melting, mixing, pressurizing, etc.) to enable sufficient time for the process to be accomplished (111). Therefore, each unit operation can be assigned to a single barrel module or several barrel modules can be dedicated to one unit operation. Likewise, screw elements are chosen and sequenced along the screw shaft to perform specific unit operations along the process length of the barrels (113). Screw elements can be broadly classified into three functional types: forwarding, mixing, and zoning. Forwarding elements, which are usually flighted, are used to forward material away from feed, vent, and drain openings and to pressurize the die at the discharge end of the extruder (113). Mixing elements are used to perform dispersive or distributive mixing, and zoning elements act as a barrier to separate unit operations (113). Modifying the screw to match the specific geometry to the required process task allows for a sequence of unit operations to take place. For example, combining forwarding screw elements with mixing screw elements allows the extruder to perform mixing and melting in addition to conveying. Figure 12 shows a combination of different screw elements.

#### *HME Process Overview*

The purpose of the screw is to convey the material from the hopper, through the various sections where the polymer achieves its homogeneous melt, and to deliver the melt to the die at a uniform rate (111). The barrel is the surface through which external heat is applied and also provides one of the surfaces for imparting shear to the material (111). The barrel usually has three or more heating zones to raise the barrel and screw to

a desired temperature (111). When the process temperature rises above the set point temperature, either air or liquid cools the barrel (111). Pressure is commonly measured at the end of the barrel and temperature is typically measured between the extruder barrel and die (111). When the material is melted, it flows through a breaker plate, filter, and shaping die, and thereafter is cooled into a solid form (111). The die determines the final shape formed during the extrusion process and is the last heating zone of the extruder (111). The final dimensions of the extrudate may differ from that formed by the die. This is due to downstream processing equipment such as pelletizers (Figure 8) or calendering devices (Figure 7). The theoretical approach to describing the melt extrusion process is generally to divide the process into four sections: feeding, conveying, extruding, and downstream processing. The following paragraphs summarize the four sections of the melt extrusion process.

### *Material Feeding*

During the HME process, different zones of the barrel are preset to specific temperatures before the process begins (106). The starting material, known as feedstock, typically consists of a powder blend containing the thermoplastic polymer, drug substance, and other processing aids such as plasticizers (106). The feedstock is fed from a hopper directly into the feed zone. In the feed zone, the screw flights are deepest or have the greatest pitch (104). The geometry of an extruder screw is shown in Figure 13.

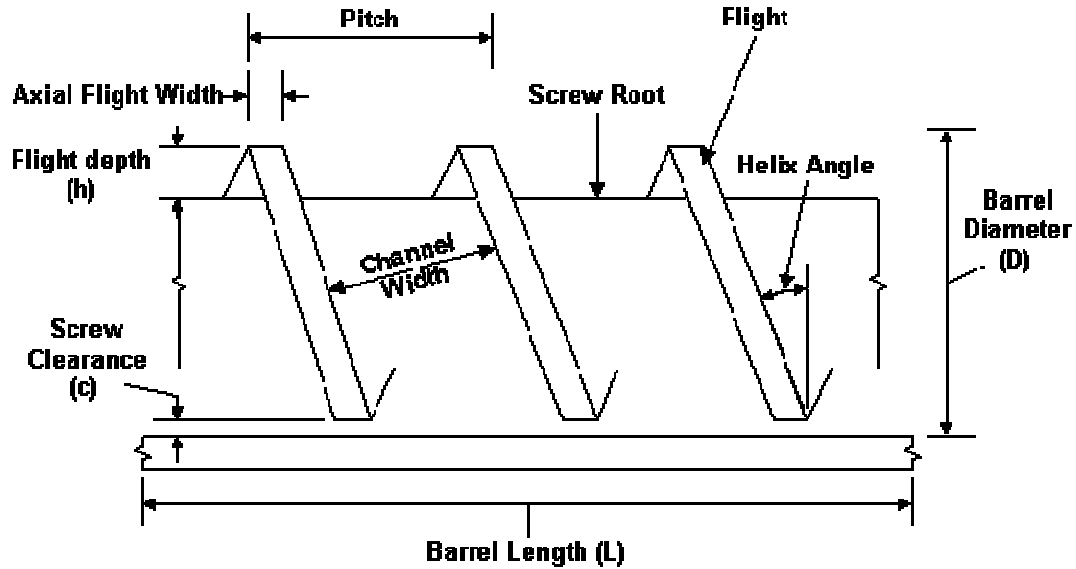


Figure 13. Geometry of an Extruder Screw

For single screw extruders, the powder-conveying mechanism depends on the frictional relationship between the raw materials and the extruder surfaces: materials must adhere to the barrel wall and must not adhere to the screw (114). Most single screw extruders are flood-fed; that is, the raw materials are filled into the hopper and as the screw rotates, the volume of material conveyed is directly related to the rotational speed, pitch, and free volume of the screw (114). An increase in screw speed results in an increase in the volume of material displaced (114). Therefore, the screw speed determines the output of the extruder as long as the screw is kept full in the feed zone (114). Thus, the conveying characteristics of a single screw extruder are directly related to the raw material properties such as particle size, particle size distribution, particle shape, bulk density, particle-particle interactions, etc. (114). Therefore, all raw materials in a blend should be similar in particle size and density; materials that are sticky or slippery will not feed well in a single screw extruder (114). Cohesive materials or very

fine powders tend to form solid bridges at the bottom of the hopper, resulting in erratic powder flow into the extruder (106).

In contrast, twin screw extruders are insensitive to raw material properties since their powder conveying mechanism does not depend on the frictional relationship between the raw materials and the extruder surfaces; raw materials which are sticky, slippery, or have different particles sizes and particle densities can easily be fed into a twin screw extruder (115). Furthermore, twin screw extruders are designed to be starve-fed; that is, the extruder screws are not filled in the feed zone (116). Since the screw is not filled, the pressure remains low while the material is being heated (115). Starve-fed extruders are equipped with either volumetric or gravimetric feeders that control the amount of material that is delivered to the extruder per unit time (115). This allows the extruder to operate at various outputs for a given screw speed, which expands the processing capabilities of the extruder (115). For both single and twin screw extruders, once the material has been introduced into the extruder through the feed hopper, it begins to transform from a solid to a partial melt as it picks up heat from conduction and mechanical friction.

#### *Conveying, Melting and Mixing*

Solids are transported to the decreasing space of the compression section of the screw where melting takes place. Extruders use two forms of energy transfer to efficiently melt and plasticize materials: thermal and mechanical energy (114). Thermal energy is typically supplied from electrical heaters that cause a polymer film to form on the inner barrel surface because of heat conduction through the barrel (114). This

melting mechanism is directly influenced by thermal energy input (114). The rotating screw flights displace the melt film, mixing the molten material back into the bulk powder (114). The temperature of the transition section is normally set at 20°C to 40°C above the glass transition temperature of the amorphous polymers or the melting point of semi-crystalline polymers (102). Thermodynamic properties of the raw materials, particle size, particle shape, the amount of material filled in the extruder screw, and the thermal gradient between the material and barrel surface influence the process (102,114). The thermal contribution to melting on a unit mass basis (Eq. 2) can be quantified as follows (114):

$$\text{Specific thermal energy} \left( \frac{kWh}{kg} \right) = \frac{\text{Thermal energy input} \left( \frac{kWh}{hr} \right)}{\text{Mass flow} \left( \frac{kg}{hr} \right)} \quad \text{Eq. 2}$$

Screw extruders are designed to convert electrical energy from the drive motor into mechanical energy via viscous dissipation (114). Viscous dissipation describes the rate at which mechanical energy is converted into heat in a viscous fluid per unit volume (114). Materials begin to melt as solids are confined to decreased clearances (twin screw) or decreased free volumes (single screw) (114). The decreasing channel volume compresses the material as it moves through the decreasing space of the melting zone (111). Compression is developed by decreasing the screws thread pitch but maintaining a constant flight depth or by decreasing flight depth while maintaining a constant thread pitch (114). Both methods result in increased pressure as the material moves along the barrel. The mechanical contribution to melting is directly influenced by mechanical

energy input from the drive motor and can be quantified on a unit mass basis (Eq. 3) as follows (114):

$$\text{Specific mechanical energy} \left( \frac{kWh}{kg} \right) = \frac{\text{Consumed motor power} \left( \frac{kWh}{hr} \right)}{\text{Mass flow} \left( \frac{kg}{hr} \right)} \quad \text{Eq. 3}$$

Thermodynamic properties as well as physical properties of the raw materials are key contributors to the efficiency of the extruder in melting via viscous dissipation (114). Materials with low melt viscosities such as lubricants and plasticizers can adversely affect the introduction of mechanical energy and thus the melting process (114). Most materials require both thermal and mechanical energy to achieve a complete melt. Most thermoplastic materials have specific mechanical energy input ranges between 0.1 and 0.4 kWh/kg (114). Specific thermal energy input values are approximately an order of magnitude less than specific mechanical energy input (114).

Once the feedstock is transported through the solids-conveying zone and is preheated, there is sufficient energy available for melting (114). Material can be pumped through a pressurized mixing element on the screw or screw elements can be designed to melt and mix simultaneously (114). Generally, there are two types of mixing for powders: dispersive and distributive. Dispersive mixing refers to mixing by the breakdown of solids; the shear stress that is produced as a result of the velocity gradient of rotating screw(s) and a stationary barrel is responsible for the size and size distribution of a constituent (114). The continued application of shear stress within the extruder screw produces a subsequent decrease in particle size, also referred to as morphology

development (114). The resulting morphology is responsible for producing a certain dissolution profile and subsequent bioavailability (114).

The magnitude of the applied stress is a function of the shear rate and the melt viscosity (Eq. 4) (114):

$$\text{Shear stress (kPa)} = \text{shear rate (sec}^{-1}\text{)} \times \text{viscosity (Pa sec)} \quad \text{Eq. 4}$$

Therefore, it is more difficult to achieve high shear stress with low melt viscosity materials than with high melt viscosity materials. Furthermore, shear rate, which describes the velocity gradient between the screw and the barrel wall, is a function of the screw's outside diameter, screw speed, and gap (Eq. 5) (114):

$$\text{Shear rate (sec}^{-1}\text{)} = \left[ \frac{\pi \times \text{screw diameter (mm)} \times \text{screw speed (rpm)}}{\text{gap (mm)} \times 60 \text{ (sec/min)}} \right] \quad \text{Eq. 5}$$

where the gap is the distance between the screw and the barrel or between the two screws in twin screw extruders. From the equations, it is apparent that material fed into the primary feed section of the extruder will experience the highest degree of dispersive mixing. That is, the viscosity is greatest in the feed section, resulting in high shear stress. In practice, shear sensitive compounds can be fed downstream into the already molten, and therefore less viscous, polymer to avoid the high stresses experienced during the melting process. Shear rates in screw extruders typically range from 10 to 10,000 sec<sup>-1</sup> (114).

Extrusion parameters that influence shear stress are used to control dispersive mixing. These parameters include: screw design, screw speed, feed rate, and barrel temperature. The configuration of the screw determines how much of the material will

experience high shear stress. The screw speed is directly proportional to shear rate; a linear effect is produced when the extruder is flood fed and a nonlinear effect is produced when the extruder is starve fed because, for starve fed extruders, increasing the screw speed at a constant feed rate will also produce a decrease in the filled screw volume (114). Feed rate is directly proportional to shear rate for flood fed extruders because an increase in feed rate corresponds to an increase in screw speed (114). For starve fed extruders, however, an increase in feed rate results in an increase in filled screw volume for a constant screw speed, resulting in a decrease in shear rate (114). As the barrel temperature is increased, the melt viscosity decreases, thereby reducing the shear stress (114).

Dispersive mixing is responsible for the size and size distribution of a constituent, while distributive mixing refers to the reorganization of components toward uniformity (114). The interchange of multiple screw channels (i.e., discrete volumes), which can split and recombine in a twin screw extruder, or interruptions in the flow channel, which provide reorientation in a single screw extruder, contribute to the content uniformity of a particular constituent (114). Single screw extruders contain only one screw channel, which limits their flexibility for improving mixing; however, twin screw extruders contain multiple screw channels that can be modified to promote distributive mixing (114). An illustration of dispersive and distributive mixing is shown in Figure 14.

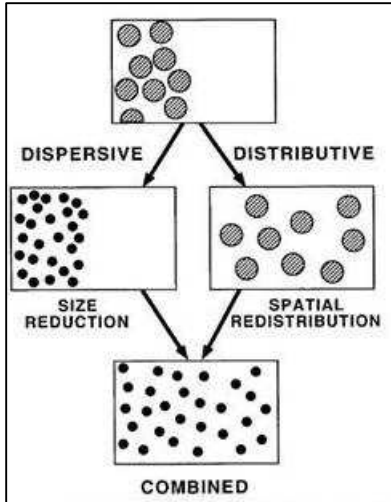


Figure 14. Illustration of Dispersive and Distributive Mixing

### *Extruding*

The in-process material reaches the metering zone in the form of a homogeneous melt suitable for extrusion. For extrudate with uniform thickness, flow must be consistent and without stagnant zones right up to the die entrance. The function of the metering zone is to reduce pulsating flow and ensure a uniform delivery rate through the die cavity (104). If the melted material cannot be sufficiently dampened by the metering section, a gear pump can be added to the end of the extruder to reduce pressure variations (104). The last heating zone of the extruder is located at the die. The die determines the final shape of the extrudate formed during the extrusion process. Examples include rod and ribbon dies (Figure 10) for the production of solid cylinders or flat sheets, respectively. The final dimensions of the extrudate however, may differ from that formed by the die due to downstream processing.

### *Downstream Processing*

Pelletization is a downstream operation for a melt extrusion process. Developed in the 1950s, pelletization is the process of cutting long strands of extrudate into pellets (117). As the extrudate exits the die in a continuous strand, it is cooled by air and fed into the feed rollers on the pelletizer, and cut to length by rotating cutting heads (117) (Figure 8). The diameter of the pellet is controlled by the diameter of the die orifice and the speed at which the rollers are pulling the strand; nearly all extrudate will be drawn down in diameter upon exiting the die (117). The pellets, typically 3mm in size or less, can then be further processed, e.g., milled, tableted, or encapsulated to obtain a final dosage form. Alternatively, extrudate can be directly shaped into the final dosage form by using a calendering device (Figure 7, above).

### *Manufacturability*

Successful production of a melt extruded solid dispersion is a function of formulation and process, and each has a key role with substantial interdependence (96). A typical formulation may contain a number of different materials that have a specific and necessary role in the formulation (96). At minimum, it consists of drug substance and stabilizing polymer; however, plasticizers, melt solubilizers, and glidants may be necessary to assist processing (96). Likewise, adjustments to temperature, screw speed and feed rate during production may alter the fluid dynamics of the process (96). A brief review of the most relevant formulation and process parameters follows.

### *Melt Residence Time*

Melt residence time plays a critical role in product performance. Melt residence time is defined as the amount of time the material exists in the molten state (96). As material enters the extruder, it displays a specific set of solid-state characteristics and has a defined temperature that is generally that of the ambient environment (96). During conveying, mechanical energy is imparted to the material along with conductive heat transfer from the barrel walls (96). This energy, 80-90% of which originates from the energy provided by the screws, increases the temperature of the material (96). Somewhere along the length of the barrel, the material transitions from solid to melt, resulting in peak observed shear and a well-delineated change of flow characteristics (96). At this point, the melt residence time begins. It is also at this time that the polymer begins to display properties characteristic of a solvent because of its low viscosity and greater molecular mobility (96). As the molten dissolution process begins, drug substance converts from crystalline to amorphous form, defining the time zero dissolution process and signaling the point at which materials begin to become more susceptible to degradation because of the absence of crystalline morphology (96). Melt residence time plays a particularly important role in the production of high-melting-point compounds and heat-sensitive compounds. In these cases, maintaining typical melt residence times, which are variable but range from 0.5 to 5 minutes, is critical for inhibiting certain decomposition processes (96). Reducing barrel temperature, along with appropriate selection of screw design and screw speed, can increase heat transfer rates from the system and help to lower localized temperatures within the process (96).

*Process Variables and Controls*

Instrumentation used to control the melt extrusion process provides insight into the performance of the formulation. The most relevant input variables of an HME process are feed rate, screw speed, and barrel temperature (102). These parameters particularly influence the mechanical energy, residence time, and temperature of the material (96). Key measurements of torque, temperature, and pressure provide information on the flow behavior of the material within the extruder (102). Torque values indicate the amount of energy being applied to the material during processing (96). Figure 15 illustrates the effect of varying feed rate, screw speed, and temperature on residence time and torque (102). It can be seen that increases in feed rate or screw speed reduce residence time, but increase extrusion torque. Torque can be reduced by increasing temperature, which reduces the melt viscosity of the polymer; however, higher processing temperatures may result in thermal degradation of the drug and/or polymer. More often, formulations exhibiting high torque values and therefore, high melt viscosities, and/or thermal degradation required the addition of a plasticizer or thermal lubricant (96,102).

HME Process Variables	Residence Time	Torque
Feed rate ↑	↓	↑
Screw speed ↑	↓	↑
Temperature ↑	↔	↓

Figure 15. Effect of Varying Feed Rate, Screw Speed, and Temperature on Residence Time and Torque. Adapted from Kolter 2010

### *Plasticizers as Thermal Processing Aids*

Melt viscosity plays a key role in determining the extrusion torque and pressure during manufacturing. Particularly with high molecular weight polymers, the melt viscosity generates excessive load on the extruder drive motor and precludes processing without the incorporation of additives to facilitate molten flow (96). The viscosity of the system is also critical for solubilization because lower melt viscosities increase diffusivity and dissolution rate of solid drug particles in the molten polymer (96). Traditionally, the viscosity of a system is lowered by adding plasticizers or other low molecular weight compounds that improve the workability and flexibility of the polymer by weakening the intermolecular forces between the polymer chains (118). In amorphous polymers, the  $T_g$  and relaxation behavior associated with it are very sensitive to the addition of small amounts of plasticizers (119). As plasticizer is added, the relaxation is shifted to a lower temperature at constant frequency (119). The explanation is that because the plasticizer molecules are small and mobile, they act to effectively expand the available free volume for segmental motion and hence speed it up (119). Some actives may also have a plasticizing effect on certain polymers. Plasticizing effects result in a reduction in elastic modulus, tensile strength, melt viscosity, and  $T_g$  (118). The toughness and flexibility of the polymer are improved and extrusion becomes possible because of its lower melt viscosity (118,120).

Reduced  $T_g$  values allow for lower thermal processing temperatures that can prevent degradation of sensitive actives (102). Lowering  $T_g$  also widens the extrusion processing range by increasing the difference between the  $T_g$  and degradation temperature ( $T_{deg}$ ) of the polymer (102). Generally, extrusion processes are run at

temperatures 20°C to 40°C above the T<sub>g</sub> and extrusion temperatures range from 90°C to 140°C (96). In a study conducted by DiNunzio et al., compositions containing a 1:2 mixture of ITZ:Eudragit L100-55 could not be effectively processed by melt extrusion due to high viscosity and decomposition of the polymers (121). Triethyl citrate (TEC) was incorporated into the melt-extruded compositions at 20% (by dry polymer weight) as a processing aid (121). Extrusion was successful; however, the T<sub>g</sub> of the system decreased from 101°C to 54°C from the addition of plasticizer and physical instability was observed in the extrudate over time (121). Miller et al. also incorporated 20% TEC into hypromellose phthalate (HPMCP) HP-55, and Eudragit L100-55/Carbopol 974P carrier systems to enable HME processing below the temperature at which thermal degradation of the polymers begins, but the physical stability of the extrudate was not reported (122). The use of plasticizers in thermal processing can significantly affect the physical stability of an amorphous solid dispersion through increased molecular mobility. In these formulations, reducing T<sub>g</sub> and promoting molecular mobility of the drug-polymer system can increase the drug's ability to separate into drug-rich domains that more readily crystallize over time (90,123,124). Crystallization during storage slows dissolution and can ultimately preclude the marketability of the formulation.

### **Stability**

One critical attribute for commercialization of amorphous solid dispersions is stability. Among various factors, polymer selection is a key consideration for developing stable dispersions (13). Once solid dispersions are produced, ideally the polymers inhibit crystallization of: 1) the amorphous solid API during dissolution; 2) the dissolved API in

a supersaturated solution; and 3) the amorphous API during storage (52,125). Stable solid dispersions, therefore, should have solid-state and supersaturated solution stability throughout the products shelf life (95).

Studies have suggested that the capacity of a polymer to inhibit crystallization often depends on interactions between the API and polymer (89,90,67). Alonzo et al. speculated that polymers inhibit crystallization of amorphous APIs during dissolution by interacting with the API's surface to delay surface crystallization (52,126). They also theorized that, after the amorphous API dissolves, polymers prevent crystallization from solution by inhibiting nucleation (52). For example, prior studies have shown both polyvinylpyrrolidone (PVP) and cellulosic polymers are effective at delaying crystallization of amorphous solids during dissolution, but PVP is much less effective than cellulosic polymers at maintaining supersaturation once an amorphous solid is in solution (89).

The stabilizing effects of polymers during storage have been attributed by some to API-polymer interactions (127,128) and by others to their ability to increase the glass transition temperature ( $T_g$ ) of the combined dispersed system (127,129). The  $T_g$  is considered to be a key parameter for stabilization because it delineates a temperature range between high and low molecular mobility (67,68). It follows that, by increasing the  $T_g$  of the system well-above storage temperatures, the molecular mobility of the drug would be reduced, which would lessen its ability to separate into drug-rich domains that would more readily crystallize over time (90,123,124). Polymers, therefore, with a high  $T_g$  relative to the drug, serve as anti-plasticizers in compatible API-polymer systems (67).

Moisture can be a factor as well. Many polymers have a relatively high T<sub>g</sub> when dry, but some exhibit marked decreases in T<sub>g</sub> with increasing water content (130). Water has a T<sub>g</sub> of about -138°C, so it can reduce the T<sub>g</sub> of amorphous systems substantially (95). Fitzpatrick et al. reported that PVP absorbed significant amounts of water when exposed to increasing levels of humidity (131). The absorbed water consequently depressed the T<sub>g</sub> of PVP from about 170°C to 34°C at 60% relative humidity (RH). This plasticizing effect induced a low-temperature glass-to-rubber transition. In contrast, the T<sub>g</sub> of hydroxypropylmethylcellulose acetate succinate (HPMCAS) only decreased from about 120°C to 95°C at 60% RH (130). Babcock et al. suggested that a dispersion with sufficiently low mobility to achieve acceptable stability should have a T<sub>g</sub> of 50°C or greater at 50% RH (130). Yet, Hancock et al.'s "aging experiments" demonstrated that amorphous solids can experience significant molecular mobility as low as 50°C below their T<sub>g</sub> (132). Accordingly, the general rule has become that the T<sub>g</sub> of a dispersed system should be at least 50°C above anticipated storage temperatures.

The T<sub>g</sub> for a combination of two compatible amorphous materials can be estimated using Gordon-Taylor-type equations (133). Based on these equations it can be inferred that, to increase the T<sub>g</sub> of a combined drug-polymer system, a significant portion of the dispersion should comprise a polymer having a relatively high T<sub>g</sub>. What is not explicitly accounted for in the equations, however, is the dependence of a polymer's T<sub>g</sub> on humidity. Babcock et al. studied the effect of humidity on a polymer's T<sub>g</sub> and observed considerable differences in the affinity for water among six common pharmaceutical polymers (130). Similar results were reported in solid dispersions containing felodipine, polymer, and water (123). Konno et al. found both polymer type

and amount influenced moisture absorption, which increased API nucleation rates (123). However, no correlations could be made between nucleation rates and the T<sub>g</sub> of the system (123).

### *Hygroscopicity of the Polymer*

Absorbed moisture can destabilize amorphous systems by lowering the T<sub>g</sub> of the polymer, weakening the interactions between the drug and polymer, and lowering the solubility or miscibility of the drug in the polymer (95). Several authors have evaluated the effect of moisture on drug solubility. Rumondor et al. showed that a small amount of moisture could significantly lower the solubility of felodipine in PVP (134). Similarly, another study showed that water could irreversibly disrupt the favorable interactions between a drug and a polymer, resulting in phase separation that eventually led to crystallization (135). Rumondor et al. developed a modified Flory-Huggins equation to estimate the effect of moisture on the interaction parameters of a water-drug-polymer ternary system (134). Their experiments showed that the ingress of water could weaken interactions between a hydrophobic drug and hydrophilic polymer, resulting in drug-rich phases that induce crystallization (134). In another study comparing different polymers, the authors concluded that the use of a hydrophobic polymer e.g., HPMCAS can be beneficial over more hydrophilic polymers e.g., PVPVA or PVP to achieve better stability (136). Friesen et al. also showed that a hydrophobic polymer provided better supersaturation during dissolution due to the formation of aggregated structures by HPMCAS (65).

Lastly, although it is well recognized that amorphous materials are more hygroscopic than their crystalline forms, Konno et al. showed that amorphous felodipine does not absorb large quantities of water on exposure to high relative humidities due to the hydrophobicity of the drug (123). However, small amounts of absorbed moisture resulted in significant increases in nucleation rate (123). A similar tendency for increased nucleation rates in the presence of moisture has been observed for another hydrophobic drug, indomethacin (137). Forming a solid dispersion of felodipine with three different polymers reduced nucleation rates relative to the drug alone (123). Each polymer had a similar inhibitory ability in the absence of moisture (67). However, in the presence of moisture, the ability of different polymers to inhibit crystallization of felodipine from solid dispersions varied considerably (123). This suggests that there is competing effect between the polymer that acts as a crystallization inhibitor and water that enhances crystallization (123).

In the presence of moisture, three pure polymers showed large variations in the amount of moisture absorbed, with PVP being the most hygroscopic, followed by HPMC and HPMCAS (123). Likewise, solid dispersions of felodipine with PVP absorbed more moisture than those containing felodipine with HPMC or HPMCAS (123). In spite of the increased hygroscopicity of the solid dispersions, nucleation rates of felodipine still were reduced relative to the drug alone (123). In addition, the dependence of nucleation rate on moisture content became less sensitive as the polymer concentration increased (0-25%) (123). For a given polymer concentration, the variation in the stabilizing ability of different polymers was attributed to their different tendencies to absorb moisture (123).

Specifically, polymers with low hygroscopicity provided better stability for amorphous systems.

### *Drug and Polymer Interactions*

In addition to low hygroscopicity, polymers with ionizable functional groups have shown improvements in the stability of amorphous systems. Enteric polymers, for example, contain carboxylic acid groups that ionize at higher pH values. Their effectiveness in solid dispersions has been attributed to two major mechanisms (96). Firstly, enteric solid dispersions typically dissolve at pH values above 5.0, depending on the polymer selected (96). This allows for targeted dissolution and supersaturation in the upper small intestine, which is the primary site of absorption for many compounds (96). It also avoids premature gastric supersaturation and potential precipitation, which can limit the bioavailability benefits of the solid dispersion (96). Secondly, the partially ionized nature of the enteric polymer after dissolution may stabilize supersaturated solutions through drug-polymer interactions (96,138,139). Several studies have attributed this behavior to a combination of steric hindrance and hydrophobic interactions (96,138,139). The greater stabilization efficiency of CAP and HPMCAS were reportedly due to the partial ionization of the polymers in solution, which slowed growth rates of drug-polymer aggregates in solution (96).

## CHAPTER 2

### PROBLEM AND OBJECTIVES

#### Statement of the Problem

Amorphous APIs are inherently metastable and any amorphous-crystalline phase transitions during dissolution and storage effectively negate their solubility advantages. Generally, the ability of a polymer to inhibit crystallization depends on interactions between the drug and polymer, and the moisture content of the solid dispersion caused by hygroscopicity of the component polymer. However, the physicochemical properties of the polymer necessary to inhibit crystallization from an amorphous state are not fully understood. The ability of polyvinyl acetate phthalate (PVAP) to inhibit crystallization of amorphous solid dispersions of itraconazole has not been explored in the literature. PVAP is a pH-dependent polymer traditionally used for enteric film coating and, as such, it may be capable of stabilizing supersaturated solutions above pH 5 through drug-polymer interactions. Furthermore, films produced from PVAP reportedly had low water vapor permeability so it may provide a stability advantage during storage over enteric polymers previously used to produce solid dispersions. While some physicochemical properties of PVAP make it a good candidate for use in solid dispersions, its use is hampered by poor processability via the most desirable method, melt extrusion; learning how to manipulate its melt extrusion processing characteristics while maintaining its

desirable properties could lead to successful formulations of amorphous solid dispersions for drug delivery.

### **Overall Objective**

The overall objective of this study is to investigate the ability of polyvinyl acetate phthalate (PVAP) to inhibit crystallization of amorphous solid dispersions of itraconazole.

### **Supporting Objectives**

1. Characterize the thermal and rheological properties of PVAP to assess its suitability for use in melt extrusion
  - a. Determine the glass transition temperature, melt viscosity and thermal decomposition temperature of PVAP
2. Determine the water affinity of PVAP to predict its suitability in amorphous solid dispersions
  - a. Measure the moisture content of PVAP as a function of various relative humidities
3. Improve the melt extrusion processability of PVAP by incorporating plasticizers or other thermal processing aids
  - a. Calculate the solubility parameter of PVAP and compare it to other excipients
  - b. Evaluate melt viscosity, glass transition temperature, and moisture content for the most promising excipients
  - c. Assess miscibility of binary polymer mixtures containing PVAP

- d. Evaluate the extrudability of binary polymer mixtures containing PVAP
  - e. Analyze the PVAP content in the melt extruded blends
4. Incorporate itraconazole into the binary polymer mixture to produce solid dispersions using melt extrusion technology
- a. Assess the miscibility of the drug in the polymer system
  - b. Evaluate the extrudability of the ternary mixtures
  - c. Analyze the itraconazole content in the melt extruded blends
  - d. Determine the physical state of itraconazole in the solid dispersions
  - e. Evaluate drug release from the solid dispersions containing PVAP
  - f. Evaluate the physical stability of the solid dispersions containing PVAP

## CHAPTER 3

### MATERIALS AND METHODS

#### Materials

##### Polyvinyl Acetate Phthalate (PVAP)

PVAP (Phthalavin 2138 clear) was provided by Colorcon, Inc., Harleysville, PA, USA. The USP34-NF 29 describes polyvinyl acetate phthalate (PVAP) as a reaction product of phthalic anhydride and a partially hydrolyzed polyvinyl acetate (19). The chemical repeat units of PVAP are shown in Figure 16.

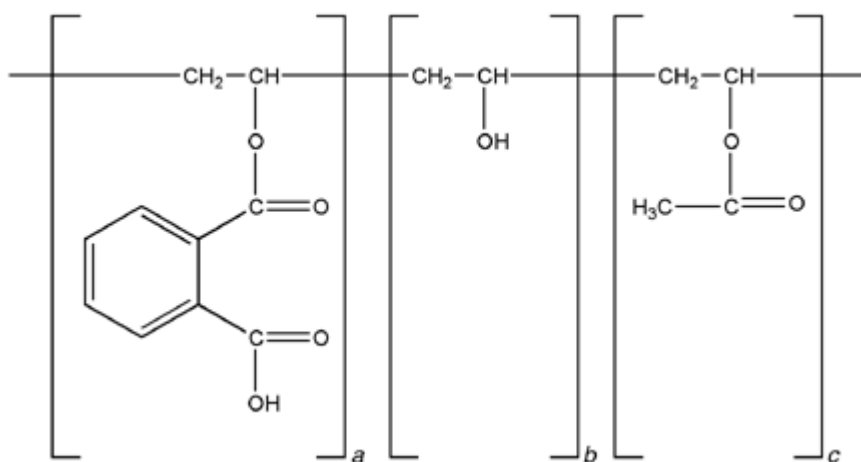


Figure 16. Chemical Repeat Units of PVAP

Similar to other enteric polymers, PVAP is practically insoluble in water and acidic solutions, but soluble in buffered solutions with a pH above 5 (140). In pharmaceutical applications, PVAP is primarily used as an enteric film coating applied to oral drug products (140). Films produced from PVAP have been shown to be much less

permeable to water vapor than those prepared from other enteric polymers such as cellulose acetate phthalate (CAP) and hydroxypropylmethylcellulose phthalate (HPMCP) (141). The low permeability of PVAP to water vapor may provide a stability advantage over enteric polymers previously used to produce solid dispersions (142).

### Salts

Phosphorous pentoxide and potassium acetate salts were of analytical grade and purchased from Sigma-Aldrich Co., St. Louis, MO, USA.

### Vinylpyrrolidone Vinyl Acetate (PVPVA)

PVPVA (Kollidon VA 64 or Copovidone) was provided by BASF SE, Ludwigshafen, Germany. Vinylpyrrolidone is a hydrophilic, water-soluble monomer where vinyl acetate is lipophilic and water-insoluble. The polymer is freely water soluble because of the ratio of the two monomers: 6 parts vinylpyrrolidone and 4 parts vinyl acetate. The chemical repeat units of PVPVA are shown in Figure 17.

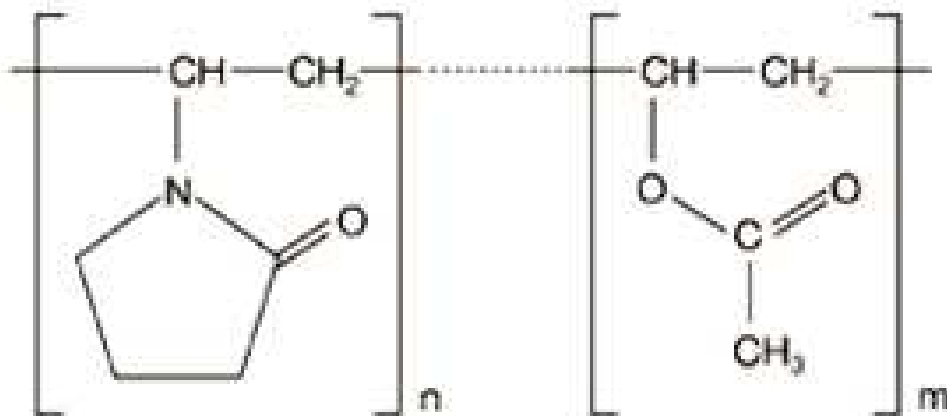


Figure 17. Chemical Repeat Units of PVPVA

In pharmaceutical applications, PVPVA is commonly used as a binder in the production of granules and tablets by wet granulation, and as a dry binder for direct compression. PVPVA has also been used as a secondary film-former in tablet coatings. PVPVA is easily extruded but the hygroscopicity of the polymer hinders its stability and therefore, limits its commercial use.

### **Itraconazole (ITZ)**

Itraconazole was purchased from Hawkins Chemical, Minneapolis, MN, USA. Itraconazole and other azole antifungal compounds such as ketoconazole and posaconazole exhibit poor solubility (96). These weak bases also have pH-dependent solubilities that present further challenges to designing a highly bioavailable drug product (96). For example, compounds similar to itraconazole ( $pK_a = 3.7$ ) show a marked reduction in solubility upon entry into neutral media, creating the need for gastric absorption or supersaturation in the intestine to enhance bioavailability (143). While conventional formulation technologies have been applied to ketoconazole drug products with sufficient exposure levels, itraconazole was the first commercially marketed amorphous solid dispersion to enhance oral bioavailability (96). Marketed as Sporanox<sup>®</sup>, the dispersion is prepared using fluid-bed technology and an organic solvent drug layering process of itraconazole and hypromellose onto sugar spheres (96,144). Although able to provide improved oral bioavailability, the product still showed variable absorption and substantial food effect that was particularly apparent in the presence of acidic beverages e.g., cola (145). Numerous attempts to improve oral bioavailability were made through the production of various manufacturing systems, including melt-

extruded dispersions (96). Attempts using melt extrusion to prepare nonionic solid dispersions with PVPVA and Eudragit E PO as carriers were successful at rendering an amorphous form; however, they failed to provide substantial bioavailability (146,147,148). Subsequent studies by Miller et al. demonstrated that the most effective delivery strategy for weakly basic compounds was to target release at the upper small intestine through the production of enteric solid dispersions (122,149). In their trials, and summarized in Table 13, increases in AUC and  $C_{max}$  were reported for enteric dispersions compared to conventional nonionic formulations in rat models (149).

Table 13. *Bioavailability of Itraconazole Solid Dispersions in Rat Models. Adapted from Miller 2008*

Formulation	Polymer	$C_{max}$ (ng/ml)	$T_{max}$ (h)	AUC (ng·h/ml)
Methocel E50	Nonionic	732 ± 187	4.9 ± 2.2	6,195 ± 1,134
Eudragit L100-55	Ionic	630 ± 695	9.9 ± 9.7	7,335 ± 10,224
Eudragit L100-55 plus 20% Carbopol	Ionic	1,198 ± 584	4.4 ± 1.6	11,107 ± 3,579
Eudragit L100-55 plus 40% Carbopol	Ionic	663 ± 186	5.6 ± 0.5	5,830 ± 1,943

Itraconazole was chosen as a model drug because of its low solubility and because it is more soluble in the low pH of the stomach (4 µg/ml) than the more neutral pH of the intestines (1 ng/ml) (142,150). Pairing itraconazole with an enteric polymer, PVAP, may reduce precipitation by delaying dissolution. Itraconazole is characterized as a poorly soluble, weak base, highly lipophilic (log P = 6.2) and a BCS Class II drug (150). It is available commercially in three forms: as drug layered multiparticulates, as a cyclodextrin-complexed oral solution, and as a solution for IV infusion (151). The chemical structure of itraconazole is shown in Figure 18.

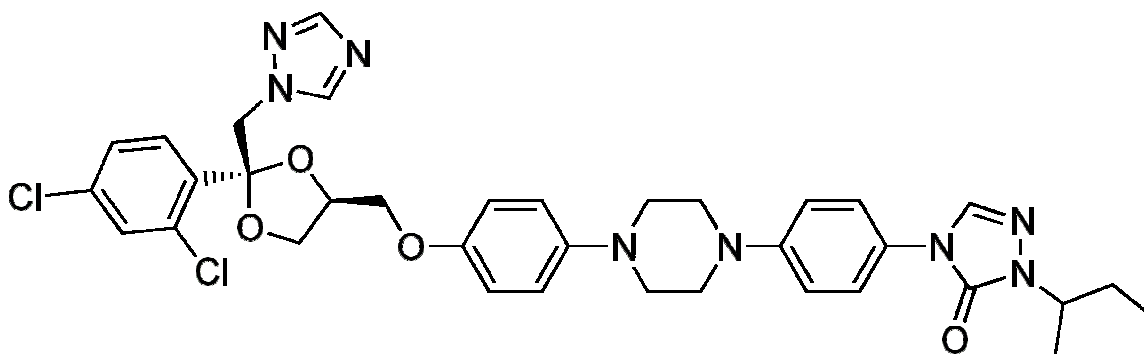


Figure 18. Chemical Structure of Itraconazole

### *Food Effect in BCS Class II Drugs*

Coadministration of oral dosage forms with meals can result in one of three scenarios: 1) the extent of absorption decreases (negative food effect); 2) the extent of absorption increases (positive food effect); and 3) no substantial change in the extent of absorption (152). Fleisher et al. suggested the extent of absorption of a poorly water-soluble, highly permeable BCS 2 drug is most likely increased, while it remains unchanged for highly water-soluble and permeable BCS 1 drugs (153). The same trend was observed by Gu et al. who evaluated the effect of food intake on the extent of absorption by analyzing clinical data on 90 marketed drug products (154). More than 70% of BCS 2 or BCS 4 drugs exhibited a positive food effect as indicated by a significant increase in the AUC in the fed state compared to the fasted state (154). The positive food effect can be ascribed primarily to several physiological changes that increase drug solubility and dissolution. Some of these changes include: 1) delayed gastric emptying that increases the time available for drug dissolution (155); 2) substantial rise in gastric and intestinal fluid volume that offers the potential for increased dissolution rates (156); and 3) release of bile from the gallbladder into the duodenum where its components (bile salts, cholesterol, and phospholipids) can solubilize dietary

lipids into mixed micelles (157). Mixed micelles have the ability to incorporate lipophilic drug molecules and increase drug solubility (158). Bile salts can also enhance the dissolution rate of poorly water-soluble drugs by improving wetting (158). In the case of weakly basic drugs such as itraconazole, variations in GI pH due to food intake can significantly increase or decrease drug solubility (2). In healthy subjects, the gastric pH in the fasted state is typically 1-3 but may temporarily increase to 4-7 after a meal (159,158). The extent of ionization of a weakly basic drug will be reduced due to the rising gastric pH, resulting in poor dissolution and/or potential precipitation of already dissolved drug molecules (2). The sensitivity to GI changes caused by food intake is often associated with unpredictable oral bioavailability (2). The pharmacokinetics of itraconazole were studied in 6 healthy male volunteers who received a single 100 mg dose of itraconazole with and without a full meal (2). In the study, only itraconazole plasma concentrations were measured (not metabolites) and the higher concentration of drug observed in fed volunteers is shown in Table 14 (2). Food effects may be reduced or eliminated by selection of an appropriate formulation design, e.g., solid dispersion-based drug delivery systems (160). The extent of oral bioavailability is affected not only by drug characteristics, e.g., solubility and GI permeability, but by a drug molecule's susceptibility to intestinal and hepatic metabolism and active influx/efflux transporters (2).

Table 14. *Pharmacokinetics of Itraconazole in Healthy Males With and Without a Meal*

Itraconazole	100 mg Fed	100 mg Fasted
C <sub>max</sub> (ng/ml)	132 ± 67	38 ± 20
T <sub>max</sub> (hours)	4.0 ± 11	3.3 ± 1.0
AUC (ng·h/ml)	1899 ± 838	722 ± 289

#### *Biopharmaceutics of Itraconazole*

Once itraconazole is delivered in solution to the intestinal lumen, it is subject to a variety of plasma membrane transporters and metabolic enzymes located in intestinal enterocytes (161). Two mechanisms have been identified as principal modulators of pre-systemic clearance/metabolism (161). The first is P-glycoprotein (P-gp). P-gp is a drug transporter found on the apical plasma membrane surface of enterocytes, where it functions to expel xenobiotics from the enterocyte back to the intestinal lumen (162). Itraconazole is both an inhibitor and substrate for P-gp (161). Therefore, the ultimate effect of P-gp on intestinal absorption of itraconazole can be mixed, or change after prolonged exposure to the drug (161). Moreover, there is significant inter-subject variability in the intestinal expression of P-gp transporters; patients diet, underlying disease, drug therapy, and genetics influence P-gp expression (162). This variability may account for some of the intra- and inter-patient variability observed in the literature for itraconazole (161).

The second mechanism of pre-systemic clearance involves intestinal metabolism by cytochrome P450 3A4 isoenzyme (CYP 3A4), which results in the production of active and inactive metabolites (161). Like P-gp, itraconazole is both a substrate and inhibitor of CYP 3A4 (163). Expression of CYP 3A4 in enterocytes shows intra- and

inter-patient variability similar to P-gp (164). Figure 19 illustrates the intestinal transport and metabolism of itraconazole (161).

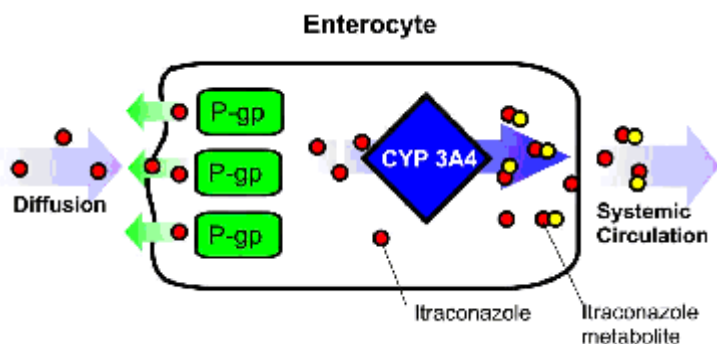


Figure 19. Intestinal Transport and Metabolism of Itraconazole

Itraconazole that is absorbed into systemic circulation is highly bound to red blood cells and plasma proteins (>99%) (165). Systemically available itraconazole is extensively metabolized in the liver to both active and inactive metabolites that are subsequently cleared by the kidneys (161). Approximately 50% of the drug is removed by first-pass metabolism in the liver (and intestinal lumen) resulting in an oral bioavailability of about 50% (166). However, this first-pass metabolism can be reversibly saturated with increasing itraconazole doses that result in an absolute bioavailability > 80% (167). The terminal elimination half-life of itraconazole after a single oral dose is about  $24 \pm 9$  hours, and about 14 hours for the active hydroxy metabolite (161). The active and inactive metabolites are excreted in the urine (161). Any remaining itraconazole (non-absorbed) is passed unchanged in the feces (165).

## Methods

Polymers for melt extrusion must exhibit thermoplastic characteristics in order to make the melt extrusion process possible and they must be thermally stable at the

extrusion temperatures employed (96). Other relevant characteristics include suitable glass transition or melt temperatures ( $T_g$  or  $T_m$ , respectively) of about  $50^\circ\text{C}$  -  $180^\circ\text{C}$  and low hygroscopicity (102). The extrudability of a polymer is mainly determined by the  $T_g$  or  $T_m$  and melt viscosity (102). As a general rule, an extrusion process runs at temperatures  $20^\circ\text{C}$  -  $40^\circ\text{C}$  above  $T_g$  (96). Once an amorphous solid dispersion is produced, drug-polymer miscibility, solid-state solubility, and drug-polymer interaction contribute to the stability of the system. Therefore, the methods in this study focused on thermal and rheological analysis, hygroscopicity, miscibility, and amorphous phase behavior.

### **Thermogravimetric Analysis (TGA)**

TGA is a suitable tool for examining the thermal sensitivity of materials. TGA has been broadly used in the study of thermal decomposition; however, it must be noted that such studies are only appropriate for materials that exhibit a weight loss upon decomposition (143). At the extrusion temperature, which is typically between  $100^\circ\text{C}$  and  $200^\circ\text{C}$ , the polymer must be stable. The difference between the  $T_g$  and degradation temperature ( $T_{deg}$ ) serves as an indication of the extrusion temperature range. Broad extrusion temperature ranges are preferred. TGA measurements were performed on a Q500 thermogravimetric analyzer (TA Instruments, New Castle, DE, USA). Three certified reference materials with nominal mass losses of 2%, 50%, and 98% at  $160^\circ\text{C}$  were used to verify the accuracy of the instrument.

### *Thermal Decomposition of PVAP*

Approximately 10 mg of sample was weighed into a platinum sample pan (TA Instruments, New Castle, DE, USA) and heated from 20°C to 1000°C at a heating rate of 20°C/min. purged under nitrogen and oxygen at a flow rate of 50 ml/min. The mass loss of PVAP as a function of temperature was reported. Experiments were performed in triplicate using fresh samples for each analysis.

### *Isothermal TGA Analysis of PVAP*

Approximately 10 mg of sample was weighed into a platinum sample pan (TA Instruments, New Castle, DE, USA) and the mass loss behavior of PVAP was recorded in nitrogen at four isothermal temperatures: 120°C, 130°C, 140°C, and 150°C. Experiments were performed in triplicate using fresh samples for each analysis.

### *Thermal Decomposition of PVPVA*

Approximately 10 mg of sample was weighed into a platinum sample pan (TA Instruments, New Castle, DE, USA) and heated from 25°C to 400°C at a heating rate of 20°C/min. purged under nitrogen and oxygen at a flow rate of 50 ml/min. The mass loss of PVP-VA as a function of temperature was reported. Experiments were performed in triplicate using fresh samples for each analysis.

### **Glass Transition Temperature (T<sub>g</sub>)**

The T<sub>g</sub> is characterized by an increase in the molecular mobility of the polymer chains, which changes the mechanical strength of the material from a hard glass to a softer rubber (68). Thermal analysis techniques can be used to characterize the T<sub>g</sub> of

amorphous polymers. The most popular techniques include differential scanning calorimetry (DSC), thermomechanical analysis (TMA), and dynamic mechanical analysis (DMA) (68). Each of these techniques detects the T<sub>g</sub> based on changes in a different material property during the glass transition. Therefore, the relative sensitivity of the different techniques varies depending on the nature of the material and experimental variables such as heating rate. Several studies have shown that DMA has about 1000 times greater sensitivity for detecting T<sub>g</sub> compared to DSC (119). Likewise, TMA has often been shown to be more sensitive than DSC at detecting T<sub>g</sub> (119). This study determined and compared the T<sub>g</sub> of PVAP using three different thermal techniques. In addition, the T<sub>g</sub> of PVPVA and ITZ were determined using DSC.

### *T<sub>g</sub> of PVAP*

#### *Conventional Differential Scanning Calorimetry (DSC)*

DSC is the most common thermal analysis technique (68). It measures heat flow to and from a sample relative to a reference and is widely used for the physical characterization of materials including identification of melting, crystallization, and thermal transition phenomena, and their associated changes in entropy and enthalpy (68). The heat capacity step change at the glass transition yields three temperature values: onset, midpoint, and endset. This T<sub>g</sub> range is helpful in identifying processing temperatures used during melt extrusion.

DSC measurements of PVAP were performed on a Q200 differential scanning calorimeter (TA Instruments, New Castle, DE, USA). Indium was used to calibrate the temperature scale and enthalpic response. Approximately 2 mg of sample was weighed

into a Tzero aluminum sample pan (TA Instruments, New Castle, DE, USA), and then the pans were hermetically sealed. Samples were heated at three different rates: 10°C/min., 15°C/min., and 30°C/min. from 0°C to 200°C under a nitrogen purge at 50 ml/min. Increasing heating rates can increase sensitivity yet, it can also shift T<sub>g</sub> to higher temperatures and broaden transitions (68). Experiments were performed in triplicate using fresh samples for each analysis.

#### *Modulated Differential Scanning Calorimetry (MDSC)*

MDSC is a high performance version of conventional DSC (68). For example, conventional DSC cannot resolve overlapping transitions. The transitions observed using conventional DSC may coincide with T<sub>g</sub> or a number of processes, making it difficult to analyze (68). MDSC has the ability to resolve overlapping transitions if the transitions separate into reversing and non-reversing heat flow signals (68). In MDSC, a sinusoidal temperature modulation is superimposed on the conventional linear temperature ramp to yield a modulated heating ramp (68). The modulated heating causes the heat flow to oscillate (68). Fourier transformation converts the modulating heat flow signal into reversing and non-reversing components, and calculates heat capacity (68). Reversing components of heat flow are those that are both thermodynamically reversible and kinetically feasible (68). Therefore, T<sub>g</sub> is observed in reversing heat flow signals. In contrast, thermal events that are not reversible or kinetically rapid appear in non-reversing heat flow signals. For example, crystallization, evaporation, and decomposition are observed in non-reversing signals (68).

MDSC measurements of PVAP were performed on a Q200 differential scanning calorimeter (TA Instruments, New Castle, DE, USA). Indium was used to calibrate the temperature scale and enthalpic response. Approximately 2 mg of sample was weighed into a Tzero aluminum sample pan (TA Instruments, New Castle, DE, USA) and then the pans were hermetically sealed. The T<sub>g</sub> was determined at a heating rate of 3°C/min. with a modulation amplitude of +/- 1.590°C every 60 sec under a nitrogen purge at 50 ml/min., and the midpoint of the transition in the reversing heat flow signal was reported. All T<sub>g</sub> values were determined from the second scan after heating the sample from -50°C to 140°C, cooling the sample to -50°C, and re-heating the sample from -50°C to 200°C. Subjecting the samples to a heat-cool-heat cycle removes thermal history of the sample. Experiments were performed in triplicate using fresh samples for each analysis.

#### *Thermomechanical Analysis (TMA)*

TMA is generally used to measure the glass transition based on changes in coefficient of thermal expansion, which result as the free volume of the material increases (168). An expansion probe on the TMA detects the increase in free volume. Another TMA approach for determining the glass transition uses instead, a penetration probe. In this mode, TMA measures the sample length as a function of temperature under load. The penetration probe applies a load to a small area of sample to measure softening. The penetration mode detects T<sub>g</sub> as a downward probe movement as the material becomes less rigid in the transition from hard glass to a softer rubber (168). For amorphous materials, the softening point corresponds to T<sub>g</sub>.

TMA measurements of PVAP were performed on a Q400 thermomechanical analyzer (TA Instruments, New Castle, DE, USA). The force exerted by the penetration probe was calibrated using three different mass values: 0 grams, 5 grams, and 10 grams. Indium was used to calibrate the temperature scale. Approximately 60 mg of PVAP was compacted into a flat-faced cylinder using a manual pellet press (TA Instruments, New Castle, DE, USA) to a sample thickness of about 1.4 mm. A penetration probe (TA Instruments, New Castle, DE, USA) applied a force of 0.02N plus 5 grams to the sample as it heated from 25°C to 200°C. The T<sub>g</sub> was determined at a heating rate of 1°C/min. under a nitrogen purge at 100 ml/min. Experiments were performed in triplicate using fresh samples for each analysis.

#### *Dynamic Mechanical Analysis (DMA)*

DMA measures mechanical stiffness (modulus) and energy absorption by subjecting the sample to oscillating mechanical stress within a linear viscoelastic region (119). The oscillating stress, measured as force per unit area, results in sample deformation (strain). The modulus is the ratio of applied stress to strain. For viscoelastic materials, the modulus has two components: 1) a component in-phase with the applied stress (storage modulus, E'), which corresponds to the elastic response of the sample, and 2) a component out-of- phase with the applied stress (loss modulus, E''), which corresponds to the viscous component of the sample (119). The ratio of the dissipated mechanical energy to stored mechanical energy is denoted by  $\tan \delta \left( \frac{E''}{E'} \right)$  (119). At the glass transition, the increase in molecular motion within the polymer results in a decrease in the storage modulus (E'). Energy is absorbed as molecular motion increases. As the

sample proceeds through the glass transition, the rate of energy absorption goes through a maximum, which corresponds to peaks in the loss modulus ( $E''$ ) and  $\tan \delta$  curves (119).

DMA measurements were performed on a Q800 dynamic mechanical analyzer (TA Instruments, New Castle, DE, USA). PVAP powder samples were secured between a parallel-plate compression clamp (plate measured 12 mm wide by 60 mm long). A slow heating rate of 1°C/min. was used to heat the samples from 30°C to 140°C. The oscillating frequency of 1 Hz was applied to a static force of 0.4N. Experiments were performed in triplicate using fresh samples for each analysis.

#### *T<sub>g</sub> of PVPVA and Itraconazole*

MDSC measurements of PVPVA and itraconazole were performed separately on a Q200 differential scanning calorimeter (TA Instruments, New Castle, DE, USA).

Indium was used to calibrate the temperature scale and enthalpic response.

Approximately 2 mg of sample was weighed into a Tzero aluminum sample pan (TA Instruments, New Castle, DE, USA) and then the pans were hermetically sealed. The  $T_g$  was determined at a heating rate of 3°C/min. with a modulation amplitude of +/- 1.590°C every 60 sec under a nitrogen purge at 50 ml/min., and the midpoint of the transition in the reversing heat flow signal was reported. All  $T_g$  values were determined from the second scan. PVP-VA was heated from -90°C to 150°C, cooling to -90C, and re-heating from -90°C to 200°C. Itraconazole was heated from -50°C to 200°C, cooling to -50C, and re-heating from -50°C to 200°C. Subjecting the samples to a heat-cool-heat cycle removes thermal history of the sample (68). Experiments were performed in triplicate using fresh samples for each analysis.

### *Tg of ITZ-PVPVA and ITZ-Polymer Blends*

Some APIs have a plasticizing effect on polymers. To evaluate the effect of ITZ on PVAP-PVPVA polymer blends, the Tg of the system at various API ratios was determined using MDSC. MDSC measurements were performed on a Q200 differential scanning calorimeter (TA Instruments, New Castle, DE, USA). Indium was used to calibrate the temperature scale and enthalpic response. Approximately 2 mg of sample was weighed into a Tzero aluminum sample pan (TA Instruments, New Castle, DE, USA) and then the pans were hermetically sealed. The Tg was determined at a heating rate of 3°C/min. with a modulation amplitude of +/- 1.590°C every 60 sec under a nitrogen purge at 50 ml/min., and the midpoint of the transition in the reversing heat flow signal was reported. All Tg values were determined from the second scan. The ITZ-PVAP-PVPVA powder blend was heated from -50°C to 150°C, cooling to -50°C, and re-heating from -50°C to 180°C. The ITZ-PVPVA powder blend was heated from 0°C to 180°C, cooling to 0°C, and re-heating from 0°C to 180°C. Experiments were performed in triplicate using fresh samples for each analysis.

### *Tg of Extruded ITZ-Polymer Blend*

MDSC measurements of ITZ-PVAP-PVPVA extrudate were performed to ensure that the ITZ was fully melted and incorporating into the polymers during extrusion. The analysis was performed on a Q200 differential scanning calorimeter (TA Instruments, New Castle, DE, USA). Indium was used to calibrate the temperature scale and enthalpic response. Approximately 2 mg of extrudate was weighed into a Tzero aluminum sample pan (TA Instruments, New Castle, DE, USA) and then the pans were hermetically sealed.

Extrudate was analyzed at a heating rate of 3°C/min. with a modulation amplitude of +/- 1.590°C every 60 sec under a nitrogen purge at 50 ml/minute, heating from -50°C to 180°C. Since the material experienced its first heat in the extruder, the samples were only heated once on the DSC and not subjected to a heat-cool-heat cycle. The transitions in the reversing heat flow signal after the first scan were evaluated for any remaining crystalline ITZ, which is observed as an endothermic melting peak. Experiments were performed in triplicate using fresh samples for each analysis.

### **Melt Viscosity of PVAP, PVPVA, PVAP-Plasticizer and PVAP-PVPVA Blends**

Besides T<sub>g</sub>, melt viscosity is another factor used to determine extrudability. Melt viscosity is influenced by molecular weight and any interactions between the functional groups on the polymer chains (102). For small-scale extruders, the limitation is approximately 10,000 Pa·s; higher viscosities generate too much torque within the extruder (102). Melt viscosities can be lowered by adding plasticizers in order to run a smoother extrusion process. Polymers should not exhibit very low viscosity either, or the extruded material will be problematic during downstream processing (102).

Viscosity studies were performed using an AR-G2 rheometer (TA Instruments, New Castle, DE, USA). The effect of temperature on viscosity was determined for the samples from 120°C to 180°C using a step oscillation procedure with strain at 1.25%, angular frequency at 6.283 rad/sec., and ramp rate of 3°C/minute. Approximately 60 mg of material was compacted into a flat-faced disk using a manual pellet press (TA Instruments, New Castle, DE, USA) to a sample thickness of about 2 mm. The samples

were placed between two 25 mm ETC steel parallel plates with the gap set at 1000  $\mu\text{m}$ . Experiments were performed in triplicate using fresh samples for each analysis.

### **Hygroscopicity of PVAP and PVPVA**

In one study, the amount of water sorbed by a solid dispersion was determined to depend on the water affinity of the polymer incorporated in the solid dispersion (123). Therefore, the water affinity of PVAP and PVPVA were evaluated to predict their suitability in amorphous systems.

#### *Sample Preparation to Evaluate the Water Affinity of PVAP and PVPVA*

Powder samples were stored either in a desiccator over saturated salt solutions or a humidity chamber (Espec SH-241, Espec North America Inc., Hudsonville, MI, USA) for 3 days at 23°C. The following salts were used to prepare saturated solutions for control of low humidity conditions: phosphorous pentoxide (0% RH) and potassium acetate (22% RH). The humidity chamber was used to maintain conditions at 35% RH, 50% RH, 75% RH, and 90% RH.

#### *TGA Analysis of PVAP After Exposure to Various Relative Humidities*

TGA measurements were performed on a Q500 thermogravimetric analyzer (TA Instruments, New Castle, DE, USA). Three certified reference materials with nominal mass losses of 2%, 50%, and 98% at 160°C were used to verify the accuracy of the instrument.

Approximately 10 mg of sample was weighed into a platinum sample pan (TA Instruments, New Castle, DE, USA) equilibrated in a desiccator or humidity chamber at

the desired relative humidity for 3 days at 23°C. Samples were heated from 20°C to 500°C at a heating rate of 20°C/min. under a nitrogen purge at 50 ml/min., and the mass loss from 20°C to 150°C was reported. Experiments were performed in triplicate using fresh samples for each analysis.

#### *Loss on Drying After Exposure to Various Relative Humidities for PVAP and PVPVA*

Loss on drying (LOD) measurements were performed on an IR-200 moisture analyzer (Denver Instrument Company, Denver, CO, USA). The balance and heaters on the moisture analyzer were calibrated prior to use.

Approximately 2 g of sample was weighed onto an aluminum sample pan (VWR International LLC, Radnor, PA, USA) equilibrated in a desiccator or humidity chamber at the desired relative humidity for 3 days at 23°C. Samples were heated to 105°C, and the moisture content was recorded as the percent weight loss. The moisture content determined by LOD was used to corroborate the mass loss reported as sorbed moisture by TGA for PVAP. For PVPVA, the moisture content determined by LOD was reported as moisture uptake.

#### *DSC Analysis of PVAP After Exposure to Various Relative Humidities*

MDSC measurements of PVAP were performed on a Q200 differential scanning calorimeter (TA Instruments, New Castle, DE, USA). Indium was used to calibrate the temperature scale and enthalpic response.

Approximately 3-5 mg of sample was weighed into a Tzero aluminum sample pan (TA Instruments, New Castle, DE, USA), equilibrated in a desiccator or humidity

chamber at the desired relative humidity for 3 days at 23°C, and then hermetically sealed to minimize the loss of sorbed water. The T<sub>g</sub> was determined at a heating rate of 3°C/min with a modulation amplitude of +/- 1.590°C every 60 sec and the midpoint of the transition in the reversing heat flow signal was reported. All T<sub>g</sub> values were determined from the first scan after heating the sample from -10°C to 150°C. Experiments were performed in triplicate using fresh samples for each analysis.

### **Solubility Parameter for PVAP, Plasticizers, Polymers and Other Excipients**

The ideal type of solid dispersion for increasing dissolution rates and providing long-term storage stability is an amorphous solution. An amorphous solution is formed when two or more components are entirely miscible in the molten state and cool to form an amorphous one-phase system. The calculated solubility parameter determined by group contribution methods can be used to predict the miscibility of compounds. Materials with similar solubility parameter values are expected to be miscible.

The solubility parameter is a measure of cohesive energy density of materials. The cohesive energy represents the total attractive forces within a material, and it can be defined as the quantity of energy needed to separate the atoms/molecules of a solid or liquid to a distance where they possess no potential energy, that is, no interactions occur between atoms and molecules. The cohesive energy of a material can be quantified in several ways. One common approach is to use the solubility parameter ( $\delta$ ). Hansen defined three partial solubility parameters ( $\delta_d$ ,  $\delta_p$ , and  $\delta_h$ ) that were combined to form the total solubility parameter ( $\delta_t$ ). The Hansen solubility parameter can be estimated based

on the methods of Hayes, Small, Hoftyzer and Van Krevelen, and Hoy. Each method predicts the cohesive energy with a mean accuracy of about 10%.

In this study, the solubility parameter for PVAP was calculated from the chemical structure using the approaches of Hoftyzer/Van Krevelen, and Hoy. The solubility parameter was determined based on the average molecular weight, repeating monomer unit, and respective homopolymers of PVAP. The mean of the Hoftyzer/Van Krevelen and Hoy values was used to determine  $\delta$  for PVAP. In addition, the solubility parameter values for other polymers and various plasticizers and excipients were determined and compared to PVAP. The units of solubility parameters are  $\text{MPa}^{1/2}$ ,  $(\text{J m}^{-3})^{1/2}$  or  $(\text{cal cm}^{-3})^{1/2}$ , where  $1 (\text{cal cm}^{-3})^{1/2}$  is equivalent to  $2.0421 \text{ MPa}^{1/2}$ .

In the Hoftyzer and Van Krevelen method

$$\delta_t = \sqrt{\delta_d^2 + \delta_p^2 + \delta_h^2} \quad \text{Eq. 6}$$

where

$$\delta_d = \frac{\sum F_{di}}{V} \quad \text{Eq. 7}$$

$$\delta_p = \frac{\sqrt{\sum F_{pi}^2}}{V} \quad \text{Eq. 8}$$

$$\delta_h = \frac{\sqrt{\sum E_{hi}}}{V} \quad \text{Eq. 9}$$

$\delta_t$  is the total solubility parameter,  $\delta_d$  is the contribution from dispersion forces,  $\delta_h$  is the contribution from hydrogen bonding,  $\delta_p$  is the contribution from polar forces,  $F_{di}$  is the group dispersion component,  $F_{pi}^2$  is the group polar component,  $E_{hi}$  is the hydrogen bonding component and  $V$  is the molar volume from Hildebrand analysis.

In the Hoy method

$$\delta_t = \frac{\left(F_t + \frac{B}{n}\right)}{V} \quad \text{Eq. 10}$$

where

$$\delta_d = \left(\delta_t^2 - \delta_p^2 - \delta_h^2\right)^{1/2} \quad \text{Eq. 11}$$

$$\delta_p = \delta_t \left[ \left( \frac{1}{\alpha^p} \right) \left( \frac{F_p}{\left(F_t + \frac{B}{n}\right)} \right) \right]^{1/2} \quad \text{Eq. 12}$$

$$\delta_h = \delta_t \left[ \frac{(\alpha^p - 1)}{\alpha^p} \right]^{1/2} \quad \text{Eq. 13}$$

$\delta_t$  is the total solubility parameter,  $\alpha$  is the molecular aggregation number describing the association of the molecules,  $n$  is the number of repeating units per effective chain segment of the polymer,  $F_t$  is the molar attraction function,  $F_p$  is the polar component,  $\Delta_T$  is the Lyderson correction for non-ideality,  $V$  is the molar volume of the structural unit of the polymer,  $B$  is a constant = 277,  $\alpha^p = 777 \frac{\Delta_T^{(p)}}{V}$ , and  $n = \frac{0.5}{\Delta_T^{(p)}}$

Compounds with similar solubility parameter ( $\delta$ ) values are likely to be miscible because the energy of mixing released by interactions within the components is balanced by the energy released by interactions between the components (169). Greenhalgh et al. grouped materials based on the difference between the solubility parameters of excipients and drugs ( $\Delta\delta$ ) (170). The authors showed that the compounds with a  $\Delta\delta < 7.0 \text{ MPa}^{1/2}$

are likely to be miscible, while compounds with  $\Delta\delta > 10.0 \text{ MPa}^{1/2}$  are likely to be immiscible with one another (170).

### **Miscibility Studies for PVAP, PVPVA and Itraconazole**

Miscibility is essential for the stability of amorphous pharmaceutical compositions because immiscibility can result in the formation of drug-rich domains that can be prone to crystallization (95). The measurement of T<sub>g</sub> was used to assess the miscibility of: 1) PVPVA in PVAP; 2) itraconazole in PVAP-PVPVA polymer blends; and 3) itraconazole in PVPVA. If the polymers are completely miscible at a given ratio, only one T<sub>g</sub> should be observed. Likewise, if ITZ is miscible in the polymers, only one T<sub>g</sub> should be observed, typically at the intermediate temperature between the drug and polymers (169). For an immiscible mixture, two T<sub>g</sub> signals should appear, one for each polymer or one for the drug and polymer. MDSC measurements were performed on a Q200 differential scanning calorimeter (TA Instruments, New Castle, DE, USA). Indium was used to calibrate the temperature scale and enthalpic response. Approximately 2 mg of sample was weighed into a Tzero aluminum sample pan (TA Instruments, New Castle, DE, USA) and then the pans were hermetically sealed. The T<sub>g</sub> was determined at a heating rate of 3°C/min. with a modulation amplitude of +/- 1.590°C every 60 sec under a nitrogen purge at 50 ml/min., and the midpoint of the transition in the reversing heat flow signal was reported. All T<sub>g</sub> values were determined from the second scan. Samples were heated from -50°C to 150°C, cooled to -50°C, and re-heating from -50°C to 200°C. Experiments were performed in triplicate using fresh samples for each analysis.

## **HME Processing**

### *Motor Load*

The extrudability of PVAP-PVPVA and ITZ-polymer blends was evaluated on a Nano-16 twin-screw co-rotating extruder with a screw diameter of 16 mm (American Leistritz Extruder Corporation, Somerville, NJ, USA). After some preliminary trials, the final extrusion parameters were set as follows: screw speed 100 rpm, feed rate 2 g/min., and melt temperature 140°C. The powder blends, in a batch size of 100 g, were fed into the extruder via a volumetric feeder. The extrusion torque during manufacturing is a key indicator of the melt viscosity; high melt viscosities generate excessive load on the extruder drive motor and preclude processing. Therefore, torque was monitored throughout the process. The torque generated from the different polymer ratios and drug loads were plotted to assess how the concentration of additive facilitated flow through the extruder.

### *Preparation of PVAP-PVPVA-ITZ Solid Dispersions*

A powder blend containing 20:40:40% PVAP:PVPVA:ITZ was melt extruded to form a solid dispersion. Melt extrusion was performed using a Nano-16 twin-screw co-rotating extruder with a screw diameter of 16 mm (American Leistritz Extruder Corporation, Somerville, NJ, USA). The extrusion parameters were set as follows: screw speed 100 rpm, feed rate 2 g/min., and melt temperature 140°C. The ITZ-powders blend was fed into the extruder via a volumetric feeder. After extrusion, the samples were cooled on a conveyor belt and subsequently pelletized.

### **Analysis of PVAP Content**

Assay testing was used to determine the content of PVAP after exposure to 130°C, 140°C and 150°C for 5 minutes, which represented the longest residence time in the extruder. PVAP analysis was performed using HPLC GPC analysis with refractive index and UV/Vis detection in a THF solvent system. Detection by UV/Vis is used to detect the phthalate groups on PVAP while the RI detection looks at the polymer as a whole. Free phthalic acid testing was performed by reverse phase HPLC to confirm and quantify the amount of PVAP degradation observed with GPC analysis.

### **Analysis of ITZ Content**

Assay testing was used to determine the content of itraconazole in the ternary solid dispersions. The solid dispersions were dissolved in dimethylsulfoxide (DMSO) and the itraconazole content was determined using an Alliance HPLC system (Waters, Milford, MA, USA) equipped with RP-18 column. Acetonitrile:tetrabutyl ammonium hydrogen sulfate (55:45) was used as mobile phase at a flow rate of 1 ml/min. The injection volume was 20 µl and absorbance was measured at a wavelength of 260 nm. The retention time for itraconazole was 4.6 min.

### **X-Ray Powder Diffraction (XRPD)**

XRPD is a widely used technique for the detection of crystallinity. XRPD is the measurement of the intensity of X-rays scattered by electrons bound to atoms and the corresponding phase shifts that occur because of the position of the atom (143). The absence of sharp Bragg's peaks corresponding to the crystalline drug suggests a

formulation is in an amorphous state (95). XRPD detects the presence of molecular order, and therefore, the disorder (amorphous state) is only implied by the absence of the order.

Prior to analysis, the instrument was calibrated using four oxide powders: ZnO, TiO<sub>2</sub>, Cr<sub>2</sub>O<sub>3</sub>, and CeO<sub>2</sub>. The physical mixtures and melt-extruded powders were analyzed using a model 1710 diffractometer (Phillips Electronic Instruments, Mahwah, NJ, USA). From the diffraction profiles, the characteristic ITZ peaks used for determining crystallinity can be identified. XRPD profiles for the melt extruded powders should lack the diffraction peaks associated with crystalline ITZ implying the samples contain amorphous ITZ. An amorphous material will yield an XRPD pattern termed a halo, which is a gradual rise and fall of the baseline with no discernible peaks.

### **Dissolution**

Development of meaningful dissolution methods for kinetically unstable systems of poorly soluble drugs is challenging. Generally, it requires consideration of physiologically relevant conditions, adequate discriminating power, and predicting in vivo performance (95). Sink conditions will not determine the ability of a system to maintain supersaturation (95). However, an overly non-sink condition can result in over discrimination and potential elimination of viable formulations (95). In this study, dissolution testing was performed in sink and non-sink conditions, in simulated gastric fluid (pH 1.2), and in 0.1N HCl (pH 1.2) for 2 hours followed by pH 6.8 buffer.

### *Sink Conditions*

Dissolution testing in sink conditions was performed to investigate the effect of polymer composition on drug release. The melt-extruded powders were compared to crystalline ITZ. A previously prepared ITZ-PVAP sample produced using a solvent evaporation technique also was compared to the melt extruded powder.

Dissolution testing was performed using a USP 25 type 2 paddle apparatus, model VK7000 (Varian, Cary, NC, USA). An equivalent of 1 mg ITZ was pre-wetted with 0.075% polysorbate 20 in deionized water and added to 900 ml of SGF pH 1.2 without enzymes. The dissolution media was maintained at  $37.0\pm 0.2^{\circ}\text{C}$  and paddle speed was maintained at 50 rpm throughout the test. Samples (5 ml) were withdrawn at 5, 10, 15, 20, 25, 30, 45, 60, 90, and 120-minute time points, filtered through a  $0.45\ \mu\text{m}$  filter, and analyzed using an Alliance HPLC system (Waters, Milford, MA, USA) equipped with an ODS-2  $5\ \mu\text{m}$   $\text{C}_{18}$  column and a UV detector. A mobile phase of acetonitrile:water:diethanolamine (70:30:0.05) at 1 ml/min eluted the ITZ peak at 5.5 min and absorbance was measured at a wavelength of 263 nm. Assuming complete dissolution, the concentration of ITZ in the dissolution vessel was 0.001 mg/ml and the solubility of ITZ in SGF (pH 1.2) is 0.004 mg/ml, which indicated the test was performed under sink conditions.

### *Non-Sink Conditions (Supersaturated)*

#### *FDA Test Method*

Itraconazole is marketed as Sporanox. Sporanox capsules were tested according to the FDA dissolution method for itraconazole to assess the marketed product's drug

release in recommended testing conditions. Dissolution testing was performed according to FDA guidelines using a USP 25 type 2 paddle apparatus model, VK7000 (Varian, Cary, NC, USA) (171). The dissolution media was maintained at  $37.0 \pm 0.2^\circ\text{C}$  and paddle speed was maintained at 100 rpm throughout the test. Samples (5 ml) were withdrawn at 5, 10, 15, 20, 25, 30, 45, 60, and 90-minute time points, filtered through a  $0.45 \mu\text{m}$  filter and analyzed using an Alliance HPLC system (Waters, Milford, MA, USA) equipped with an ODS-2  $5 \mu\text{m}$   $\text{C}_{18}$  column and a UV detector. A mobile phase of acetonitrile:water:diethanolamine (70:30:0.05) at 1 ml/min eluted the ITZ peak at 5.5 min and absorbance was measured at a wavelength of 263 nm. The contents of one capsule containing 100 mg of itraconazole was placed in 900 ml of USP simulated gastric fluid (SGF) without enzymes (pH 1.2) to obtain a concentration of 0.11 mg/ml, assuming complete dissolution. The solubility of ITZ at pH 1.2, however, is only 0.004 mg/ml, which indicates the FDA dissolution test method is performed under non-sink conditions.

#### *USP Enteric Test Method A*

Polymers with pH-dependent dissolution properties have been investigated extensively for their use in pharmaceutical applications intended for delayed drug release. These polymers have been widely used for targeted drug delivery to the small intestine. Enteric polymers such as PVAP show low solubility in acidic conditions due to free carboxylic acid functional groups on the molecule that remain unionized at low pH. As the pH of the media increases to a specific value, above pH 5 for PVAP, the functional groups begin to ionize, resulting in increased hydrophilicity and solubility. To evaluate the enteric functionality of PVAP and better simulate the conditions a solid dispersion

would be experiencing in the GI tract, dissolution testing was performed according to USP enteric test method A. The method A procedure specifies that the dosage form be tested in 750 ml 0.1N hydrochloric acid (HCl) at 37°C for 2 hours (acid phase) followed by the addition of 250 ml sodium phosphate buffer to obtain a final pH of 6.8±0.05 (buffer phase).

The concept of generating and maintaining supersaturation was described as the "spring and parachute approach" by Guzman et al. (172). In the case of a molecular dispersion (solid solutions), release of drug molecules is dictated by dissolution of the polymer (spring action) and leads to a supersaturated state of drug in solution (172). Eventually, the kinetically unstable drug concentrations decline (parachute action) (172). The ability of an amorphous solid dispersion to achieve and maintain supersaturation is commonly assessed (143). This can be accomplished by adding an amount of solid dispersion to the dissolution vessel such that the amount added contains an excess amount of drug relative to the intrinsic solubility and thereby, upon complete dissolution, a theoretical level of supersaturation is achieved (143). For example, in one study of melt extruded itraconazole formulations, 180 mg of extrudate containing 60 mg of itraconazole was added to each 750-ml dissolution vessel (149). Assuming complete dissolution, this amount corresponds to 80 µg/ml, representing 20X supersaturation because the intrinsic solubility of itraconazole in acidic conditions is 4 µg/ml. In other studies, itraconazole was evaluated at a level equivalent to 10X equilibrium solubility (173,121,174).

In this study, dissolution testing was performed in supersaturated conditions (20X ITZ equilibrium solubility) in order to determine the maximum concentration ( $C_{max}$ ), and

the duration of supersaturation ( $T_{\max}$ ), which depends both upon dissolution of the extrudate and the ability of the polymers to inhibit precipitation of ITZ.

Dissolution testing was performed on the melt-extruded powders using a USP 25 dissolution apparatus model VK7000 (Varian, Cary, NC, USA). Dissolution was conducted according to USP enteric test method A for delayed release dosage forms using 100-ml glass dissolution vessels and stirring with appropriate, small paddles. An equivalent of 8.8 mg ITZ (20X ITZ equilibrium solubility) was pre-wetted with 5 ml 0.008% polysorbate 20 in 0.1N HCl and added to 70 ml 0.1N HCl (75 ml total). The dissolution media was maintained at  $37.0\pm 0.2^{\circ}\text{C}$  and the paddle speed was maintained at 50 rpm through the test. After 2 hours, 0.2M tribasic sodium phosphate was equilibrated at  $37.0\pm 0.2^{\circ}\text{C}$  and added to the dissolution vessels. The dissolution media had a final pH of 6.8. For each time point, 3 ml of medium was withdrawn and filtered using a  $0.45\ \mu\text{m}$  filter, diluted with acetonitrile to minimize precipitation, and analyzed using an Alliance HPLC system (Waters, Milford, MA, USA) equipped with an ODS-2  $5\ \mu\text{m}\ \text{C}_{18}$  column and a UV detector. A mobile phase of acetonitrile:water:diethanolamine (70:30:0.05) at 1 ml/min eluted the ITZ peak at 5.5 min and absorbance was measured at a wavelength of 263 nm.

Of crucial importance to supersaturation dissolution studies is the prevention of precipitation in the withdrawn samples, which can cause inaccurately low results and accidental solubilization of withdrawn particles by the mobile phase, yielding positive deviations (143). To prevent this from occurring, withdrawn samples were immediately diluted with acetonitrile, a component of the mobile phase. The dilution was then accounted for in the HPLC analysis.

### *Area Under the Supersaturated Dissolution Curves*

The area under the supersaturated dissolution curves (AUC) was calculated using the trapezoidal method to determine the duration or cumulative extent of supersaturation in the acid (pH 1.2) and buffer (pH 6.8) phases for each formulation.

### **Stability**

Development of poorly water-soluble drugs often relies on the use of an altered drug form such as the amorphous form of the compound (143). In this study, amorphous solid dispersions of itraconazole were produced using a melt extrusion processing technique. While this formulation strategy can enhance aqueous solubility, it is often plagued by stability issues, mainly recrystallization of the amorphous drug and subsequent loss of solubility and bioavailability. As such, it is necessary to gain an understanding of the stability of the drug in the formulation over time.

The International Conference on Harmonization (ICH) has set guidelines for stability testing of formulations relative to the intended storage conditions upon geographic region for distribution (143). Table 15 outlines the storage conditions to be used for short term, long term, and accelerated stability testing (143). Accelerated conditions are often used during preformulation studies because the timeline is significantly shortened (143). However, because stability of solid dispersions can be problematic, for this study, the melt-extruded powders were stored in high-density polyethylene bottles for 6 months at 30°C/65%RH and tested for changes in crystallinity determined by XRPD and for drug release under supersaturated dissolution testing conditions.

Table 15. ICH Guidelines for Stability Testing Conditions

<i>Room Temperature Storage Conditions</i>		
Stability Study	Storage Conditions	Minimum Time Period
Long term	25°C±2°C/60%RH±5%RH or 30°C±2°C/65%RH±5%RH	12
Intermediate	30°C±2°C/65%RH±5%RH	6
Accelerated	40°C±2°C/75%RH±5%RH	6
<i>Refrigerated Storage Conditions</i>		
Long term	5°C±3C	12
Accelerated	25°C±2C/60%RH±5%RH	6
<i>Freezer Storage Conditions</i>		
Long term	-20°C±5C	12

## CHAPTER 4

### RESULTS AND DISCUSSION

#### Results

##### Thermal Decomposition of PVAP

TGA measured the mass of PVAP as a function of temperature. The initial mass loss of about 3.8% was due to moisture, which agreed with LOD results and met the product specification from the manufacturer of not more than 5%. The decomposition in nitrogen occurred in three mass loss steps (Figure 20) that coincided with three homopolymers of PVAP (inset, Figure 20). The onset of the first decomposition was about 150°C. Thermogravimetric curves in nitrogen and oxygen were superimposable indicating that PVAP was susceptible to thermal, but not oxidative degradation. About 4% carbon-black formed after decomposition in nitrogen. The baseline shifted at 650°C when the nitrogen gas was switched to oxygen.

The TGA data was visually confirmed by heating samples of PVAP to 140°C, 160°C and 180°C. The sample heated to 140°C, which was below the decomposition temperature detected by TGA, showed no discoloration. However, samples heated above the first mass loss detected by TGA (150°C) discolored slightly at 160°C and severely at 180°C (Figure 20). The visual observations were in agreement with the TGA analysis.

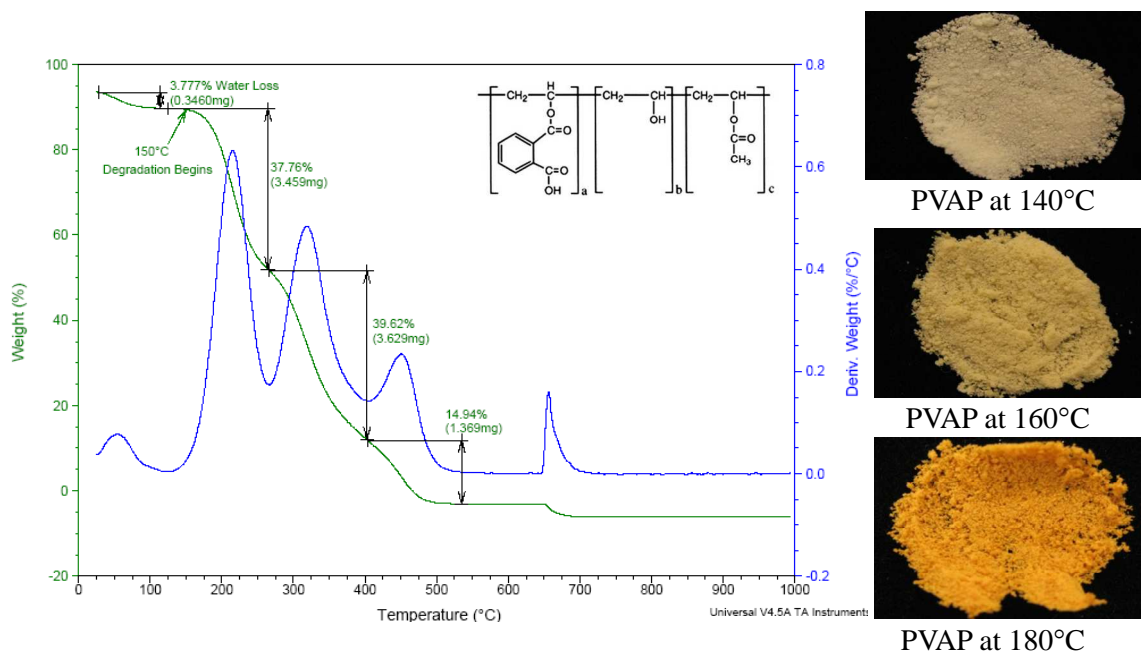


Figure 20. TGA Analysis of PVAP, Chemical Structure of PVAP (inset), and Visual Observations of PVAP Heated to Various Temperatures

TGA provides a quantitative measurement of the mass change, but does not identify the nature of the material lost. TGA curves comparing PVAP and polyvinyl acetate (PVA), a monomer component of PVAP, suggested the first mass loss at 150°C was the phthalate group of PVAP (Figure 21). TGA was coupled to a mass spectrometer (MS) in an attempt to analyze the gases evolved during TGA analysis; however, the data was inconclusive. The TGA-MS data could not differentiate the gases that evolved at similar temperatures and, therefore, could not confirm that it was the phthalate group at 150°C.

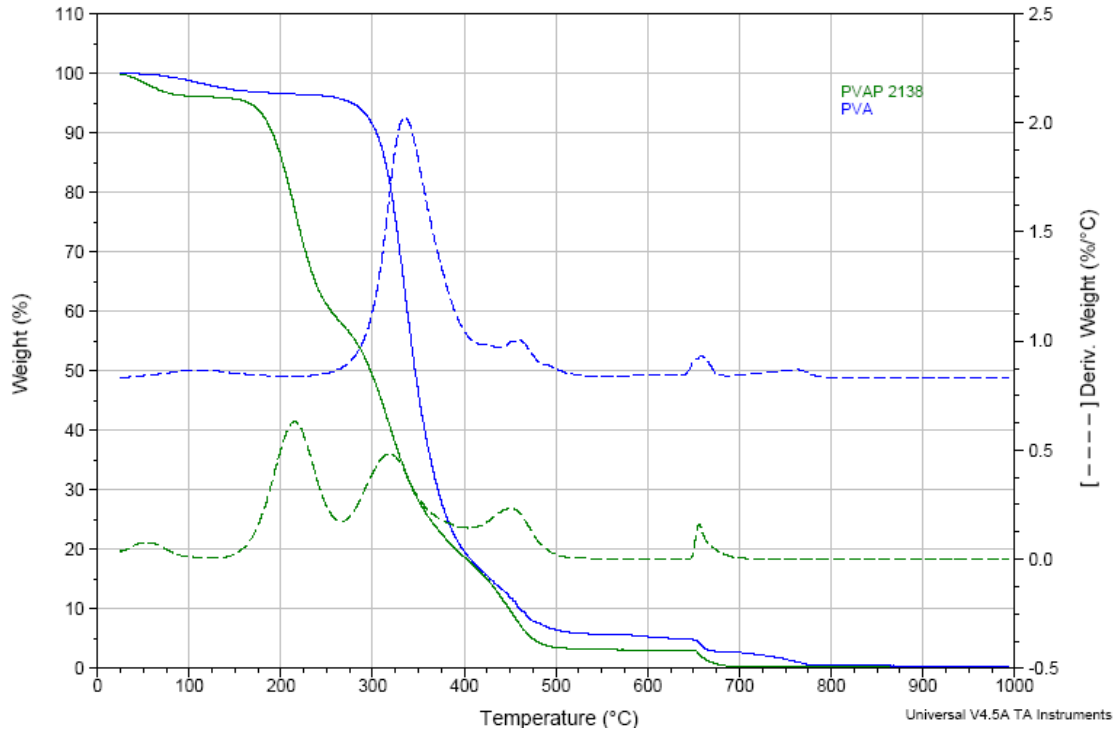


Figure 21. TGA Analysis of PVAP (blue line) Compared to PVA (green line)

### **Isothermal TGA of PVAP**

The mass-loss behavior of PVAP was evaluated in nitrogen at four isothermal temperatures: 120°C, 130°C, 140°C, and 150°C. The thermogravimetric curves showed water loss of about 3% within the first 3 minutes, and then the mass of PVAP remained constant from 4 to 6 minutes (Figure 22). The steady weight of PVAP indicated little to no decomposition up to 6 minutes for each temperature studied. This is important because the residence time in extruders is typically 0.5 min. to 5 min. After 6 minutes, the rate of decomposition increased notably for the highest temperatures tested, but remained relatively constant at the lower temperatures (Figure 22). After correcting for moisture loss, the mass loss of PVAP after 20 minutes was approximately 0.5%, 1%, 3%, and 6% for samples held at 120°C, 130°C, 140°C, and 150°C, respectively.

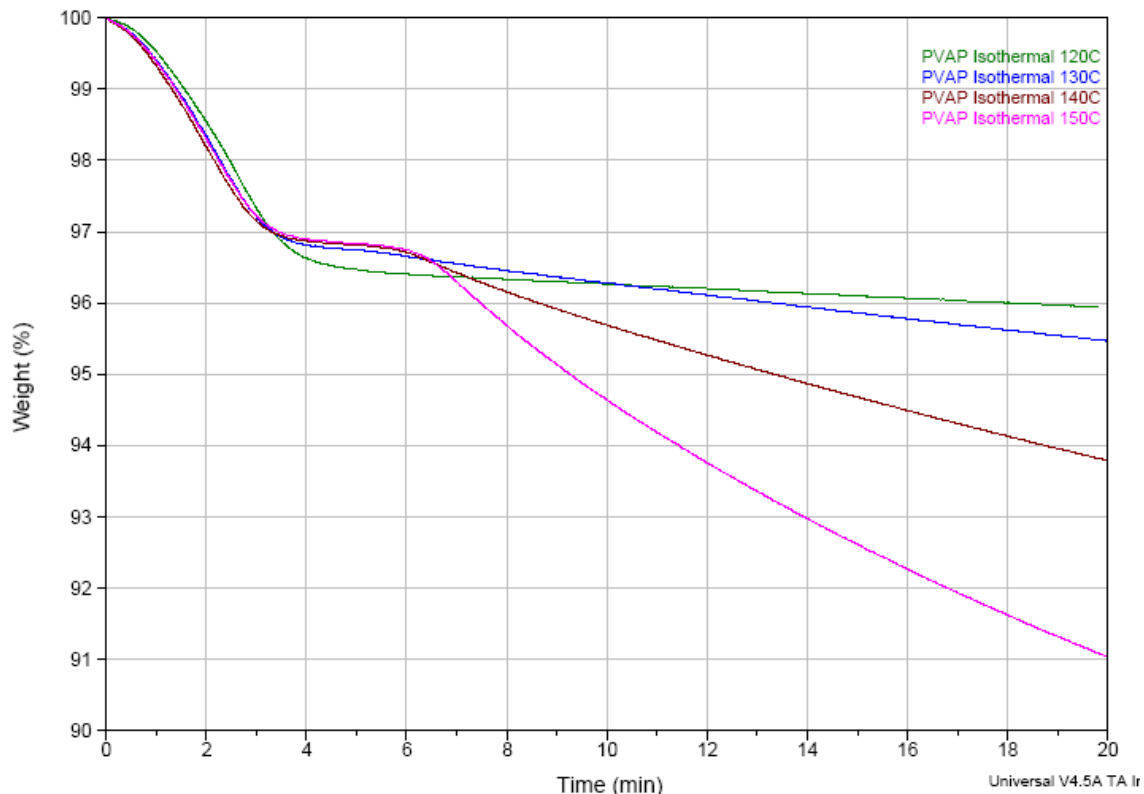


Figure 22. Isothermal TGA Analysis of PVAP at 120°C (green line), 130°C (blue line), 140°C (brown line), and 150°C (pink line)

### Glass Transition Temperature (T<sub>g</sub>) of PVAP

#### *Conventional Differential Scanning Calorimetry (DSC)*

DSC measured heat flow as a function of temperature. The Handbook of Pharmaceutical Excipients reports the T<sub>g</sub> of PVAP at 78°C (140). The experimental results in this study, however, showed two transitions: one at about 80°C and another at 120°C (Figure 23). The transition at 80°C was very broad and the one at 120°C was very small. Increasing the heating rate from 10°C/min. to 30°C/min., unfortunately, decreased sensitivity; transitions shifted to higher temperatures and broadened. The transitions around 80°C and 120°C may coincide with T<sub>g</sub> or a number of processes, making it difficult to interpret. MDSC has the ability to resolve overlapping transitions if the

transitions separate into reversing and nonreversing heat flow signals.

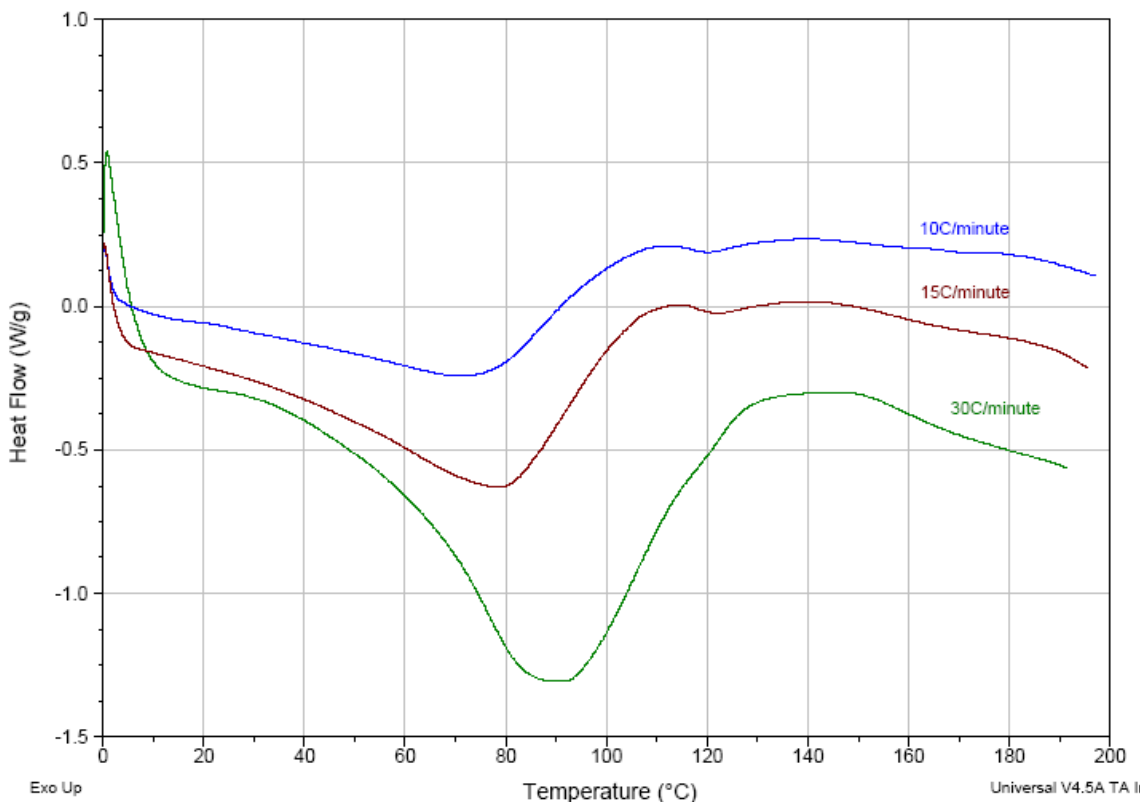


Figure 23. Conventional DSC Thermograms of PVAP at 10°C/min. (blue line), 15°C/min. (red line), and 30°C/min. (green line)

#### *Modulated DSC (MDSC)*

MDSC separated the total heat flow signal into reversing and nonreversing signals.  $T_g$  is observed in the reversing heat flow signal, where crystallization and evaporation are observed in non-reversing signals. PVAP was heated at a linear rate to an elevated temperature, and then cooled at a linear rate before heating again (Figure 24). In the reversing heat flow signal (brown line), a transition appeared around 100°C in the first heating scan, during cooling and then again in the second heating scan. This transition, therefore, is the  $T_g$  of PVAP, which ranges from about 109°C to 118°C in the second heating scan. Furthermore, this confirmed the transition observed at 80°C by

conventional DSC and reported in the Handbook of Pharmaceutical Excipients as 78°C is not the Tg of PVAP. Instead, it is reasonable to conclude this earlier transition is in fact a water loss peak. In the first heating scan, the water loss peak appeared in the non-reversing heat flow signal (blue line) together with the endothermic relaxation peak (green line). Upon cooling and reheating, these peaks were no longer present because the water had been driven off.

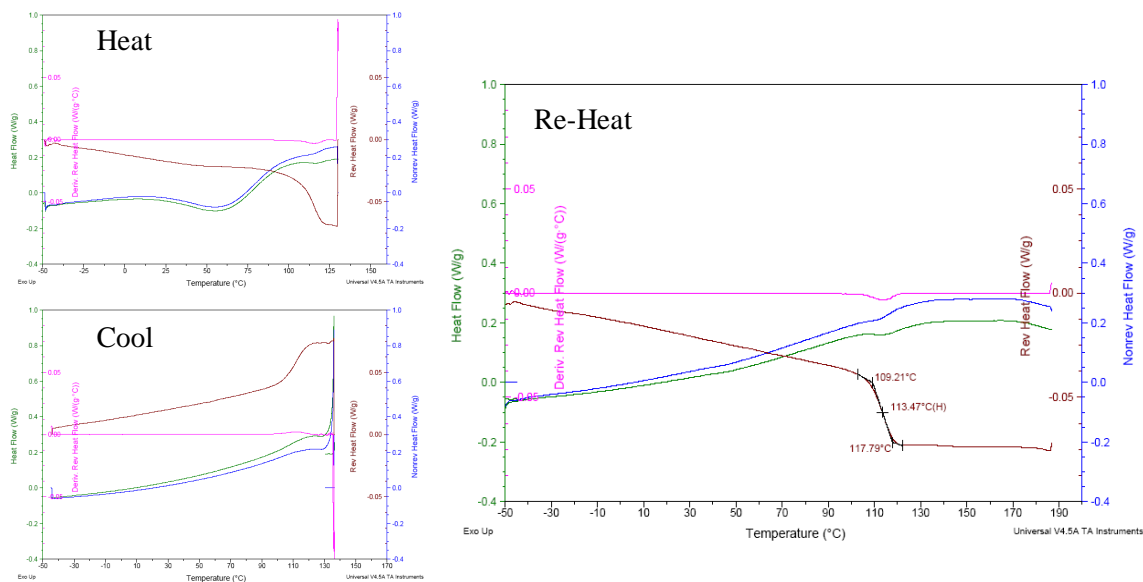


Figure 24. MDSC Heat-Cool-Heat Cycles for PVAP

### *Thermomechanical Analysis (TMA)*

TMA measured changes in sample length as a function of temperature under load. A penetration probe applied the load to a small area of sample to measure softening. For amorphous polymers, the softening point is close to Tg. The Tg of PVAP ranged from about 113°C to 133°C (Figure 25). This agreed with the experimental results obtained from MDSC, which confirms the Tg of PVAP.

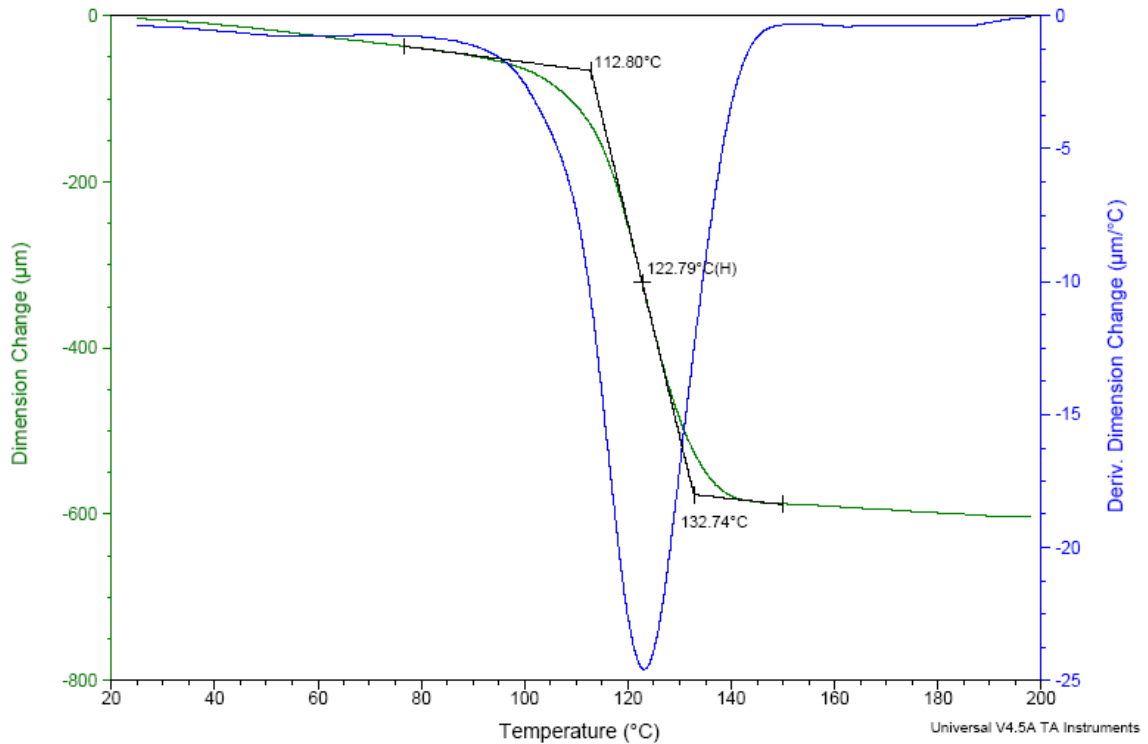


Figure 25. TMA Analysis of PVAP

### *Dynamic Mechanical Analysis (DMA)*

DMA detected transitions arising from molecular motions or relaxations. A sinusoidal stress was applied to the sample and the material's response (strain) was measured.  $T_g$  is determined from either the peak in loss modulus ( $E''$ ) or peak in  $\tan \delta$ . The  $\tan \delta$  peak corresponds more closely to the transition midpoint, while the loss modulus peak more closely denotes the onset from the glassy state into the transition. The transitions around 40°C and 80°C correspond to the vinyl acetate and vinyl alcohol homopolymers, respectively.  $T_g$  onset (peak  $E''$ ) for PVAP was about 125°C (Figure 26). PVAP was softest at about 130°C; however, decomposition occurred at about 150°C (from TGA data).

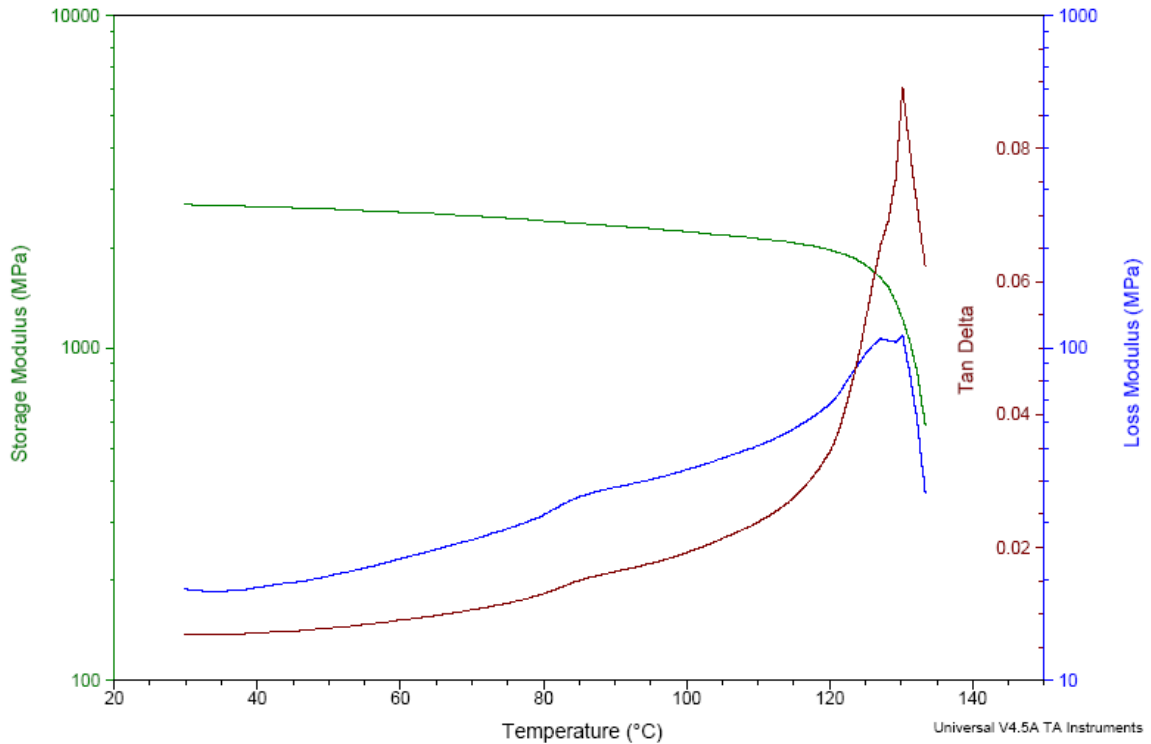


Figure 26. Storage and Loss Modulus versus Temperature by DMA for PVAP

### *Thermal Analysis Summary*

TGA was used to evaluate the thermal stability of PVAP. MDSC, TMA, and DMA were used to determine and confirm the T<sub>g</sub> of PVAP. Each thermal technique for detecting T<sub>g</sub> is based on changes in a different material property during the glass transition. Furthermore, each technique differs in sample size and sensitivity, which leads to differences in T<sub>g</sub> ranges. Table 16 summarizes the thermal analysis results for PVAP. From the data, it is apparent that PVAP has a narrow processing window for melt extrusion. That is, T<sub>g</sub> is about 120°C, which is suitable for melt extrusion and ideal for stabilizing an amorphous dispersion, however, T<sub>deg</sub> is only 150°C. To broaden the processing temperature range, plasticizers and other excipients/polymers were investigated for their ability to lower the T<sub>g</sub> of PVAP slightly so it would be further away

from  $T_{deg}$  while maintaining a  $T_g$  sufficiently high to provide stability to an amorphous solid dispersion.

Table 16. *Thermal Analysis Summary of PVAP*

Method	Thermal Results	Property Measured
TGA	Decomposition begins at 150°C	Mass (changes in mass)
MDSC	$T_g$ 109°C – 118°C	Heat capacity (changes in molar volume)
TMA	$T_g$ 113°C – 133°C	Length or Softening (dimensional changes)
DMA	$T_g$ onset 125°C, Softest at 130°C	Viscoelastic properties (molecular motions)

### **Melt Viscosity of PVAP**

The melt viscosity was obtained from 120°C to 180°C, which represents a typical extrusion processing temperature range, at constant frequency (1 Hz). PVAP showed a decrease in viscosity with rising temperature up to 150°C (Figure 27). Above 150°C, the viscosity of PVAP increased with rising temperature. This increase may be due to an initial cross-linking of the polymer chains. Given the mass loss observed by TGA at 150°C and the increased melt viscosity at 150°C, extruding PVAP must be performed below 150°C to preserve its properties. Components added to PVAP such as plasticizers, polymers or other excipients, ideally, should not only lower the  $T_g$  of PVAP but also function as a processing aid by lowering its melt viscosity.

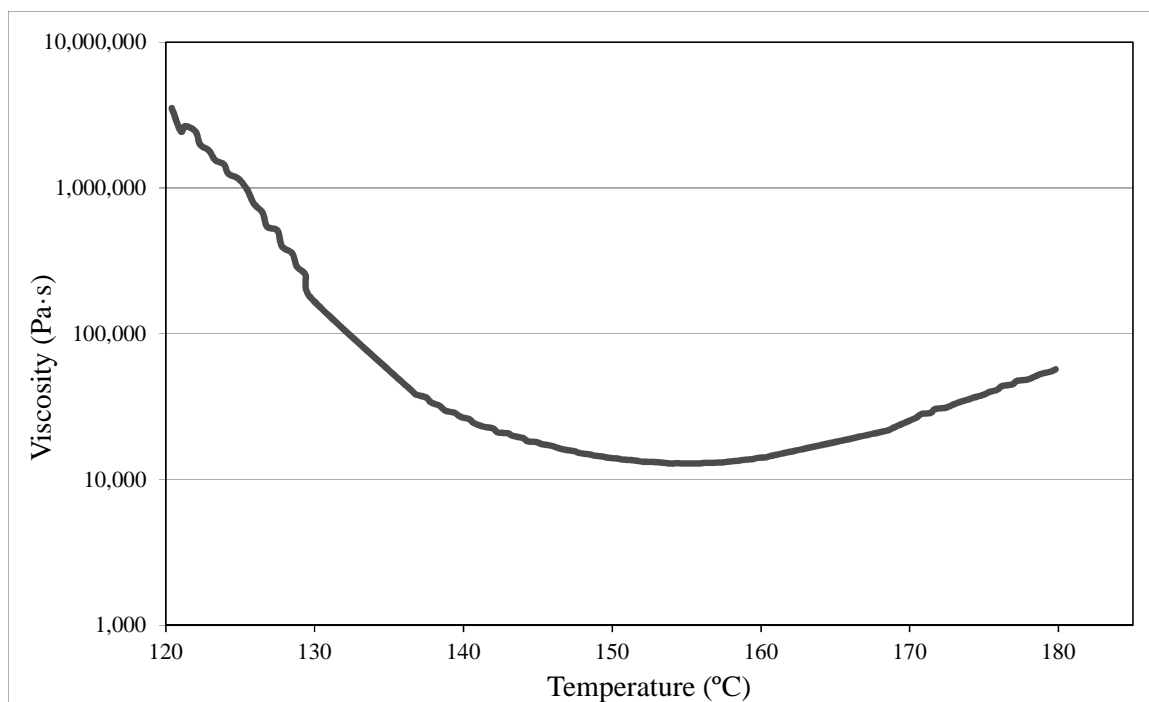


Figure 27. Melt Viscosity of PVAP

### Hygroscopicity of PVAP

#### *TGA and Loss on Drying of PVAP After Exposure to Various Relative Humidities*

The stabilizing ability of various polymers has been correlated to the moisture content of the solid dispersion caused by hygroscopicity of the component polymer (123). To evaluate the hygroscopic properties of PVAP, samples were exposed for 3 days to varying relative humidities from 0% to 90%. Figure 28 shows the mass loss and moisture content for PVAP as a function of relative humidity. The moisture content determined by LOD corroborated the mass loss categorized as sorbed moisture by TGA. The results show that, although the amount of moisture sorbed by PVAP increased with increasing relative humidity, the polymer had a low affinity for water. That is, PVAP only sorbed about 8% moisture after 3 days at 90% RH.

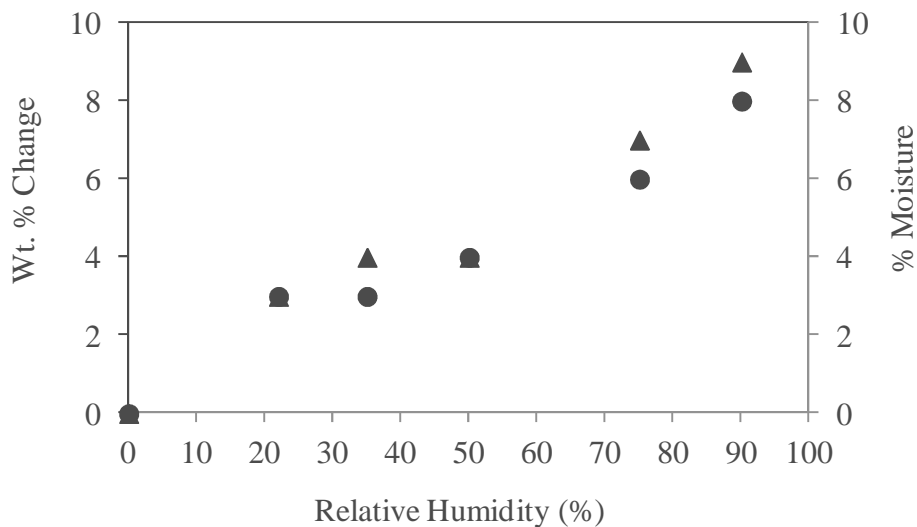


Figure 28. Moisture Uptake for PVAP as a Function of Humidity. Symbols Represent the Mass Loss Determined by TGA (Circles) and Moisture Content Determined by LOD (Triangles)

*DSC Analysis of PVAP After Exposure to Various Relative Humidities*

Moisture absorption can result in plasticization and enhanced molecular mobility, which can lead to crystallization (123). For that reason, the ability of water to plasticize PVAP was investigated by measuring the glass transition temperature of samples exposed for 3 days to varying relative humidities from 0% to 90%. The Tg midpoint of the PVAP transition as a function of relative humidity is shown in Figure 29. It can be seen that the Tg of PVAP (121°C) remained relatively constant with increasing relative humidity. From this data, it is apparent that water is not an efficient plasticizer for PVAP. Furthermore, it is reasonable to conclude that PVAP is slightly hygroscopic (140) and that water uptake determined by TGA after 3 days at different relative humidities was predominantly surface adsorption.

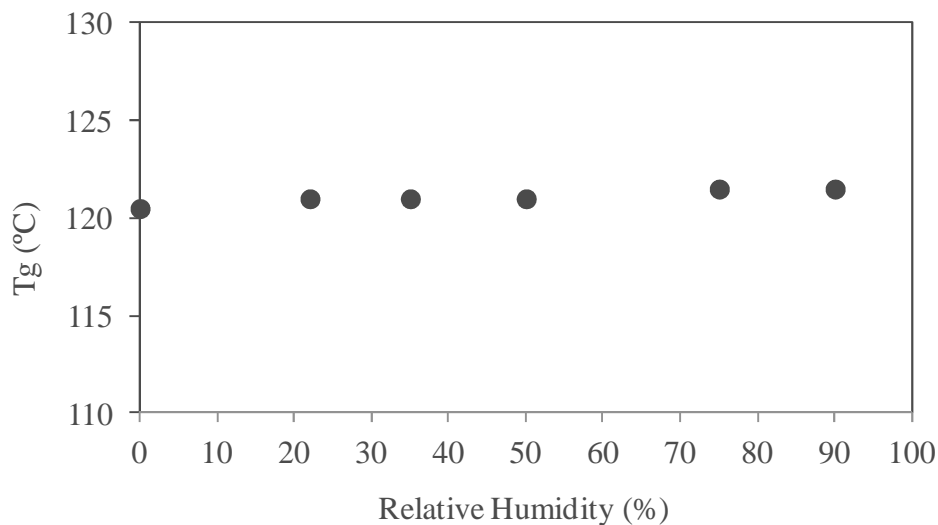


Figure 29. The T<sub>g</sub> of PVAP with Increasing Humidity as Measured by MDSC in the Reversing Heat Flow Signal

#### *Water-Solid Interactions*

There are two primary water-solid associations: adsorption of water onto the solid surface and absorption of water into the bulk structure (175). Adsorption of water molecules to a solid surface can result from attractive forces (physical adsorption) or binding forces (chemical adsorption). The ability of water to absorb into a bulk solid depends on the number and type of polar functional groups capable of hydrogen bonding, and on the amount of free volume in a polymer network (123,176). In an amorphous solid, one indication that water has advanced from surface adsorption to bulk absorption is a change in glass transition temperature.

In the case of PVAP, the water content of the polymer increased to only 8% at 90% RH, and it showed no depression in T<sub>g</sub> from 0% to 90% RH. Both results suggest that the water uptake by PVAP was limited to surface adsorption after 3 days at 23°C. Structurally, PVAP includes the polar functional groups capable of forming hydrogen bonds that might enable it to absorb water into its bulk. However, it appears that

hydrophobic and steric barriers from the benzene rings and weak hydrogen bonding between water and PVAP's acetate and phthalate carbonyl groups may be hindering the intermolecular bond formation required for absorption (176,177,178). This is consistent with observations from Taylor et al. who reported that the strength of the hydrogen bond formed with water depended on the chemistry of the polymer, which in turn affected moisture absorption (176). Their results showed that polyvinyl acetate (PVAc), a monomer component of PVAP, took up only about 3% water at 94% RH compared to PVP, which absorbed more than 40% water at the equivalent relative humidity (176). The larger magnitude of moisture absorption into PVP compared to PVAc correlated with the stronger water-pyrrolidone hydrogen bond as compared to the water-acetate hydrogen bond (176).

In addition to the chemical structure of the polymer, its physical state has also been shown to influence the extent of its interactions with water (176). More water-polymer interactions were reported for polyvinyl pyrrolidone-co-vinyl acetate (PVPVA) when the polymer existed in the rubbery state (176). This is presumably a result of the increased accessibility of bonding sites as a consequence of increased free volume and polymer chain mobility (176).

In this study, PVAP was exposed to varying relative humidities from 0% to 90% for 3 days at 23°C. The increase in the water content of PVAP did not have a plasticizing effect on PVAP, as reflected in its steady T<sub>g</sub>, which implied that PVAP remained in the glassy state throughout the experiment. It seems the physical state of PVAP, therefore, was unfavorable for interactions with water.

### *Moisture Uptake Summary*

PVAP did not absorb water on exposure to high relative humidities. Its low affinity for moisture is attributable to weak solid-water interactions. The slight hygroscopicity demonstrated by PVAP may provide a stability advantage for solid dispersions during storage.

### **Solubility Parameter**

The calculated solubility parameter can be used as an initial tool to predict the miscibility of materials. For this study, firstly, the Hansen solubility parameter of PVAP was determined based on the methods of Hoftyzer/Van Krevelen and Hoy. Hansen defined three partial solubility parameters ( $\delta_d$ ,  $\delta_p$ , and  $\delta_h$ ) that were combined to form the total solubility parameter ( $\delta_t$ ). Secondly, the solubility parameter of various polymers, plasticizers, and excipients were matched to those of PVAP by observing the relative difference in the total solubility parameter ( $\Delta\delta$ ). Lastly, the solubility parameter for itraconazole, the model drug used in this study, was compared to PVAP.

### *Method of Hoftyzer and Van Krevelen*

The solubility parameter results for PVAP based on the method of Hoftyzer and Van Krevelen are presented below. Given the various functional groups on PVAP (Figure 30), the values of  $F_{di}$ ,  $F_{pi}^2$ ,  $E_{hi}$  and  $V$  were obtained from chemical handbooks and summarized in Table 17. The partial and total solubility parameters were calculated from the group contributions and shown in Table 18.

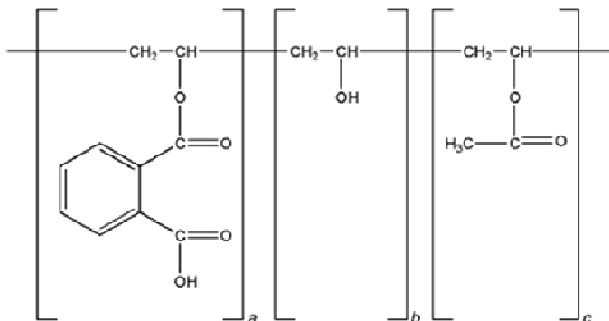


Figure 30. Chemical Repeat Units of PVAP

Table 17. Group Contributions for PVAP (Method of Hoftyzer/Van Krevelen)

Group <sub>z</sub>	F <sub>di</sub>	F <sub>pi</sub> <sup>2</sup>	E <sub>hi</sub>	Σ <sup>2</sup> V/cm <sup>3</sup> mol <sup>-1</sup>
(3) CH <sub>2</sub>	810	0	0	48.3
(3) CH	240	0	0	-3.0
(2) COO <sup>-</sup>	780	980	14,000	36.0
(1) COOH	530	420	10,000	28.5
(1) Phenylene	1270	110	0	52.4
(1) OH	210	500	20,000	10.0
(1) CH <sub>3</sub>	420	0	0	33.5
Σ	4260	2010	44,000	205.7
Avg. MW	707,160	333,660	7,304,000	34,146.2

Table 18. Hansen Solubility Parameters for PVAP (Method of Hoftyzer/Van Krevelen)

Solubility Parameter	δ <sub>d</sub>	δ <sub>p</sub>	δ <sub>h</sub>	δ <sub>t</sub>
Average MW	20.7	0.02	14.6	25.3
Monomer Unit	20.7	0.20	14.6	25.3
Homopolymer (a)	22.3	0.28	12.2	25.4
Homopolymer (b)	22.3	0.89	28.2	36.0
Homopolymer (c)	12.4	0.33	10.3	20.2

### *Method of Hoy*

The Hansen solubility parameter can be estimated based on different methods and each method predicts the cohesive energy with a mean accuracy of about 10%.

Therefore, the solubility parameter for PVAP was calculated using two different approaches. The second approach, based on the method of Hoy, is presented below.

Given the various functional groups on PVAP (Figure 30), the values of  $F_t$ ,  $F_p$ ,  $\Delta_T^{(P)}$  and  $V$  were obtained from chemical handbooks and summarized in Table 19. The solubility parameter components were predicted from group contributions and shown in Table 20.

Table 19. *Group Contributions for PVAP (Method of Hoy)*

Group <sub>z</sub>	$F_t$	$F_p$	$\Delta_T^{(P)}$	$V$
(3) CH <sub>2</sub>	807	0	0.06	46.65
(3) CH	528	0	0.039	28.68
(2) COO <sup>-</sup>	1280	1056	0.1	47.4
(1) COOH	565	415	0.039	26.1
(1) Phenylene	20.2	-13.3	0.0015	-
(1) OH	675	675	0.049	12.45
(1) CH <sub>3</sub>	303.5	0	0.022	21.55
$\Sigma$	4178.7	2132.7	0.3105	182.83
Avg. MW	693664.2	354028.2	51.543	30349.78

Table 20. *Hansen Solubility Parameters for PVAP (Method of Hoy)*

Solubility Parameter	$\delta_d$	$\delta_p$	$\delta_h$	$\delta_t$
Average MW	14.8	14.5	11.7	23.8
Monomer Unit	14.8	14.5	11.7	23.8
Homopolymer (a)	13.9	15.0	10.9	23.2
Homopolymer (b)	15.4	18.1	19.9	31.0
Homopolymer (c)	15.2	11.6	7.6	20.6

### *Solubility Parameter Summary*

In this study, the average of the Hoftyzer/Van Krevelan and Hoy values have been used to determine the solubility parameter of PVAP. The two methods predicted similar total solubility parameter ( $\delta$ ) values for PVAP. A summary of the values is listed in Table 21. The calculated solubility parameter for the average molecular weight of PVAP is  $24.6 \text{ MPa}^{1/2}$ . Drugs and/or excipients with similar solubility parameter values are likely to be miscible with PVAP. More specifically, Greenhalgh et al. showed that compounds with a  $\Delta\delta < 7.0 \text{ MPa}^{1/2}$  are likely to be miscible and compounds with  $\Delta\delta > 10.0 \text{ MPa}^{1/2}$  are likely to be immiscible. Therefore, drugs and excipients with a  $\delta$  of 18-32  $\text{MPa}^{1/2}$  are likely to be miscible with PVAP and form glass solutions or one-phase systems when melt extruded. However, drugs and excipients with a  $\delta$  less than 15 or greater than 35  $\text{MPa}^{1/2}$  are likely to be immiscible with PVAP and are not expected to form a glass solution, but instead, form a two-phase solid dispersion when melt extruded.

Table 21. *Total Solubility Parameter for PVAP*

PVAP	Solubility Parameter ( $\delta$ )		
	Hofsteyer/Van Krevelen (MPa) <sup>1/2</sup>	Hoy (MPa) <sup>1/2</sup>	Mean (MPa) <sup>1/2</sup>
Average MW	25.3	23.8	24.6
Monomer Unit	25.3	23.8	24.6
Homopolymer (a)	25.4	23.2	24.3
Homopolymer (b)	36.0	31.0	33.5
Homopolymer (c)	20.2	20.6	20.4

*Solubility Parameters for Plasticizers, Polymers and Other Excipients*

To broaden the processing temperature range of PVAP, plasticizers were investigated for their ability to lower the T<sub>g</sub> of PVAP so it would be further away from T<sub>deg</sub> of PVAP but not so low that it jeopardized storage stability. Plasticizers were selected based on estimates of the solubility parameter calculated from the approaches of Hofsteyer/Van Krevelen and Hoy. A list of plasticizers and their corresponding solubility parameter values is listed in Table 22. As an alternative to plasticizers, miscible polymers and other excipients can be used to improve the processability of PVAP. Therefore, the solubility parameters for various polymers and excipients were determined and listed in Table 23 and Table 24, respectively.

Table 22. *Difference in Solubility Parameter ( $\Delta\delta$ ) of PVAP and Various Plasticizers*

Plasticizer	Solubility Parameter ( $\delta$ ) (MPa) <sup>1/2</sup>	$\Delta\delta$ (MPa) <sup>1/2</sup> $\Delta\delta < 7$ likely miscible $\Delta\delta > 10$ likely immiscible	Pharmaceutical Regulatory Status
PVAP	24.6	-	US, EU
Triethyl citrate	21.0-20.4	3.6-4.6	US, EU, JP
Triacetin	22.0-20.0	2.6-4.6	Global
Polyethylene glycol (PEG) 200 - 6000	22.4 - 26.1	1.2-2.2	Global
Glycerin	33.8	9.2	US, EU, JP
Propylene glycol	30.3-25.8	5.7-1.2	Global
Dibutyl phthalate	20.2-19.0	4.4-5.6	EU
Diethyl phthalate	20.5	4.1	US, EU
Dibutyl sebacate	18.8	5.8	US, EU, IN
Medium chain triglycerides	20.0	4.6	US, EU, JP, IN
Palmitic acid	16.1	8.5	US, EU, JP

Table 23. *Difference in Solubility Parameter ( $\Delta\delta$ ) of PVAP and Various Polymers*

Polymer	Solubility Parameter ( $\delta$ ) (MPa) <sup>1/2</sup>	$\Delta\delta$ (MPa <sup>1/2</sup> ) $\Delta\delta < 7$ likely to be miscible $\Delta\delta > 10$ likely to be immiscible
PVAP	24.6	-
PEO	34.7	10.1
EPO	21.3	3.3
Soluplus	19.4	5.2
PVA	34.4-19.9	9.8-4.7
CAP	27.2-21.7	2.6-2.9
EC	21.1-19.4	3.5-5.2
HEC	25.5-19.8	0.9-4.8
HPC	25.5-20.8	0.9-3.8
HPMC	30.6-22.8	6.0-1.8
HPMCP	26.4-17.2	1.8-7.4
MC	21.3	3.3
PVP	21.4	3.2
Methacrylic acid	19.0	5.6
Methyl methacrylate	17.9	6.7

Table 24. *Difference in Solubility Parameter ( $\Delta\delta$ ) of PVAP and Various Excipients*

Excipient	Solubility Parameter ( $\delta$ ) (MPa) <sup>1/2</sup>	$\Delta\delta$ (MPa <sup>1/2</sup> ) $\Delta\delta < 7$ likely to be miscible $\Delta\delta > 10$ likely to be immiscible
PVAP	24.6	-
Tweens / Polysorbates	29.4-24.4	4.8-0.2
Citric acid	29.4	4.8
Sorbic acid	24.4	0.2
Mannitol	39.1	14.5
Sucrose	34.8-32.8	10.2-8.2
Lactose (anhydrous)	33.2	8.6
MCC	30.2	5.6
Butyl paraben	21.6	3.0
Methyl paraben	24.5	0.1
Cetyl alcohol	18.3	6.3
Ethylene glycol	29.6	5.0
Magnesium stearate	18.2	6.4
Stearic acid	17.6-15.8	7.0-8.8
Oleic acid	16.1-15.8	8.5-8.8

### **Melt Viscosity of PVAP and Plasticizers**

Several plasticizers were evaluated from Table 22, however, it was found that levels as high as 30% - 40% w/w were required to reduce the melt viscosity of PVAP and improve its extrusion processability. The high levels of plasticizer required for PVAP were consistent with the work conducted by Mehuys et al. who extruded hollow cylindrical tubes of PVAP, filled the tubes with drug, and then crimped the ends of the cylinders to produce what they called, extruded enteric capsules (179). They reported that PVAP extruded into clear and flexible films at 125°C when it contained 40% w/w

triacetin or triethyl citrate (TEC), however, PVAP-cylinders containing less than 40% triacetin or TEC were brittle and difficult to extrude. Furthermore, the PVAP mixtures containing 40% plasticizer reportedly had T<sub>g</sub> values of 44.9°C with triacetin and 44.1°C with TEC (179). These low T<sub>g</sub> values would be detrimental for amorphous solid dispersions over time.

Sample mixtures of PVAP containing 30%, 40% and 50% TEC or triacetin were prepared. Pictures of these samples are shown as examples (Figure 31 and Figure 32). All the plasticizers evaluated performed similarly, except polyethylene glycol, which is also shown in Figure 33. The PVAP-plasticizer mixtures were heated to 100°C, 120°C, 140°C, and 160°C to assess their miscibility and melt characteristics. At 30% TEC, the PVAP-plasticizer mixtures were transparent and completely melted at 140°C. At 40% and 50% TEC, the PVAP-plasticizer mixtures were transparent and completely melted at 100°C (Figure 31). This suggested the PVAP-plasticizer mixtures were miscible and TEC was plasticizing PVAP because as the concentration of TEC increased, the melt temperature of PVAP decreased. The levels of TEC needed to plasticize PVAP, however, are significantly high and would pose a stability concern during storage. Triacetin also appeared to be lowering the T<sub>g</sub> of PVAP based on melt characteristics; however, the melts were opaque, which suggests at least partial immiscibility between the polymer and plasticizer (Figure 32). Lastly, based on the Hansen solubility parameter, PVAP should be miscible with polyethylene glycol (PEG). However, at each plasticizer level studied (up to 50% w/w), at or below 140°C, the material only partially melted and most likely, only the PEG melted based on the visual observations of pure PVAP at 140°C during TGA testing (Figure 20). At 160°C, the partially melted material

discolored, which was most likely PVAP discoloring based on the decomposition data obtained by TGA. This suggested PVAP and PEG were immiscible. Pictures of the partial melts and discolored melts are shown in Figure 33. The observed behavior of the PVAP and PEG mixture was consistent with expectations based on their partial solubility parameters; although their parameters were similar, they were distinct enough to predict the two components would be immiscible. The partial and total solubility parameters for PVAP and PEG are shown in Table 25 for comparison. Furthermore, it appears that PVA, a monomer component of PVAP, is not miscible with PEG.

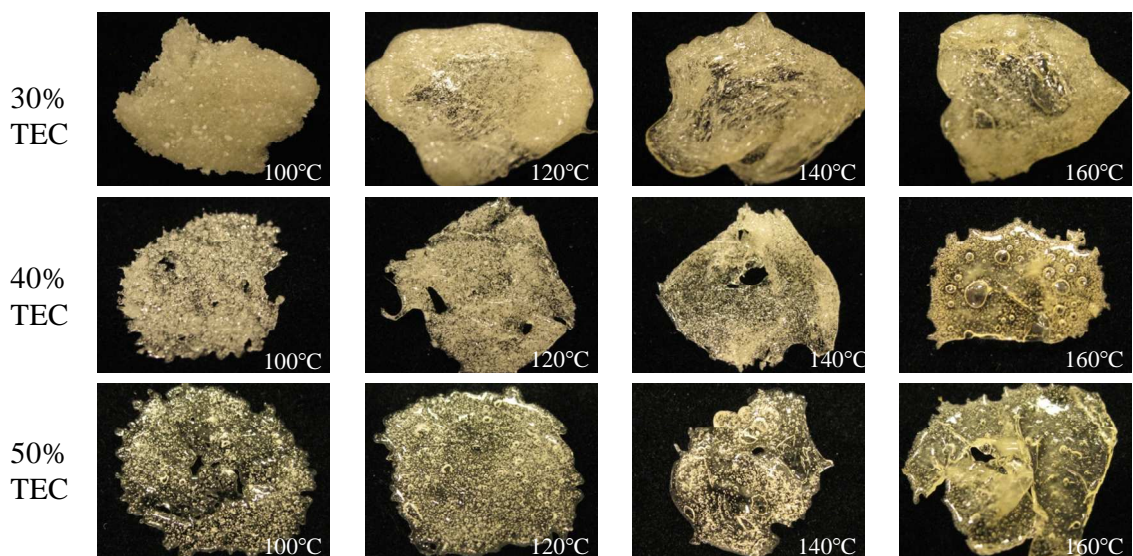


Figure 31. PVAP Mixtures Containing 30%, 40% and 50% w/w TEC and Heated to 100°C, 120°C, 140°C and 160°C

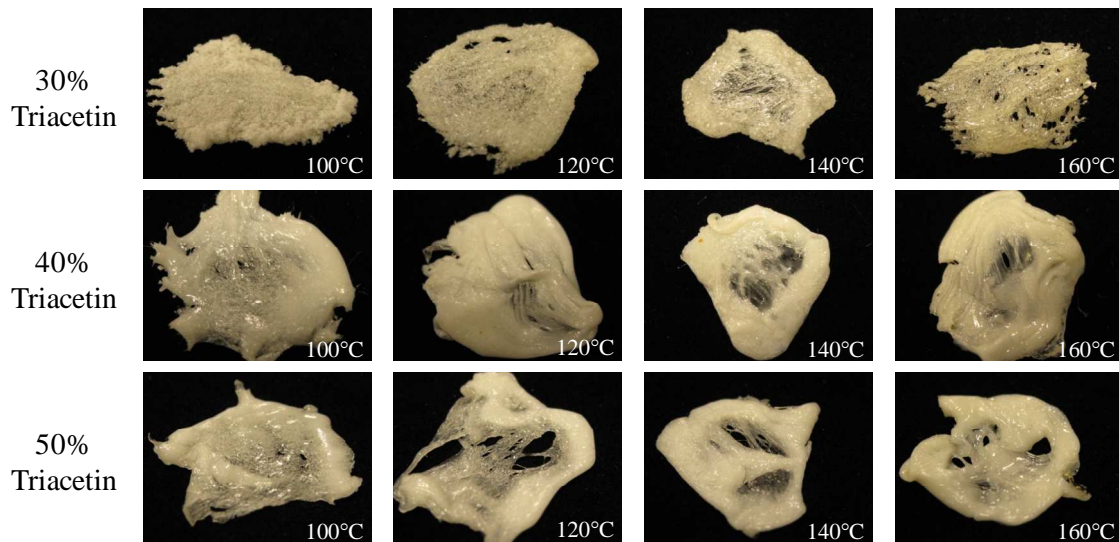


Figure 32. PVAP Mixtures Containing 30%, 40% and 50% w/w Triacetin and Heated to 100°C, 120°C, 140°C and 160°C



Figure 33. PVAP Mixtures Containing 50% PEG 400 or PEG 3350 and Heated to 100°C, 120°C, 140°C and 160°C

Table 25. *Partial and Total Solubility Parameters for PVAP, PVA, and PEG*

Polymer	Solubility Parameters (MPa) <sup>1/2</sup>			
	$\delta_d$	$\delta_p$	$\delta_h$	$\delta_t$
PVAP co-polymer	20.7	0.20	14.6	25.3
PVA co-polymer	16.4	14.7	24.2	32.7
Homopolymer (a), phthalate	22.3	0.28	12.2	25.4
Homopolymer (b), polyvinyl alcohol	22.3	0.89	28.2	36.0
Homopolymer (c), polyvinyl acetate	12.4	0.33	10.3	20.2
PEG	17.5	1.0	9.4	19.9

### **PVPVA as an Alternative to Plasticizers**

As an alternative to plasticizers, miscible polymers and other excipients were evaluated for their ability to aid in the processability of PVAP. Ghebremeskel et al. studied the effect of surfactants on the processability of various polymer-API blends (118). The authors showed surfactants decreased T<sub>g</sub> and melt viscosity, which improved the processability of the melt extruded blends (118). One example of a polymer that appears to be miscible with PVAP is PVPVA; the difference in their total solubility parameters ( $\Delta\delta$ ) was 5.6 MPa<sup>1/2</sup>, shown in Table 26.

PVPVA is commonly used in melt extrusion, however, its hygroscopicity has been cited as the cause for instability of amorphous systems during storage; its commercial pharmaceutical use is limited for this reason (102,180,181). PVPVA is easily extruded at 120°C to 130°C without additives (96) so it appears particularly well suited as a secondary polymer or processing aid for PVAP. Therefore, PVPVA was characterized alone and then in combination with PVAP. In addition, the solubility parameter for itraconazole was compared to PVAP and PVPVA and based on  $\Delta\delta$ , the

drug is predicted to be miscible with both polymers (Table 26). Miscibility will also be determined using Tg measurements by DSC for the ITZ-polymer blends.

Table 26. *Partial and Total Solubility Parameters for PVAP, PVPVA, and Itraconazole*

Polymer	$\delta_d$	$\delta_p$	$\delta_h$	$\delta_{total}$	$\Delta\delta$ (MPa) <sup>1/2</sup> $\Delta\delta < 7$ likely miscible $\Delta\delta > 10$ likely immiscible
PVAP	20.7	0.02	14.6	25.3	-
PVPVA	17.4	0.5	9.2	19.7	5.6
ITZ	19.4	5.4	10.3	22.6	2.7 for ITZ-PVAP 2.9 for ITZ-PVPVA

### Characterization of PVPVA

#### *MDSC of PVPVA*

MDSC was used to separate the total heat flow signal into reversing and non-reversing signals. PVPVA was heated at a linear rate to an elevated temperature, and then cooled at a linear rate before heating again. In the reversing heat flow signal, a transition appeared around 100°C in the first heating scan (blue line), during cooling (red line) and then again in the second heating scan (green line). This transition is the Tg of PVPVA, which ranged from about 95°C to 115°C in the second heating scan. The Tg midpoint of PVPVA was 107°C (Figure 34). This was consistent with the Tg of 101°C reported by the manufacturer (102). There also appears to be a secondary transition for PVPVA around -20°C.

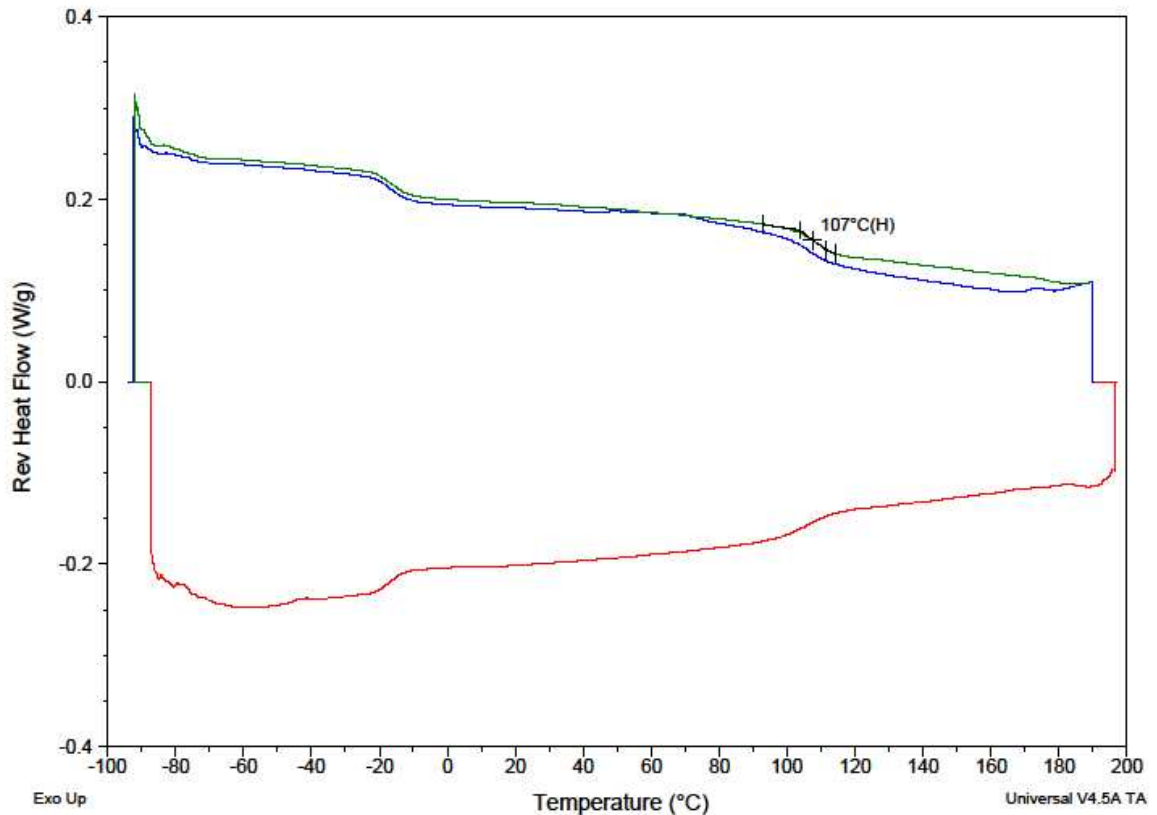


Figure 34. MDSC Heat (blue line), Cool (red line), Heat (green line) Cycle for PVPVA

### *TGA of PVPVA*

TGA measured the mass of PVPVA as a function of temperature. The initial mass loss of about 3.0% was due to moisture, which agreed with LOD results. The decomposition in nitrogen was observed as a large mass loss step with an onset of about 253°C (Figure 35). The manufacturer reports  $T_{deg}$  by TGA analysis of PVPVA at 230°C (102). Since extrusion temperatures rarely exceed 180°C and the  $T_{deg}$  of PVAP is 150°C, the discrepancy between  $T_{deg}$  determined in this study for PVPVA and that of the manufacturer is minor and most likely results from different analysts interpreting the trace.

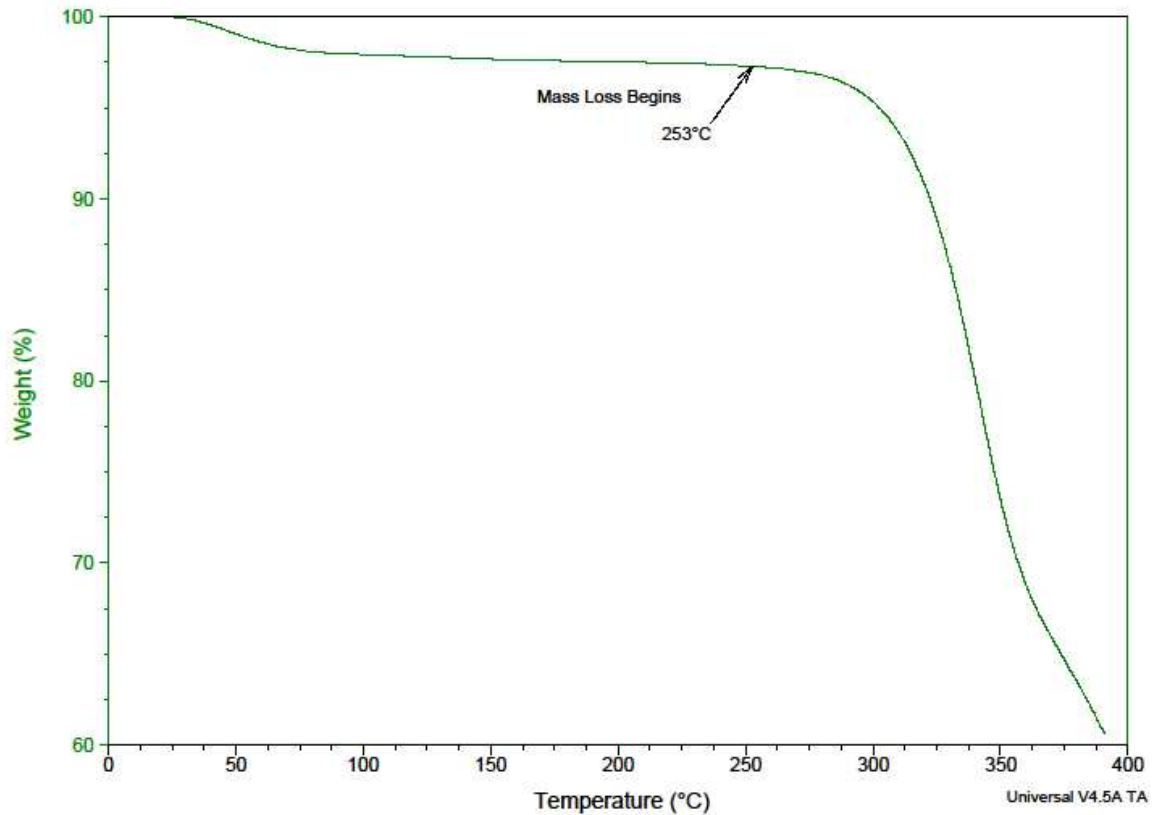


Figure 35. Weight Loss (%) as a Function of Temperature by TGA for PVPVA

#### *Melt Viscosity of PVPVA*

The melt viscosity for PVPVA was obtained from 120°C to 180°C at constant frequency (1 Hz). PVPVA showed a decrease in viscosity with increasing temperature across the entire temperature range studied. This is ideal thermoplastic behavior for a polymer used in melt extrusion. Unlike PVAP, which increased in viscosity above 150°C, PVPVA continued to decrease in viscosity up to 180°C (Figure 36).

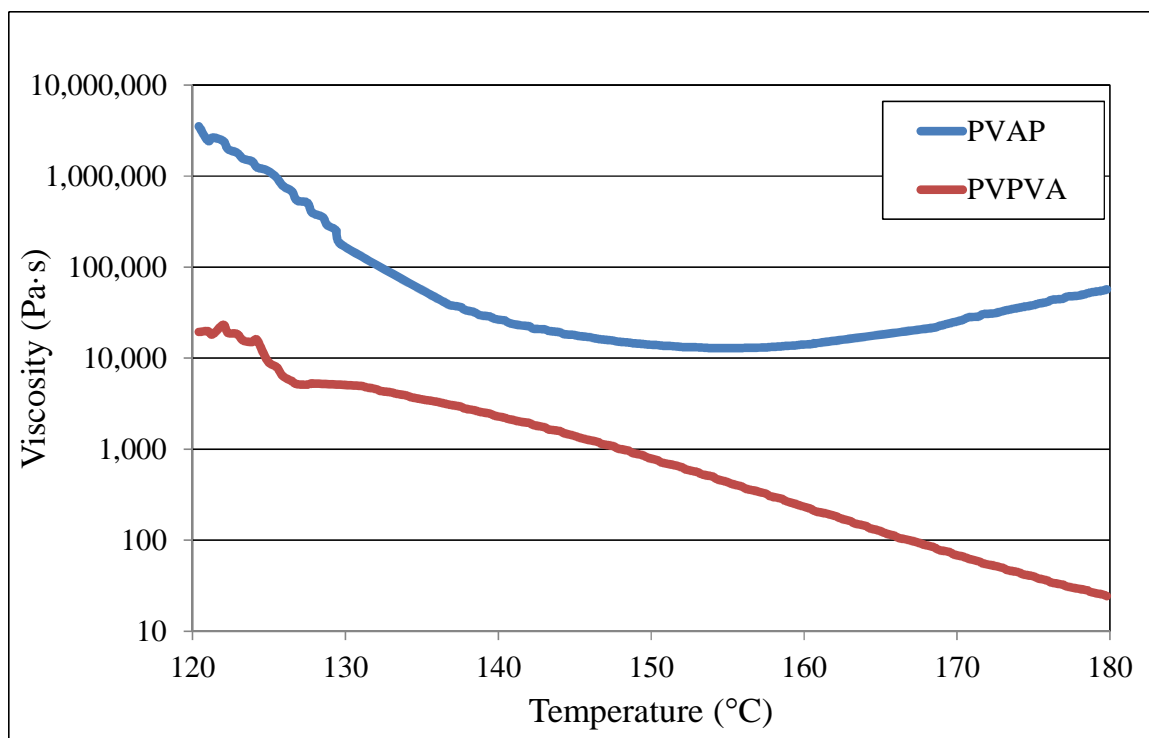


Figure 36. Melt Viscosity of PVPVA and PVAP

#### *Moisture Uptake of PVPVA*

One issue with using PVPVA is its hygroscopicity. Solubilizers that absorb too much water from the ambient air can cause unwanted crystallization of amorphous API in a solid dispersion (181). A hygroscopicity that is too great may also cause problems in processing the dosage form (181). To evaluate the hygroscopic properties of PVPVA, samples were exposed for 3 days to varying relative humidities from 0% to 90%. Figure 37 shows the moisture content determined by LOD for PVPVA as a function of relative humidity. The results show that the amount of moisture sorbed by PVPVA increased with increasing relative humidity. At 20% RH, PVPVA sorbed about 8% moisture compared to only 3% for PVAP. Above 30% RH, the moisture uptake of PVPVA continued to increase and became alarmingly high. PVPVA sorbed nearly 40% moisture after 3 days at 90% RH compared to only about 8% for PVAP. Based on this consistent

data, PVPVA is more hygroscopic than PVAP. Similar results were reported from sorption isotherms for PVPVA by Kolter et al. (102).

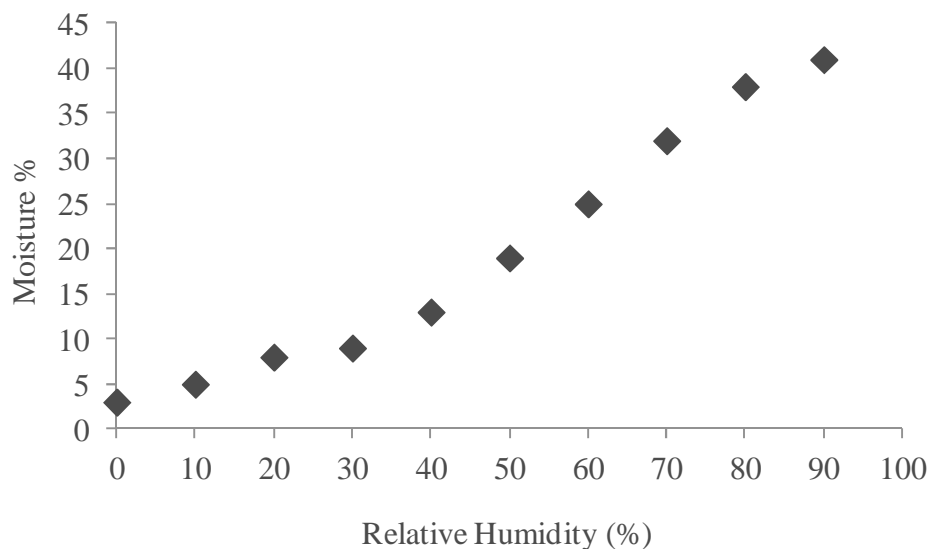


Figure 37. Moisture Uptake for PVPVA by LOD as a Function of Humidity

#### *PVPVA Characterization Summary*

PVPVA is commonly used in melt extrusion but its hygroscopicity has precluded its more widespread commercial pharmaceutical use. The polymer has a broad melt extrusion processing range owing to its  $T_g$  of about  $107^\circ\text{C}$  and  $T_{deg}$  of about  $250^\circ\text{C}$ . The polymer extrudes easily, without the need for additional plasticizers or thermal lubricants, at  $120^\circ\text{C}$  to  $130^\circ\text{C}$ . Furthermore, its melt viscosity decreases with increasing temperature, which is ideal for melt extrusion. The properties of PVPVA make it a particularly good candidate for co-extrusion with PVAP. By combining PVAP with PVPVA, which has a low  $T_g$  relative to PVAP but high  $T_g$  relative to plasticizers, the processability of PVAP may improve without impacting the stability of the extrudate. Furthermore, PVAP is much less hygroscopic than PVPVA so it may provide a stability

advantage for solid dispersions during storage. Therefore, blends of PVAP and PVPVA were evaluated further for miscibility by MDSC analysis.

### **Miscibility of PVAP-PVPVA Polymer Blends**

Polymers are miscible if they form a single, one-phase system. The most widely used experimental technique to determine miscibility uses the measurement of T<sub>g</sub> via DSC (68). Generally, the observation of a single glass transition somewhere between the T<sub>g</sub> values of the individual component polymers indicates a single, uniform composition and therefore a miscible system. Conversely, an immiscible blend will show two glass transition temperatures with T<sub>g</sub> values corresponding to those of the individual components.

The miscibility of PVAP and PVPVA were assessed at the following ratios: 10:90%, 20:80%, 30:70%, 40:60% and 50:50% w/w PVAP:PVPVA. From the thermograms, the two polymers appeared miscible at 10:90%, 20:80%, and 30:70% w/w PVAP:PVPVA. That is, only one T<sub>g</sub> was observed for the polymer blends (Figure 38). At 40:60% and 50:50% w/w PVAP:PVPVA, however, very small changes in the appearance of the transitions, a trough midway through the transition, suggested there were two T<sub>g</sub> values and therefore, at these ratios, the two polymers are not completely miscible, but instead, only partially miscible. Therefore, 10%, 20%, and 30% w/w PVAP was selected for melt extrusion processing. The MDSC data also showed the T<sub>g</sub> values of the combined polymer systems, which were lower than that of PVAP but higher than PVPVA. This also indicated the polymers were at least partially miscible at all ratios

studied. More importantly, lowering the  $T_g$  of PVAP by adding PVPVA should allow extrusion to occur at lower temperatures, further away from  $T_{deg}$  of PVAP.

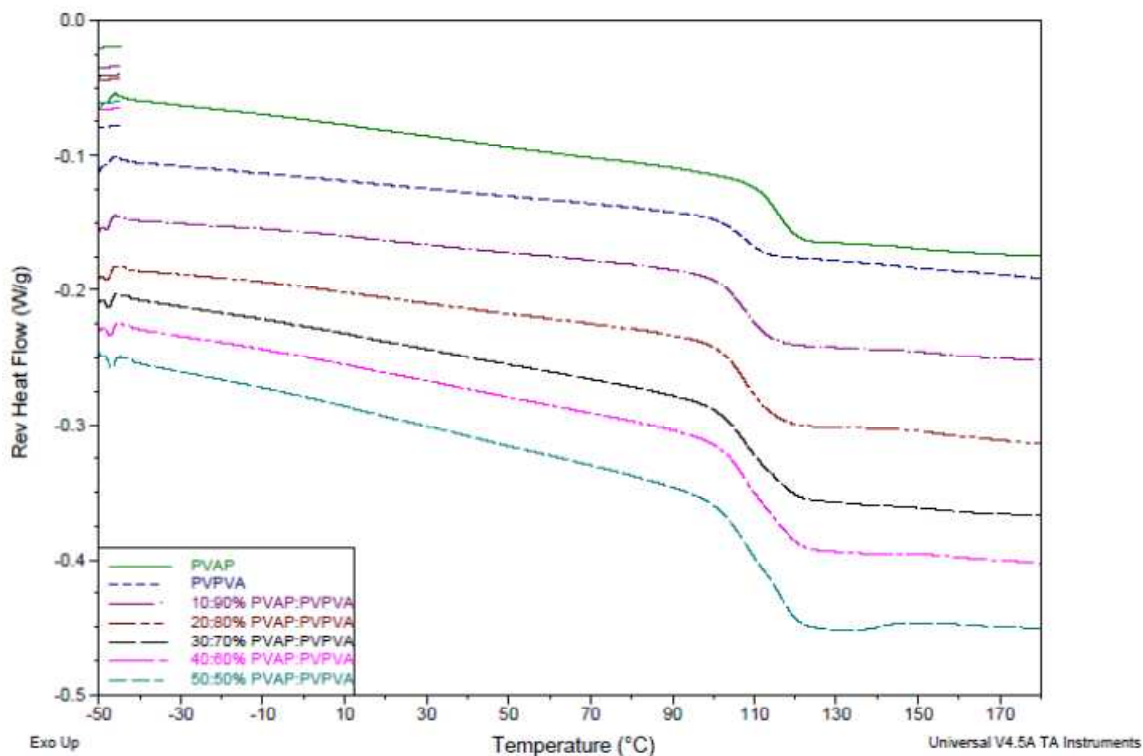


Figure 38. MDSC Analysis of PVAP-PVPVA Polymer Blends

### Processability of the Polymer Blends

The torque generated during the extrusion process is a key indicator of the melt viscosity. Torque was monitored throughout the process because high melt viscosities generate excessive torque and complicate manufacturing. The torque generated by the different polymer ratios was plotted to assess how the concentration of PVPVA facilitated flow through the extruder. PVAP is very difficult to extrude on its own because of its high melt viscosity and low decomposition temperature. However, the processability of PVAP improved significantly when mixed with PVPVA. The three ratios: 10:90%, 20:80%, and 30:70% w/w performed similarly in the extruder (Figure

39). Each blend extruded with similar torque and therefore, similar melt viscosity values. In an effort to maintain the integrity of the solid dispersion over time, the polymer blend containing the highest level of PVAP (30%) was selected for solid dispersion preparation with itraconazole.

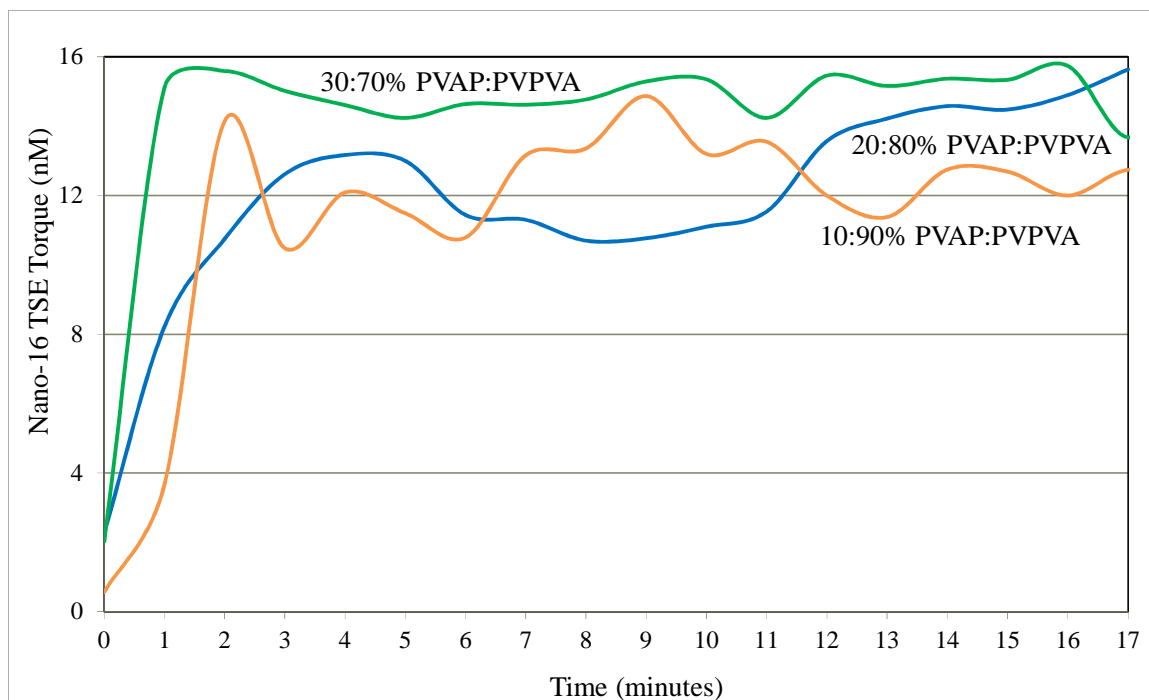


Figure 39. Torque Generated from Different Polymer Ratios as a Function of Extrusion Time

### Analysis of PVAP Content

Assay testing was used to determine the content of PVAP after exposure to 130°C, 140°C and 150°C for 5 minutes, which represented the longest residence time in the extruder. Below its decomposition temperature (150°C), PVAP remained fairly stable, although a slight decrease in PVAP content, and corresponding increase in free phthalic acid degradant content, was apparent as early as 140°C (Table 27). This behavior indicated that extrusion temperatures should not exceed 140°C and, more preferably, should remain below 140°C.

Table 27. *PVAP Content as a Function of Temperature*

Sample ID	% PVAP UV/Vis	% PVAP RI	% Free Phthalic Acid
PVAP	104.8	104.2	0.43
PVAP at 130°C	102.7	103.1	0.48
PVAP at 140°C	101.8	102.1	0.75
PVAP at 150°C	47.2	41.3	2.0

### **Melt Viscosity of the Polymer Blend**

Overall, the processability of PVAP improved significantly when mixed with PVPVA. One explanation for the improved processability is a reduction in the melt viscosity of PVAP caused by PVPVA lowering its T<sub>g</sub> or acting as a thermal lubricant. From Figure 40, it is apparent that the melt viscosity of pure PVPVA is much lower than pure PVAP. Furthermore, the polymer blend (30:70% PVAP:PVPVA) had a much lower melt viscosity than pure PVAP. PVPVA seems to be acting as a thermal lubricant for PVAP, lowering its melt viscosity and increasing its plasticity, even at temperatures above T<sub>deg</sub> of PVAP. Furthermore, PVPVA reduced the T<sub>g</sub> of PVAP from 116°C to 109°C, indicating PVPVA also acts as a plasticizer for PVAP at miscible polymer blend ratios. Plasticizing effects result in a reduction in T<sub>g</sub> and melt viscosity (118).

Similar improvements in extrusion processing were reported with PVPVA and other polymers (102). Kolter et al. combined PVPVA with Kollidon SR (polyvinyl acetate/polyvinyl pyrrolidone), Kollicoat IR (polyvinyl alcohol/polyethylene graft copolymer), Kollidon 30 (vinylpyrrolidone MW 50,000), and Kollidon 90F (vinylpyrrolidone MW 1,250,000) to produce different blends (102). The polymer ratios were varied from 0:100% to 100:0% w/w to investigate the effect of polymer

composition on the minimum processing temperature by extrusion (102). The tested polymer combinations are summarized in Table 28. PVPVA had almost no effect on the extrusion processing temperature of Kollidon SR; all blends extruded at 140°C (102). For all compositions with Kollicoat IR, the blends extruded at 150°C, versus 160°C to 190°C for the pure polymer (102). Pure polymers of Kollidon 30 and Kollidon 90 F were reportedly impossible to extrude due to their high T<sub>g</sub> and melt viscosities (102). However, in the presence of PVPVA, Kollidon 30 could be melt extruded successfully (102). Moreover, relatively low processing temperatures were required with higher amounts of PVPVA (102). For Kollidon 90F, processing of the blend was possible but only with 70% w/w PVPVA (102). Unfortunately, the T<sub>g</sub> values for the polymer blends were not reported in their study.

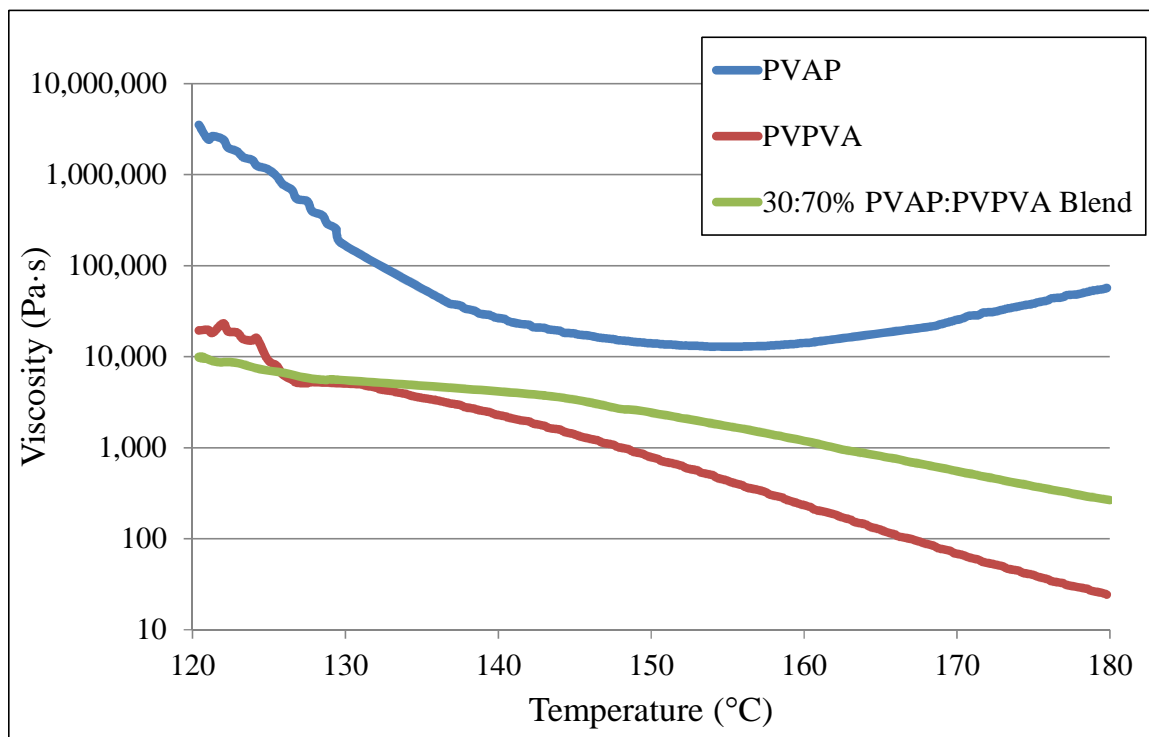


Figure 40. Melt Viscosities for Pure PVAP, Pure PVPVA, and 30:70% PVAP:PVPVA Polymer Blend

Table 28. *Polymer Combinations Tested for Processability by Melt Extrusion. Adapted from Kolter 2010*

Polymer	Kollidon SR PVAc-PVP	Kollicoat IR PVA-PEG	Kollidon 30 PVP MW 50,000	Kollidon 90F PVP MW 1,250,000
PVPVA	70:30	70:30	70:30	70:30
	50:50	50:50	50:50	-
	30:70	30:70	30:70	-
Extrusion Outcome	No effect on processing temperature, pure polymer extruded at 140°C	All blends were extruded at 150°C versus 160°C to 190°C for pure Kollicoat IR	Pure Kollidon 30 could not be extruded. Blends with PVPVA were successfully extruded	Pure Kollidon 90F could not be extruded. Only blends of 70% PVPVA were extrudable

### Itraconazole

#### *T<sub>g</sub> and T<sub>m</sub> of ITZ*

Crystalline itraconazole was transformed to the glassy state by cooling it from the melt (Figure 41). The melting endotherm for itraconazole was observed at about 166°C in the MDSC total heat flow signal. Upon cooling, no re-crystallization exotherm was observed within the temperature range corresponding to the melt in the total heat flow signal; however, exotherms between 90°C and 45°C appeared in the reversing heat flow signal (Figure 41). These peaks appeared again as endotherms upon re-heating. Six et al. investigated the thermal properties of glassy itraconazole and reported two reversible transitions: the first at 90°C represents the transition of the isotropic liquid to the formation of a chiral nematic mesophase and the second transition is likely caused by rotational restrictions of the molecules (182). The T<sub>g</sub> was identified by the authors at 59°C (182). Therefore, the T<sub>m</sub>, T<sub>g</sub>, and T<sub>deg</sub> of itraconazole were found to be 166°C, 59°C and 300°C, respectively, indicating the drug was suitable for melt extrusion.

The physical properties of a drug substance such as the  $T_g$  of the amorphous form can be used to identify the type of glass formed and its propensity for recrystallization (96). Current theories suggest that amorphous forms may exist as a weak or strong glass, which is assessed by the  $\frac{T_m}{T_g}$  ratio (183,184,185). Ratios greater than 1.3 indicate the material is a weak glass and will have a propensity to recrystallize on storage due to the large thermodynamic driving force, whereas ratios less than 1.3 indicate a strong glass and low kinetic barrier for molecular diffusion (that is, their diffusion coefficient at a given temperature is relatively high) (65). Thus, the  $\frac{T_m}{T_g}$  ratio combines both a thermodynamic parameter ( $T_m$ ) and a kinetic parameter ( $T_g$ ) (65). In the case of itraconazole,  $\frac{T_m}{T_g} = \frac{166}{59} = 2.8$  indicating, according to theory, ITZ is a weak glass and will have a propensity to recrystallize. Therefore, sufficient polymeric stabilization by, for example, dispersing ITZ in a high  $T_g$  polymer, is most likely critical for a stable amorphous system.

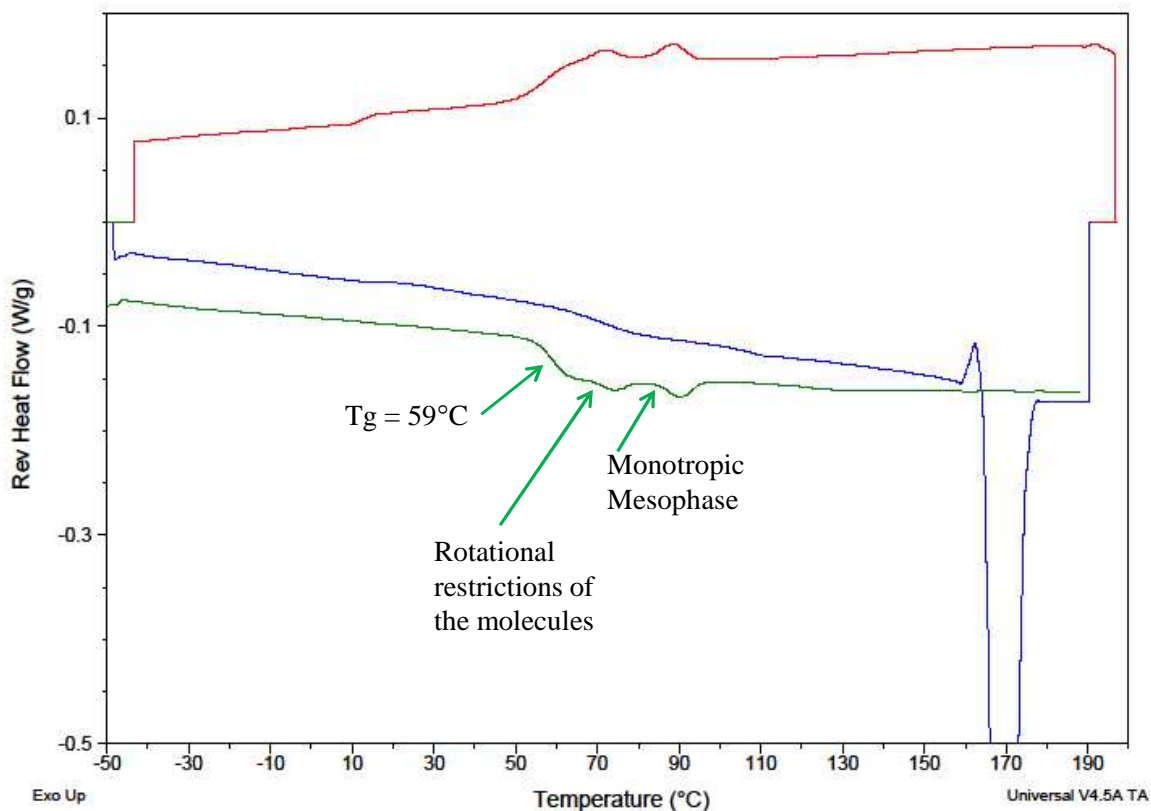


Figure 41. MDSC Analysis for ITZ: Heat (blue line), Cool (red line), Re-heat (green line)

### Miscibility of PVAP-PVPVA-ITZ Blends

Qualitatively, the miscibility of a drug and polymer can be assessed by DSC measurements by mixing them and heating them to observe the changes in  $T_g$ . A single  $T_g$  suggests miscibility, two  $T_g$ 's corresponding to individual components suggests complete immiscibility, and two  $T_g$ 's in between the two individual component  $T_g$ 's suggests partial miscibility. Generally, miscibility of drug and polymer are assessed on the second heating scan after the system has been heated beyond the melting point of the drug. In this case, however, the temperature used during MDSC experiments (first heat) cannot exceed the  $T_{deg}$  of PVAP ( $150^\circ\text{C}$ ) even though the  $T_m$  of ITZ is  $166^\circ\text{C}$ . Although

this presented a potential challenge for thermal analysis, it is not expected to be an issue during extrusion. This is because at least 80-90% of the energy in an extruder is supplied via the extrusion screws and materials soften and/or melt mainly by frictional heat. In practice, the barrel temperatures on an extruder therefore, are routinely set lower than the  $T_m$  of the drug. PVAP and ITZ should extrude simultaneously with processing temperatures below both the  $T_m$  of ITZ and  $T_{deg}$  of PVAP.

Powders containing 30:70%, 40:60%, 50:50% and 60:40% API:polymer blend were analyzed by MDSC. The ratio of API to polymer blend varied, but the polymer blend itself always contained a 1:2 ratio of PVAP:PVPVA. This polymer blend ratio was believed to be within the miscible range based on previous experiments. At the API:polymer ratios studied, each thermogram showed two  $T_g$  values (Figure 42). This either meant that the drug was not miscible in the polymer blend (one  $T_g$  for the drug and one  $T_g$  for the polymer blend) or, the polymers were not completely miscible and the drug had miscibility in both polymers (one  $T_g$  for ITZ-PVPVA and one  $T_g$  for ITZ-PVAP).

Janssens et al. reported amorphous/amorphous phase separation for ITZ-Eudragit E100 mixtures (186). The authors reported that amorphous/amorphous phase separation could be distinguished by the presence of two consecutive glass transitions and in the particular case of ITZ, by the presence of endotherms at 74°C and 90°C that are characteristic of its chiral nematic mesophase (186). This peculiar phase behavior was convenient for identifying a separate glassy itraconazole phase and was considered to be a signature of phase separation. In this study, two separate glass transitions were observed for all the ITZ:polymer blend samples, but there were no discernible mesophase

endotherms. This suggested the two T<sub>g</sub> were not from the amorphous drug and amorphous polymer blend.

A second scenario explaining the two T<sub>g</sub> values was the polymers were not completely miscible with one another but the drug was miscibility in both polymers. To investigate this further, MDSC was performed on ITZ:PVPVA blends (without PVAP) at 10:90%, 20:80%, and 40:60% w/w. For the samples containing less than 40% ITZ, only a single glass transition was detected (Figure 43). The single T<sub>g</sub> also decreased with increasing ITZ potency and no melting endotherms were detected up to 40% ITZ, both indicating miscibility. At 40% ITZ, however, phase separation and partial immiscibility occurred with PVPVA. At the highest drug load (40%), the melting endotherm for ITZ could be observed at about 150°C (Figure 43). This is caused by recrystallization occurring upon heating without sufficient polymeric stabilization. The recrystallization of ITZ occurred at 40% drug load in the blends containing PVPVA but not in the mixtures containing a mixture of PVAP and PVPVA (Figure 42). This suggested PVAP was providing some additional stabilization against crystallization through molecular interactions with ITZ. Therefore, it is likely that the polymer combination together with ITZ forms a two-phase system: one consisting of an ITZ-PVAP phase and the other one consisting of an ITZ-PVPVA phase. Furthermore, the two polymers, originally thought to be completely miscible with one another and capable of forming a single, one-phase system at 30:70% w/w PVAP:PVPVA, must only be partially miscible at this ratio.

Upon very close inspection of the PVAP:PVPVA transitions (without ITZ), the shape of the 30:70% PVAP:PVPVA trace resembles the 40:60% and 50:50% w/w polymer blends, which were originally identified as being partially miscible.

Furthermore, the calculated solubility parameter values predicted miscibility between PVAP and PVPVA because  $\Delta\delta_t$  was less than 7, but  $\Delta\delta_t$  is also as high as  $5.6 \text{ MPa}^{1/2}$ . Moreover, the relative difference in  $\delta_h$  is  $5.4 \text{ MPa}^{1/2}$ . Bustamante et al. showed that hydrogen bonding and polarity of the polymer largely determine polymer-solvent interactions or in this case, polymer-polymer interactions (187). In addition, for polar polymers with hydrogen bonding groups, the acidic and basic characteristics play an important role in their interactions with drugs, excipients, and solvents (187). These characteristics, however, are not taken into account with the single Hansen hydrogen bonding parameter,  $\delta_h$  (187). Therefore, it is difficult to rely solely on the calculated solubility parameter and predicted miscibility for PVAP and PVPVA. Both polymers have a vinyl acetate monomer component (like dissolves like) but the vinyl alcohol and phthalate groups of PVAP and pyrrolidone group of PVPVA may not be miscible. Lastly, the glass transition temperatures of PVAP and PVPVA are somewhat close,  $116^\circ\text{C}$  and  $107^\circ\text{C}$ , respectively, and this can complicate the detection of their compositions since two consecutive or overlapping Tg transitions might appear as one broad Tg (186).

Combining two polymers with a drug and forming two separate drug-polymer phases was previously observed with ITZ and Eudragit E100 -PVPVA blends following hot stage extrusion (147). The authors reported no detectable sign of the chiral nematic mesophase in the polymer blends, although it was clearly present in the Eudragit E100 dispersion (147). All of the ITZ was molecularly dispersed in the Eudragit E100 and PVPVA phases (147). Improvements in dissolution rate were observed for the ternary ITZ-PVPVA-E100 dispersion over the binary ITZ-PVPVA dispersions (147).

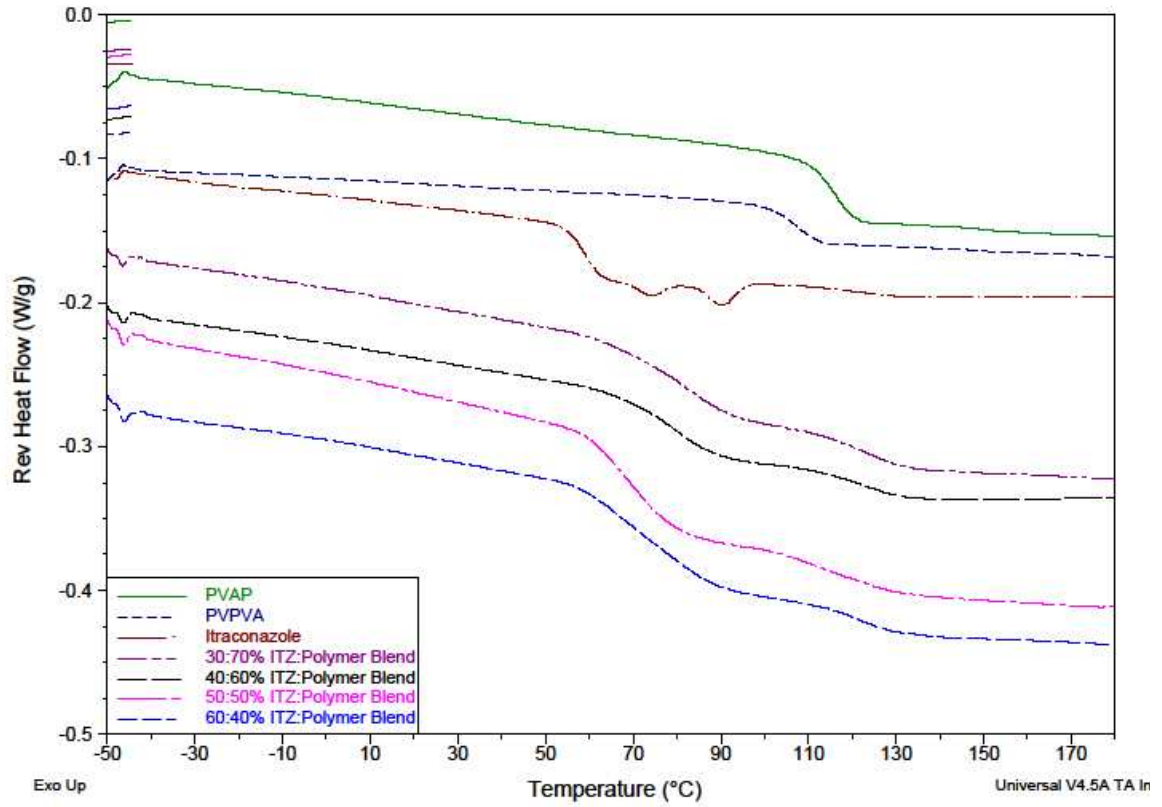


Figure 42. MDSC Analysis of ITZ:Polymer (1:2 PVAP:PVPVA) Powder Blends

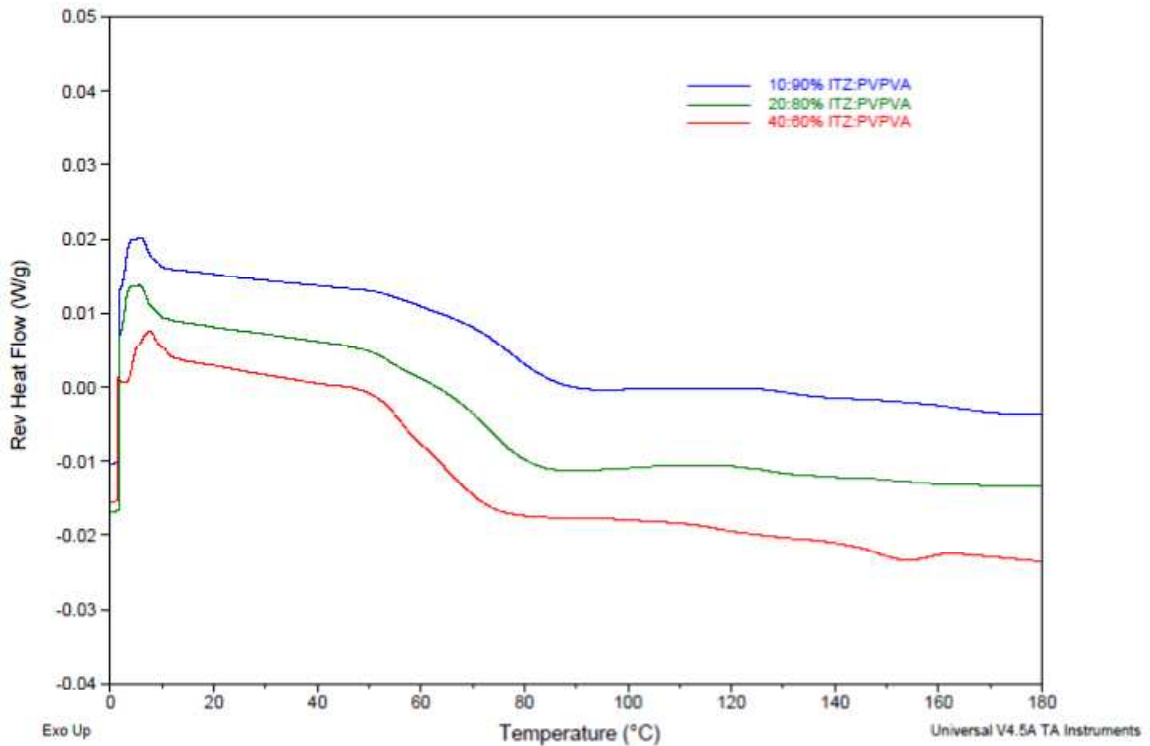


Figure 43. MDSC Analysis of ITZ:PVPVA Powder Blends

### **Processability of ITZ-Polymer Blends**

In some formulations, the drug itself can act as a plasticizer during processing, reducing melt viscosity and extrusion torque. Rambali et al. optimized a melt extrusion formulation containing itraconazole, hypromellose, and hydroxypropyl- $\beta$ -cyclodextrin by adjusting the level of ITZ in the formulation until suitable torque values were achieved during thermal processing (188). The authors reported that itraconazole acted as a plasticizer for the melt because formulations with higher drug loading had lower torque values. For example, a formulation with 20% ITZ had a torque of 45%, whereas at 43% ITZ the torque reduced to 34% (188). Similar results were observed in this study. That is, all formulations containing ITZ had lower torque values than those without ITZ (Figure 44). Incorporating ITZ into the polymer blend further facilitated thermal processing.

Extrudate containing 40:20:40% w/w ITZ:PVAP:PVPVA was produced by melt extruding the powder blend at 140°C. The formation of a solid dispersion at a processing temperature approximately 26°C below the melting temperature of ITZ represents solubilization of ITZ by the molten polymer during processing and indicates miscibility of ITZ with the PVAP:PVPVA polymer blend (122). The amber colored extrudate was transparent, as shown in Figure 45.

Sporanox, the marketed brand for itraconazole capsules, contains 100 mg of ITZ at a 40:60% ratio of ITZ:hypromellose. The API and polymer are dissolved in methylene chloride then coated onto sugar spheres. In the experimental melt-extruded blends, the API to polymer ratio was selected to emulate Sporanox and to evaluate the effect of

PVAP in the polymer blend at a level where recrystallization would otherwise occur with pure PVPVA.

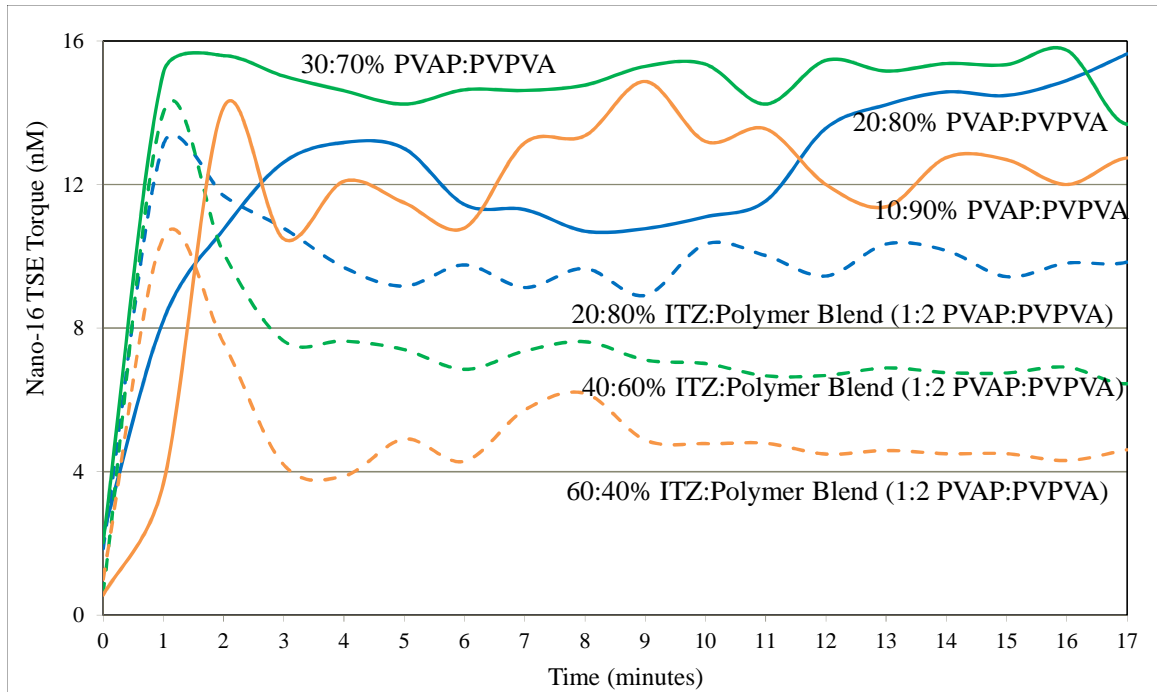


Figure 44. Torque Generated from Different Polymer Blends Versus ITZ-Polymer Blends as a Function of Extrusion Time



Figure 45. Extrudate Containing ITZ-PVPVA and ITZ-PVAP-PVPVA on a Black (Left) and White (Right) Background

### Analysis of ITZ Content

Assay testing was used to determine the content of ITZ in the ternary solid dispersions. The assay values ranged from 92.6% to 98.5%. This indicated the drug remained stable during the melt extrusion process. The results of the assay testing are summarized in Table 29.

Table 29. Assay Results for ITZ in the Ternary Solid Dispersions

Extruded Samples	Label Claim (mg/g)	Label Claim (%)
20:80% ITZ:Polymer Blend (1:2 PVAP:PVPVA)	200	92.6
40:60% ITZ:Polymer Blend (1:2 PVAP:PVPVA)	400	98.5
60:40% ITZ:Polymer Blend (1:2 PVAP:PVPVA)	600	95.0

### Miscibility of ITZ-PVAP-PVPVA Extrudate

A powder blend containing 40:20:40% ITZ:PVAP:PVPVA was melt extruded to form a solid dispersion. The 40% ratio of ITZ to polymer was selected to emulate Sporanox, the marketed itraconazole product. The balance of the formulation was divided into a 20:40% ratio of PVAP:PVPVA based on previous studies. After the blend was melt extruded, a sample of the extrudate was analyzed by MDSC (Figure 46). The sample was only exposed to one heat cycle on the DSC because the extruder performed the first melt. In the total heat flow signal, no melting endotherm for itraconazole was observed, and in the reversing heat flow signal, two Tg transitions were observed: one indicating an ITZ-PVAP phase and the other indicating an ITZ-PVPVA phase. It can be

concluded that crystalline ITZ was successfully transformed to a glassy state and solubilized by the molten polymers during processing.

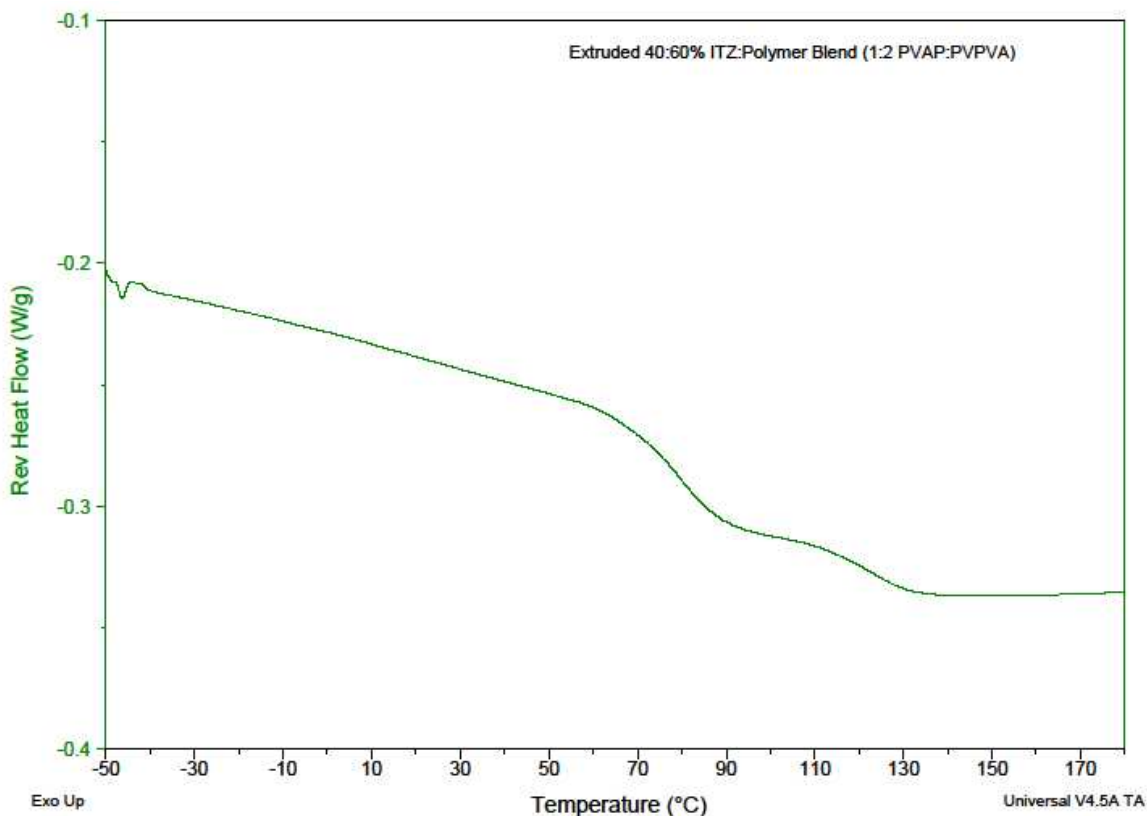


Figure 46. MDSC Analysis of Extruded 40:60% ITZ:Polymer Blend (1:2 PVAP:PVPVA)

### X-Ray Diffraction (XRD)

The crystallinity of the melt-extruded powder blend was examined using XRD and the profiles are depicted in Figure 47. From the diffraction profiles, the characteristic ITZ peaks (most intense) for determining crystallinity of the melt extruded sample are located at 17.45 and 17.95 (doublet), 20.30, and 23.45 two theta degrees. The XRD profile for the melt extruded blend containing 40:20:40% ITZ:PVAP:PVPVA lacked the diffraction peaks associated with crystalline ITZ, implying the samples contained amorphous ITZ.

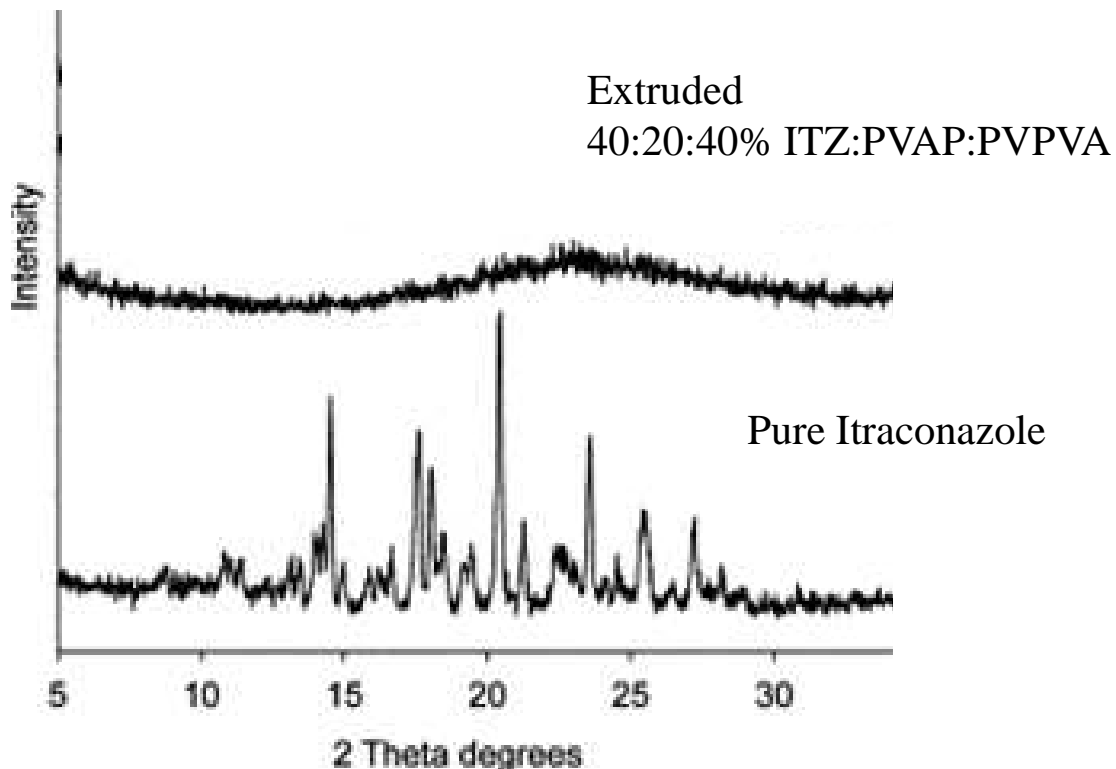


Figure 47. X-Ray Diffraction Profiles for the Melt Extruded Powder Blend Containing 40:60% ITZ:Polymer Blend (1:2 PVAP:PVPVA)

## Dissolution

### *Sink Conditions*

Sink dissolution studies in SGF were performed to investigate the effect of polymer composition on drug release. The results are shown in Figure 48.

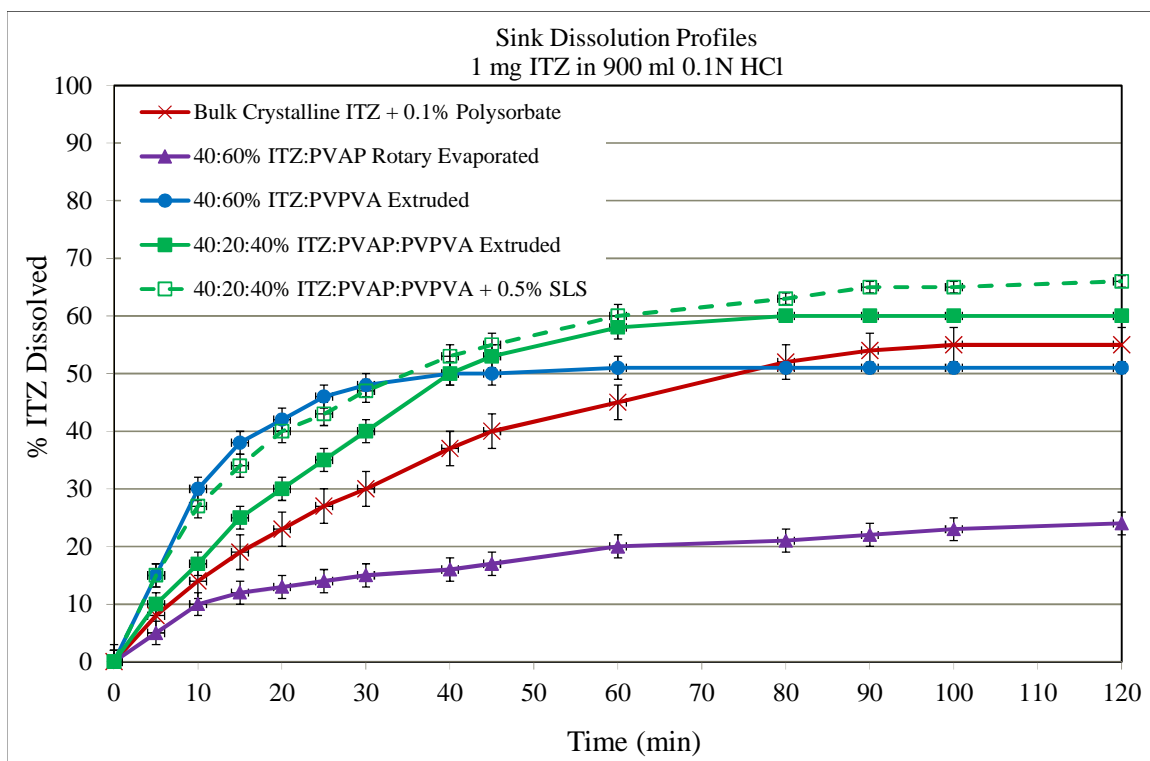


Figure 48. Sink Dissolution Profiles of Melt Extruded Powders Containing Binary and Ternary Mixtures of ITZ in SGF

Melt extruded powders were compared to crystalline ITZ which was 58% dissolved after 2 hours. The dissolution profiles showed the fastest dissolution rate from 40:60% ITZ-PVPVA extrudate, although drug release slowed after 60 minutes and only 75% ITZ released at 120 minutes. When PVAP was incorporated into the melt extruded blend (20:40:40% PVAP:PVPVA:ITZ), dissolution rates were faster than crystalline ITZ but slower than ITZ-PVPVA extruded blends. Drug release from the ternary blends also slowed after 60 minutes and only 63% ITZ released at 120 minutes. The slower drug release observed from the ternary blend was anticipated because PVAP is practically insoluble in acidic solutions. Adding surfactant (0.5% SLS) increased the initial drug release up to 40 minutes but then slowed and resembled the sample profile without SLS. A previously prepared ITZ-PVAP (40:60% w/w) sample produced using a solvent

evaporation technique also was compared to the melt extruded powder. The ITZ-PVAP sample showed that after 120 minutes, only 23% ITZ was released. This further confirmed the influence of the enteric PVAP polymer on the dissolution rate of ITZ in SGF.

Although all melt extruded powders lacked any crystalline ITZ according to XRD, the total amount of ITZ released was never higher than 75%, compared to 58% for crystalline ITZ, despite the amorphous morphology and considerably higher surface area caused by the intense mixing inside the extruder. Overhoff et al. observed similar results with ITZ in 0.1N HCl under sink conditions (142). After 2 hours in acid, their data showed 65% released for crystalline micronized ITZ and not more than 25% ITZ release from Eudragit L100-55 and 70% ITZ release from HPMCP HP-55 dispersions, both produced by ultra-rapid freezing (142). The insoluble enteric polymers in their study and this study appear to be slowing drug release. The drug release presumably occurs through a drug dissolution/diffusion process without the enteric polymer dissolving.

Pure PVPVA, however, is 100% dissolved after only 4 minutes in SGF according to the data generated by Six et al. (paddle method; 100 rpm) (147). Yet, in this study and the study conducted by Qian et al., PVPVA dissolution profiles showed only 75% ITZ released after 2 hours in SGF and 78% BMS-A released after 1 hour in pH 4.5 buffer, respectively, both in sink conditions (189,125,89). Quin et al. showed that the incomplete drug release from their PVPVA solid dispersion formulations produced by spray drying was due to slow paddle speed (189). In another dissolution study where the paddle speed was increased from 50 rpm to 75 rpm, the authors stated 100% of BMS-A released from PVPVA formulations (189). They also noted that the second polymer they

evaluated, HPMC-AS, showed incomplete drug release at 50 rpm due to the pH-dependent solubility of the polymer and drug release profiles from HPMC-AS remained unchanged at 75 rpm (189).

#### *Non-Sink Conditions (Supersaturated)*

##### *Sporanox FDA Test Method*

The marketed multiparticulate capsule formulation, Sporanox, was tested according to the FDA recommended dissolution guidelines for ITZ. The contents of one capsule containing 100 mg of itraconazole was placed in 900 ml of USP simulated gastric fluid (SGF) without enzymes (pH 1.2) to obtain a concentration of 0.11 mg/ml, assuming complete dissolution. The solubility of ITZ at pH 1.2, however, is only 0.004 mg/ml, indicating the FDA test method is conducted in non-sink conditions. The dissolution profiles are presented in Figure 49. Although the FDA test method specified sampling up to 90 minutes, an additional time point was added at 120 minutes since less than 100% ITZ was dissolved at 90 minutes. Variability was observed among the 6 capsules tested and while the FDA test method does not specify release criteria, drug release ranged from 67% to 98% after 90 minutes. After 120 minutes, drug release ranged from 76% to 100%. In the following section, Sporanox capsules were tested according to USP enteric test method A to better simulate in vivo conditions.

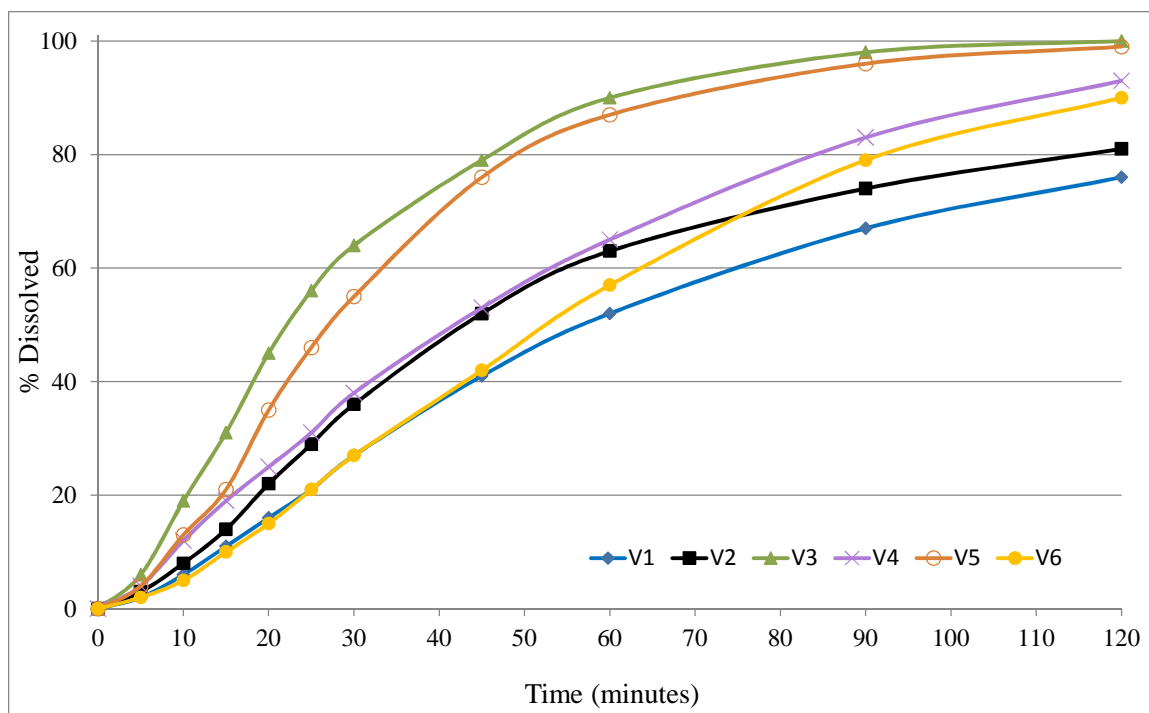


Figure 49. Dissolution Results for Sporanox Capsules using FDA Test Method in SGF

#### *USP Enteric Test Method A*

Friesen et al. proposed a mechanism of supersaturation and bioavailability enhancement for drug-polymer dispersions and explained that, after aqueous dissolution, the drug can be present in various forms including nanosized suspended polymer/drug assemblies, drug in bile salt/lecithin micelles, truly supersaturated free drug in solution, and drug in precipitate (65). In the context of this work, the term supersaturation refers to an apparent supersaturation, i.e., increased drug concentrations that include all species that pass through a 0.45  $\mu\text{m}$  filter. According to Babcock et al., the concentration of free drug, that is, drug in solution and not in colloidal particles is the true, rather than an apparent, supersaturation, and this higher free drug concentration provides a higher driving force for passive diffusional transintestinal absorption (190). The nanosized

polymer/drug assemblies have been demonstrated to be labile; they provide more free drug as free drug is removed from the system (190).

Dissolution studies were performed under supersaturated conditions (20X the equilibrium solubility of crystalline ITZ in the media) to determine the maximum concentration, and cumulative supersaturation, which depends both upon dissolution of the extrudate and the ability of the polymers to inhibit precipitation of ITZ. The dissolution studies were conducted according to the USP 25 enteric test method A, and the results are shown in Figure 50. After 2 hours in 0.1N HCl, aliquots were removed and the ITZ concentration was determined. The rank order for the maximum concentration or largest extent of supersaturation was as follows: Sporanox > 40:60% ITZ:PVPVA > 40:20:40% ITZ:PVAP:PVPVA > 40:60% ITZ:PVAP > crystalline ITZ.

Adjusting the dissolution medium after 2 hours from pH 1.2 to pH 6.8 changed the extent of supersaturation for all the samples tested. The Sporanox and 40:60% ITZ:PVPVA samples precipitated in the dissolution vessel and the extent of supersaturation in pH 6.8 fell to zero. The dissolution vessels became extremely turbid and milky white immediately after the pH change. Conversely, samples containing PVAP showed an increase in ITZ concentration in pH 6.8. Upon addition of the buffer (and increase in pH) an increase in supersaturation was observed as the PVAP dissolved and released the entrapped amorphous ITZ, leading to the maximum extent of supersaturation for the composition. It was also observed that the degree of supersaturation increased more with ternary blends than binary blends containing PVAP. The supersaturation profiles also indicate that the compositions that achieved a high degree of supersaturation were also subject to subsequent losses in supersaturation,

regardless of the stabilizing polymer(s). PVAP appears to have had two effects. Firstly, it reduced ITZ precipitation in acid by delaying dissolution. Secondly, it reduced the crystallization tendency of ITZ during dissolution (in pH 6.8), thereby generating supersaturated solutions for 90 minutes; although, losses in the extent of supersaturation were observed. Table 30 lists the equilibrium solubility of ITZ in pH 1.2 and pH 6.8, the maximum concentration of ITZ in the acid and buffer phases from dissolution testing, and the saturation solubility of ITZ in dimethyl sulfoxide (DMSO) for comparison.

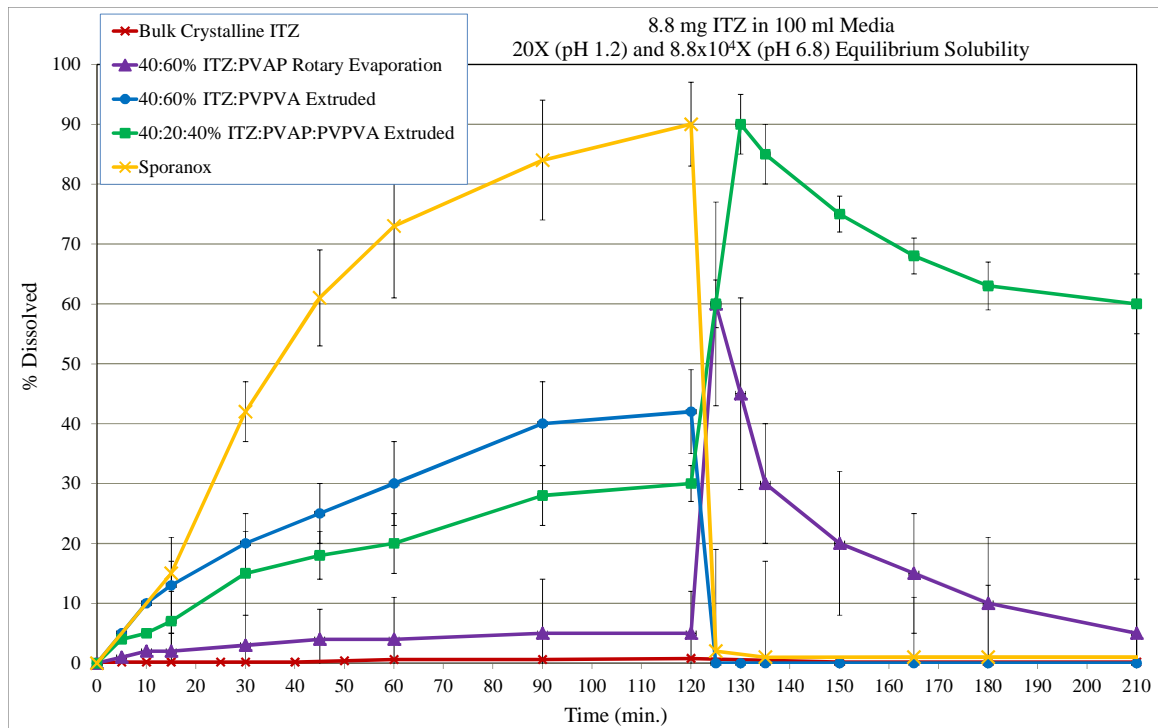


Figure 50. Supersaturated Dissolution Profiles of Melt Extruded Powders Containing Binary and Ternary Mixtures of ITZ in 0.1N HCl for 2 hours followed by pH 6.8 Buffer

Table 30. *Equilibrium Solubility of Pure ITZ, Concentrations of ITZ in Acid and Buffer Phases from Supersaturated Dissolution Testing, and ITZ Saturation Solubility in DMSO*

Solubility	C <sub>max</sub> in pH 1.2 (mg/ml)	C <sub>max</sub> in pH 6.8 (mg/ml)
Pure Itraconazole	0.004	1x10 <sup>-6</sup>
Sporanox (40:60% ITZ:HPMC)	0.0792	-
Rotary Evaporated 40:60% ITZ:PVAP	0.0045	0.053
Melt Extruded 40:60% ITZ:PVPVA	0.0370	-
Melt Extruded 40:20:40% ITZ:PVAP:PVPVA	0.0264	0.079
Pure Itraconazole in DMSO	0.5 mg/ml	

#### *Area Under the Curve*

Area under the supersaturated dissolution curves (AUC<sub>dissl</sub>) were calculated for the acidic phase (AUC<sub>0.1N HCl</sub>), neutral phase (AUC<sub>pH 6.8 buffer</sub>), and total dissolution test (AUC<sub>total</sub>) for each evaluated composition to provide a quantitative means of comparing the extent and duration of supersaturation at each stage of testing. These results are listed in Table 31. The AUC<sub>dissl</sub> results reveal that the greatest total extent of supersaturation (AUC<sub>total</sub>) was produced by the ITZ:PVAP:PVPVA and Sporanox formulations and the greatest acid phase release (AUC<sub>0.1N HCl</sub>) was produced by the Sporanox formulation, which contained an immediate release, pH-independent polymer (HPMC). However, the AUC in the neutral phase (AUC<sub>pH 6.8</sub>) is a key metric by which to evaluate the different compositions because it is expected to correlate to *in vivo* absorption (122).

The ITZ:PVAP:PVPVA formulation showed a substantially higher AUC<sub>pH 6.8</sub> value compared to the other formulations. When compared to other published data, the AUC<sub>0.1N HCl</sub> value for the 40:20:40% ITZ:PVAP:PVPVA formulation was in agreement with the values Overhoff et al. generated from Eudragit L100-55 and HPMCP HP-55

containing solid dispersions (142) and all AUC values for 40:20:40% ITZ:PVAP:PVPVA were greater than those reported by Miller et al. for Eudragit L100-55 and Carbopol 974P combinations (122).

Table 31. *Area Under the Supersaturated Dissolution Curve (AUC) for the Acid Phase, Neutral Phase, and Total Dissolution Test*

Formulation	AUC <sub>dissolution</sub>		
	AUC <sub>0.1N HCl</sub> (mg·min)	AUC <sub>pH 6.8 Buffer</sub> (mg·min)	AUC <sub>total</sub> (mg·min)
Sporanox (40% ITZ)	9727	160	9887
40:60% ITZ:PVPVA	5445	0	5445
40:60% ITZ:PVAP	613	1650	2263
40:20:40% ITZ:PVAP:PVPVA	2565	7338	9903

## Stability

### *X-Ray Diffraction (XRD)*

The crystallinity of the melt extruded powder blend was examined using XRD after 6 months of storage at 30°C/65% RH and the profiles are depicted in Figure 51. The XRD profiles for the melt extruded blend containing 40:20:40% ITZ:PVAP:PVPVA lacked the diffraction peaks associated with crystalline ITZ, indicating the samples maintained ITZ in its amorphous form throughout 6 months of storage at 30°C/65% RH.

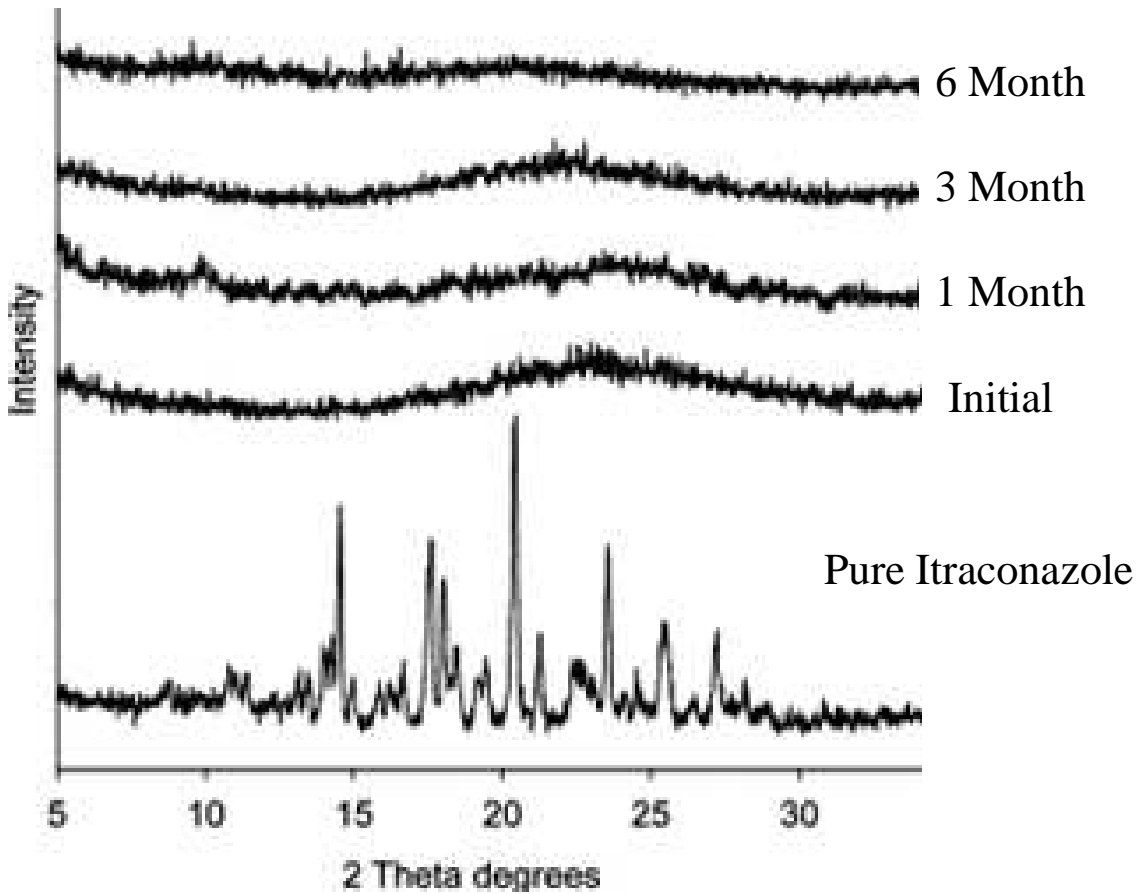


Figure 51. X-Ray Diffraction Profiles for Melt Extruded Powder Blend Containing 40:60% ITZ:Polymer Blend (1:2 PVAP:PVPVA) After 1, 3, and 6 Months of Storage at 30°C/65% RH

USP Enteric Test Method A

Dissolution studies were performed under supersaturated conditions (20X the crystalline ITZ equilibrium solubility) after 6 months of storage at 30°C/65% RH. The dissolution studies were conducted according to the USP 25 enteric test method A, and the results are shown in Figure 52. Similar dissolution profiles were observed in the acid and buffer phases for the melt extruded polymer blend containing 40:20:40% ITZ:PVAP:PVPVA. The extrudate also remained transparent after 6 month of storage compared to ITZ:PVPVA blends that turned opaque (Figure 53).

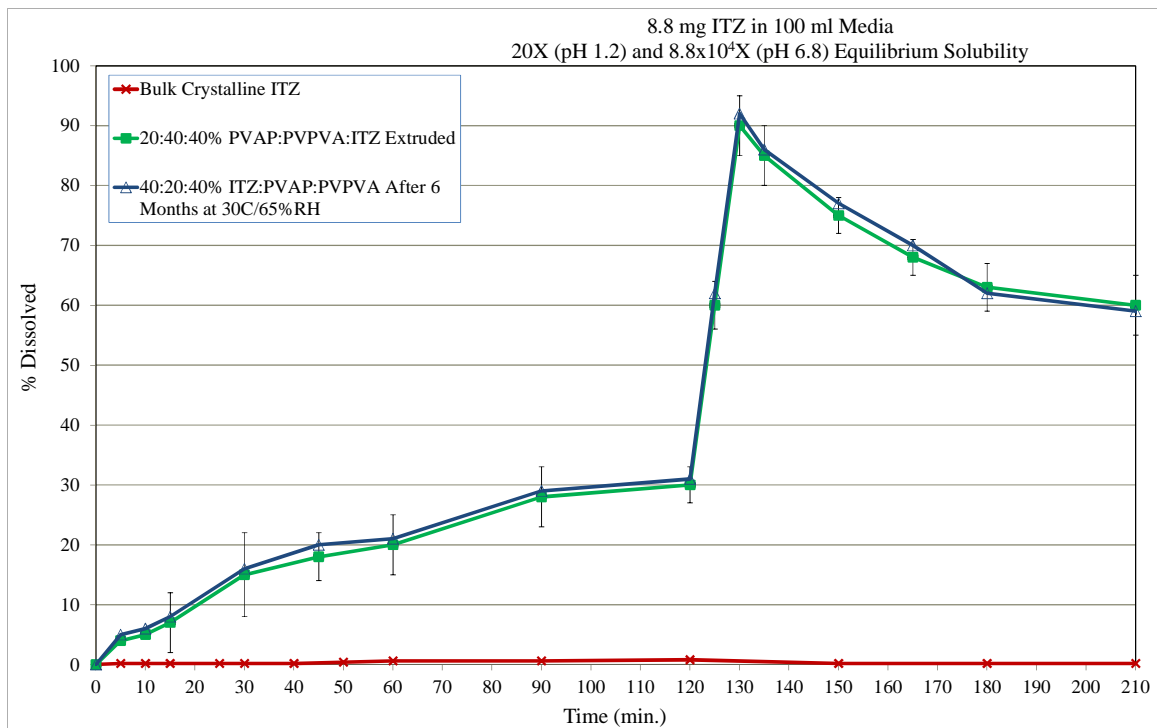


Figure 52. Supersaturated Dissolution Profiles of Melt Extruded Powders Containing 40:20:40% ITZ:PVAP:PVPVA in 0.1N HCl for 2 hours followed by pH 6.8 Buffer Before and After 6 Months of Storage at 30°C/65%RH



Figure 53. Extruded ITZ-PVAP-PVPVA (left) and ITZ-PVPVA (right) Solid Dispersions After 6 Months of Storage at 30°C/65%RH

## Discussion

### *ITZ Miscibility in Polymers*

Craig et al. described the mechanism of drug release from solid dispersions (191). They concluded that when the drug was molecularly dispersed within the polymer (i.e. solid solution) drug release was polymer mediated (191). However, if localized regions of pure drug existed (i.e. solid dispersion), and were sufficiently large, dissolution of the drug may also be drug mediated (191). Moreover, Six et al. reported that ITZ miscibility within a polymer system is not critical to achieve rapid dissolution rates and that both the polymer and the physical state of ITZ contribute to its dissolution (146,147). This is because dissolved polymer releases miscible drug and aids wetting of any immiscible ITZ domains, while having ITZ in an amorphous state contributes to the dissolution process by largely removing the crystalline heat of fusion and increasing solubility (146,147). In this study, ITZ appeared to be molecularly dispersed within the polymers and in an amorphous state, both of which contributed to its faster dissolution rates compared to crystalline ITZ.

Several authors have reported the miscibility of ITZ in various polymers. In one study, Six et al. found limited miscibility of ITZ (13% w/w) with Eudragit E100 (soluble in low pH) following melt extrusion, yet Overhoff et al. reported the miscibility of ITZ in Eudragit L100-55 (soluble above pH 5.5) at levels greater than 60% w/w (146,192,147,142). Miller et al. compared the molecular structures of Eudragit E100 and Eudragit L100-55 and attributed the effects of miscibility of ITZ with these polymers to acidic functional groups contained on Eudragit L100-55 that are not present on Eudragit E100 (122). According to the authors, the acidic functional groups improved the

solubility of ITZ in aqueous media and enhanced the miscibility of ITZ with acrylic polymers in the solid state (122). Van den Mooter et al. first introduced the affinity of weakly basic drugs with polymers containing acidic functional groups and the stabilizing effects of these polymers on the drug molecules in the supersaturated solution state and solid state (195). The authors credited the improved solution and amorphous solid-state stability to the formation of a salt between basic drugs and acidic polymers (195).

Similar to the study conducted by Miller et al., this study incorporated ITZ into a polymer that contains acidic functional groups. The polymethacrylate used by Miller et al. (Eudragit L100-55) and polyvinyl derivative used in this study (PVAP) both have free carboxylic acid groups on the methacrylic acid or phthalyl group of their respective polymer. These carboxylic acid groups remain un-ionized in acidic conditions and become ionized in neutral and weakly alkaline conditions. Both Eudragit L100-55 and PVAP are ionized above pH 5.5 or pH 5.0, respectively, and this charge is thought to not only improve the solubility of ITZ in aqueous media through drug-polymer associations, but also enhance the miscibility of ITZ in the solid state (122). In addition, polymers with ionizable functional groups have been used to specifically target drug supersaturation to the small intestine.

### *Targeting Supersaturated Drug Delivery*

Although numerous publications demonstrate improved oral bioavailability of poorly water-soluble drugs using supersaturated formulations, few studies have been published that illustrate specific targeting of drug supersaturation to the small intestine by the use of pH-dependent polymers.

In one such study, Kondo et al. investigated both pH-independent polymers (povidone and copovidone) and pH-dependent polymers (hypromellose phthalate (HPMCP) HP-55) as a means of improving the bioavailability of an anticancer drug, HO-221 (193). *In vivo* studies with these formulations showed that absorption of HO-221 achieved with the HPMCP HP55 formulations was twice that of the povidone and copovidone co-precipitates (193). The authors speculated the outcome was a result of targeting the onset of HO-221 supersaturation to the small intestine versus the stomach (193). Transient supersaturation was thought to be responsible for the poor absorption of the pH-independent formulations due to precipitation of HO-221 before passage into the small intestine (193). Conversely, the pH-dependent polymer (HPMCP HP-55) directed supersaturation of HO-221 to the small intestine and maximized the exposure of absorptive surface area to elevated drug concentrations (193).

Another pH-dependent solid dispersion system was evaluated to improve the absorption of albendazole, a poorly water-soluble drug with a pH solubility profile similar to ITZ (194). The intestinal absorption of albendazole was variable and highly dependent on gastric pH (194). The researchers evaluated the use of HPMCP HP55 in a solid dispersion to improve the intestinal absorption of the drug (194). *In vitro* two-stage dissolution testing showed improved albendazole supersaturation following pH change from 1.2 to 6.5 (194). *In vivo* studies were conducted with polymer combinations consisting of HPMCP HP-55 and hypromellose, which generated a 3.2 fold increase in bioavailability compared to crystalline drug in rabbits with elevated gastric pH (194). Improvements were attributed to targeted supersaturation of albendazole to the small intestine by pH-dependent drug release of the solid dispersion formulation (194).

In another study, Miller et al. demonstrated that Methocel E50 and Eudragit L100-55 produced substantially greater *in vivo* absorption than immediate release formulations owing to improved supersaturation of ITZ in the small intestine (149). Additionally, the authors demonstrated the stabilizing effect of Carbopol 974P on supersaturated levels of ITZ *in vitro* and its absorption-enhancing effects *in vivo* when incorporated into an Eudragit L100-55 polymer matrix (122). The combination of polymers yielded targeted intestinal delivery that was able to generate prolonged supersaturation of ITZ within the small intestine (122).

In this study, the *in vitro* release of ITZ from the dispersions containing PVAP was minimal in acid (2.6 mg after 2 hours) but rapid following the pH change, with peak ITZ release occurring 10 minutes into the neutral phase of dissolution testing (7.9 mg). The combination of PVAP and PVPVA as a polymer carrier for amorphous ITZ yielded a targeted intestinal delivery system that generated prolonged supersaturation of ITZ in a pH that was representative of the small intestine. These results suggest the potential for improved therapy with orally delivered ITZ via intestinal targeting with prolonged supersaturation caused by the ionization of PVAP, a pH-dependent polymer.

#### *Influence of PVAP on Amorphous Solid Dispersions of ITZ*

Owing to the abundance of carboxylic acid functional groups contained on the PVAP polymer network, it is plausible that its incorporation with PVPVA improved the formation of an ITZ solid solution during HME processing and contributed to the physical stability of the solid dispersion over time. Above pH 5, PVAP is at least partially ionized and this charge may support stable drug-polymer solutions or nanosized

drug-polymer aggregates; the charge on the polymer minimizes formation of large polymer aggregates that may not be capable of releasing free drug. In addition, the more hydrophobic regions of PVAP, its acetate substituents, may provide sites for drug association, while hydrophilic PVPVA, its pyrrolidone moieties, permit stable formation of hydrated drug-polymer structures in aqueous media. Since PVAP contains substituents that are hydrophobic, even when PVAP becomes ionized, as it does at the pH in the small intestine, the polymer is still only sparingly soluble and exists as colloidal polymer aggregates in aqueous solutions. In its non-ionized state (as it is in a solid dispersion before dissolution) PVAP has a high T<sub>g</sub> even when exposed to high relative humidity. Under both low and high humidity conditions, the T<sub>g</sub> of PVAP remains about 120°C. Similar to all amorphous materials, when exposed to humidity, PVAP sorbs moisture. However, the relative hydrophobicity of PVAP results in much less sorption of water (only 8% at 90% RH after 3 days) than is observed for typical water-soluble polymers and the sorbed water does not plasticize the polymer (or increase its mobility). In order to maintain a stable solid dispersion, the molecular mobility of the dispersion must be low to minimize diffusion and crystallization of the drug molecules during storage. The low hygroscopicity of PVAP combined with the higher T<sub>g</sub> values for the drug-polymer systems reduced the mobility of drug molecules dispersed in the polymers and appeared to improve the physical stability during storage over time. Specifically, the PVPVA-ITZ rich portion of the ternary dispersion had a T<sub>g</sub> = 80°C and the PVAP-ITZ rich portion of the ternary dispersion had a T<sub>g</sub> = 115°C, whereas pure ITZ had a T<sub>g</sub> of only 59°C. In addition, the partial miscibility of PVAP in PVPVA increased the T<sub>g</sub> of the ITZ-PVPVA rich portion of the ternary dispersion by acting as an anti-plasticizer.

Without PVAP, ITZ-PVPVA binary dispersions had a  $T_g$  of only 63°C compared to ITZ-PVAP-PVPVA dispersions that had a  $T_g = 80^\circ\text{C}$ . The anti-plasticization of PVPVA caused by PVAP also improved storage stability.

## **CHAPTER 5**

### **CONCLUSIONS**

The processability of PVAP by melt extrusion was improved by adding PVPVA. The PVAP-PVPVA polymer blends were partially miscible and, when co-extruded with itraconazole, produced predominantly PVAP-ITZ and PVPVA-ITZ solid solutions. PVAP improved amorphous drug stability by preventing precipitation at low pH, facilitating supersaturated solutions at higher pH, and acted as an effective anti-plasticizer through drug-polymer and polymer-polymer associations.

#### **Future Direction**

PVAP cannot be melt extruded alone. It requires the addition of a plasticizer or thermal processing aid. In some formulations, the drug itself can act as a plasticizer during processing, reducing melt viscosity and extrusion torque. The ability of PVAP to be plasticized by APIs (certain types and levels) should be evaluated before discounting the use of PVAP in melt extrusion. If a particular API can act as a plasticizer for PVAP, then co-extrusion of drug and PVAP alone may be possible and the ability of PVAP to stabilize amorphous dispersions through specific drug-polymer associations could be studied.

## BIBLIOGRAPHY

1. Buckley S, Fischer S, Fricker G, Brandl M. In vitro models to evaluate the permeability of poorly soluble drug entities: Challenges and perspectives. *Eur J Pharm Sci.* 2012; 45(3): p. 235-250.
2. Bosselmann S, Williams III R. Route-Specific Challenges in the Delivery of Poorly Water-Soluble Drugs. In Miller D, editor. *Formulating Poorly Water Soluble Drugs.* 1st ed. New York: Springer; 2012. p. 1-26.
3. Williams R, Watts A. *Formulating Poorly Water Soluble Drugs.* 1st ed. Miller D, editor. New York: Springer; 2012.
4. Lee V, Yang J. Oral Drug Delivery. In Swarbrick J, editor. *Drug Delivery and Targeting for Pharmacists and Pharmaceutical Scientists.* London: Taylor & Francis; 2001.
5. Levine R. Factors affecting gastrointestinal absorption of drugs. *Am J Dig Dis.* 1970; 15: p. 171-188.
6. Martinez M, Amidon G. A mechanistic approach to understanding the factors affecting drug absorption: a review of fundamentals. *J Clin Pharmacol.* 2002; 42: p. 620-643.
7. Wilding I. The Enterion Capsule: A Novel Technology for Understanding the Biopharmaceutical Complexity of New Molecular Entities (NMEs). *Drug Dev Technol.* 2001.
8. Krill S. *The Drug Delivery Companies Report.* PharmaVentures; 2000.
9. Lipinski C, Lombardo F, Dominy B, Feeney P. Experimental and computational approaches to estimate solubility and permeability in drug discovery and development settings. *Adv Drug Deliv Rev.* 2012; 46: p. 3-26.
10. SciFinder. [[www.scifinder.cas.org](http://www.scifinder.cas.org)].; 2013.
11. Di L, Fish P, Mano T. Bridging solubility between drug discovery and development. *Drug Discov Today.* 2012; 17(9/10): p. 486-495.
12. Lipinski C. Drug-like properties and the causes of poor solubility and poor permeability. *J Pharmacol Toxicol Methods.* 2000; 44: p. 235-249.

13. Smithey D, Gao P, Taylor L. Amorphous solid dispersions: An enabling formulation technology for oral delivery of poorly water soluble drugs. *AAPS Newsmagazine*. 2013; p. 10-14.
14. Keseru MG, Makara GM. Hit discovery and hit-to-lead approaches. *Drug Discov Today*. 2006; 11: p. 741-748.
15. Wells JA, McClendon CL. Reaching for high-hanging fruit in drug discovery at protein-protein interfaces. *Nature*. 2007; 450: p. 1001-1009.
16. Waring MJ. Lipophilicity in drug discovery. *Expert Opin Drug Discov*. 2010; 5: p. 235-248.
17. Stegemann S, Leveiller F, Franchi D, de Jong H, Linden H. When poor solubility becomes an issue: From early stage to proof of concept. *Eur J Pharm Sci*. 2007; 31: p. 249-261.
18. Lipinski C. Poor aqueous solubility: an industry wide problem in drug discovery. *Am Pharm Rev*. 2002; 5: p. 82-85.
19. USP-35 , NF-30. USP-NF Online. [Online].; 2013 [cited 2013 March 17. Available from: <http://www.uspnf.com/uspnf/display?cmd=jsp&page=chooser>.
20. Martin A. *Physical Pharmacy*. 4th ed. Mundorff G, editor. Maryland: Lippincott Williams & Wilkins; 1993.
21. Kawabata Y, Wada K, Nakatani M, Yamada S, Onoue S. Formulation design for poorly water-soluble drugs based on biopharmaceutics classification system: Basic approaches and practical applications. *Int J Pharm*. 2011; 420: p. 1-10.
22. Takagi T, Ramachandran C, Bermejo M, Yamashita S, Yu L, Amidon G. A provisional biopharmaceutical classification of the top 200 oral drug products in the United States, Great Britain, Spain, and Japan. *Mol Pharm*. 2006; 3: p. 631-643.
23. Hayes D, Morella AM, inventors; Improved pharmaceutical compositions for poorly soluble drugs. Europe patent EP1239831. 2002 September 18.
24. Horter D, Dressman J. Influence of physicochemical properties on dissolution of drugs in the gastrointestinal tract. *Adv Drug Deliv Rev*. 2001; 46: p. 75-87.

25. Amidon GL, Lennernas H, Shah VP, Crison JR. A theoretical basis for a biopharmaceutical drug classification: the correlation of in vitro drug product dissolution and in vivo bioavailability. *Pharm Res.* 1995; 12: p. 413-420.
26. U.S. Department of Health and Human Services. Food and Drug Administration. Center for Drug Evaluation and Research (CDER). [Online].; 2000 [cited 2013 March. Available from: <http://www.fda.gov/downloads/Drugs/./Guidances/ucm070246.pdf>.
27. Remington JP. Remington: The Science and Practice of Pharmacy. 21st ed. Troy D, editor. Maryland: Lippincott Williams & Wilkins; 2006.
28. Cook J, Addicks W, Wu Y. Application of the biopharmaceutical classification system in clinical drug development - an industry view. *The AAPS Journal.* 2008: p. 306-301.
29. Ku M, Dulin W. A biopharmaceutical classification-based Right-First-Time formulation approach to reduce human pharmacokinetic variability and project cycle time from First-In-Human to clinical Proof-of-Concept. *Pharmaceutical Development & Technology.* 2010: p. 1-18.
30. Fasano A. Innovative strategies for the oral delivery of drugs and peptides. *Trends in Biotechnology.* 1998: p. 152-157.
31. Thanou M, Verhoef J, Junginger H. Chitosan and its derivatives as intestinal absorption enhancers. *Advanced Drug Delivery Reviews.* 2001; 50: p. 91-101.
32. Zhang F, DiNunzio J. Solubilized Formulations. In Miller D, editor. *Formulating Poorly Water Soluble Drugs.* New York: Springer; 2012. p. 171-208.
33. Incivek. Incivek Prescribing Information. [Online].; 2011.
34. European Medicines Agency. Zelboraf (vemurafenib) CHMP assessment report, Procedure EMEA/H/C/002409. [Online].; 2012.
35. Di L, Kerns E, Carter G. Drug-like property concepts in pharmaceutical design. *Curr Pharm Des.* 2009; 15: p. 2184-2194.
36. Ali S, Kolter K. Challenges and Opportunities in Oral Formulation Development. *Am Pharm Rev.* 2012: p. 14-21.

37. Griffin B. Advances in lipid-based formulations: Overcoming the challenges in low bioavailability for poorly water soluble drug compounds. *Am Pharm Rev.* 2012; p. 41-47.
38. Serajuddin A. Salt formation to improve drug solubility. *Adv Drug Deliv Rev.* 2007; 59: p. 603-616.
39. Swarbrick J. Salt Forms: Pharmaceutical Aspects. In Corrigan O. *Encyclopedia of Pharmaceutical Technology, Third Edition.*: Informa Healthcare; 2006.
40. Serajuddin A, Pudipeddi M. Salt-selection strategies. In *Handbook of Pharmaceutical Salts: Properties, Selection, and Use.*: Wiley-VCH, Weinheim; 2002. p. 135-160.
41. Blagden N, Matas M, Gavan P, York P. Crystal engineering of active pharmaceutical ingredients to improve solubility and dissolution rates. *Adv Drug Deliv Rev.* 2007; 59: p. 617-630.
42. Singhal D, Curatolo W. Drug polymorphism and dosage form design: a practical perspective. *Adv Drug Deliv Rev.* 2004; 56: p. 335-347.
43. El-Nabarawi M, El-Miligi M, Khalil I. Optimization of class II BCS drugs using solid dispersion technique. *Int J Pharm Pharm Sci.* 2012; 4.
44. Riis T, Bauer-Brandl A, Wagner T, Kranz H. pH independent drug release of an extremely poorly soluble weakly acidic drug from multiparticulate extended release formulations. *Eur J Pharm Biopharm.* 2007; 65: p. 78-84.
45. Kranz H, Guthmann C, Wagner T, Lipp R, Reinhard J. Development of a single unit extended release formulation for ZK811752, a weakly basic drug. *Eur J Pharm Sci.* 2005; 26: p. 47-53.
46. Siepe S, Lueckel B, Kramer A, Ries A, Gurny R. Strategies for the design of hydrophilic matrix tablets with controlled microenvironmental pH. *Int J Pharm.* 2006; 316: p. 14-20.
47. Tran P, Tran H, Lee B. Modulation of microenvironmental pH and crystallinity of ionizable telmisartan using alkalizers in solid dispersions for controlled release. *J Control Release.* 2008; 129: p. 59-65.
48. Badawy S, Hussain M. Microenvironmental pH modulation in solid dosage forms. *J Pharm Sci.* 2007; 96: p. 948-959.

49. Davis M, Brewster M. Cyclodextrin-based pharmaceuticals: past, present, and future. *Nat Rev Drug Discov.* 2004; 3: p. 1023-1035.
50. Mu H, Holm R, Mullertz A. Lipid-based formulations for oral administration of poorly water-soluble drugs. *Int J Pharm.* 2013.
51. Kohli K, Chopra S, Dhar D, Arora S, Khar R. Self-emulsifying drug delivery systems: an approach to enhance oral bioavailability. *Drug Discov Today.* 2010; 15: p. 958-965.
52. Alonzo D, Zhang G, Zhou D, Gao Y, Taylor L. Understanding the behavior of amorphous pharmaceutical systems during dissolution. *Pharm Res.* 2010; 27: p. 608-618.
53. Hancock B, Parks M. What is the true solubility advantage for amorphous pharmaceuticals. *Pharm Res.* 2000; 17: p. 397-404.
54. Huang L, Tong W. Impact of solid state properties on developability assessment of drug candidates. *Adv Drug Deliv Rev.* 2004; 56: p. 321-334.
55. Tesconi M, Landis M. Practical aspects of solubility determination and considerations for enabling formulation technologies. *Am Pharm Rev.* 2013 March: p. 14-18.
56. Pudipeddi M, Serajuddin A. Trends in solubility of polymorphs. *J Pharm Sci.* 2005; 94: p. 929-939.
57. Khankari R, Grant D. Pharmaceutical hydrates. *Thermochim Acta.* 1995; 248: p. 61-79.
58. Myrdal P, Jozwiakowski M. *Water Insoluble Drug Formulations.* 2nd ed. Li R, editor. Boca Raton, FL: CRC Press; 2008.
59. Hancock B, Zografi G. Characteristics and significance of the amorphous state in pharmaceutical systems. *J Pharm Sci.* 1997; 86: p. 1-11.
60. Hancock B. Disordered drug delivery: destiny, dynamics and the Deborah number. *J Pharm Pharmacol.* 2002; 54: p. 737-746.
61. Solids / Crystal Structure aS. [Document].; 2012 [cited 2013 April 27. Available from: <http://chemconnections.org/crystals/pdf/crys-solids.pdf>.

62. Amorphous S. Department of Electronic Materials Engineering. [Online].; 2013 [cited 2013 April 27. Available from: <http://physics.anu.edu.au/eme/research/amorphous.php>.
63. Ross K, Arnfield S, Cenkowski S. A Polymer Science Approach to Physico-Chemical Characterization and Processing of Pulse Seeds. [Online].; 2013 [cited 2013 April 28. Available from: <http://www.intechopen.com/books/polymer-science/a-polymer-science-approach-to-physico-chemical-characterization-and-processing-of-pulse-seeds>.
64. Laitinen R, Lobmann K, Strachan C, Grohganz H, Rades T. Emerging trends in the stabilization of amorphous drugs. *Int J Pharm.* 2012 April.
65. Friesen D, Shanker R, Crew M, Smithey D, Curatolo W, Nightingale J. Hydroxypropyl methylcellulose acetate succinate-based spray-dried dispersions: an overview. *Mol Pharm.* 2008; 5: p. 1003-1019.
66. Kaushal A, Gupta P, Basal A. Amorphous drug delivery systems: molecular aspects, design and performance. *Crit Rev Ther Drug Carrier Syst.* 2004; 21: p. 133-193.
67. Konno H, Taylor L. Influence of different polymers on the crystallization tendency of molecularly dispersed amorphous felodine. *J Pharm Sci.* 2006; 95: p. 2692-2705.
68. Menczel J, Judovits L, Prime R, Bair H, Reading M, Swier S. Thermal analysis of polymers. 1st ed. Menczel J, Prime R, editors. Hoboken: John Wiley & Sons, Inc; 2009.
69. Marsac P, Konno H, Taylor L. A comparison of the physical stability of amorphous felodipine and nifedipine systems. *Pharm Res.* 2006; 23: p. 2306-2316.
70. Zhou D, Grant D, Zhang G, Law D, Schmitt E. Physical stability of amorphous pharmaceuticals: importance of configurational thermodynamic quantities and molecular mobility. *J Pharm Sci.* 2002; 8: p. 1863-1872.
71. Andronis V, Zografi G. Molecular mobility of supercooled amorphous indomethacin, determination by dynamic mechanical analysis. *Pharm Res.* 1997; 14: p. 410-414.

72. Grzybowska K, Paluch M, Grzybowski A, Wojnarowska Z, Hawelek L, Kolodziejczyk K, et al. Molecular dynamics and physical stability of amorphous anti-inflammatory drug: celecoxib. *J Phys Chem. ; B*114: p. 12792-12801.
73. Ambike A, Mahadik K, Paradkar A. Physico-chemical characterization and stability study of glassy simvastatin. *Drug Dev Ind Pharm.* 2005; 31: p. 895-899.
74. Fukuoka E, Makita M, Yamamura S. Glassy state of pharmaceuticals III: thermal properties and stability of glassy pharmaceuticals and their binary glass systems. *Chem Pharm Bull.* 1989; 37: p. 1047-1050.
75. Kaushal A, Bansal A. Thermodynamic behavior of glassy state of structurally related compounds. *Eur J Pharm Biopharm.* 2008; 69: p. 1067-1076.
76. Graeser K, Patterson J, Rades T. Applying thermodynamic and kinetic parameters to predict the physical stability of two differently prepared amorphous forms of simvastatin. *Curr Drug Deliv.* 2009; 6: p. 374-382.
77. Karmwar P, Graeser K, Gordon K, Strachan C, Rades T. Investigation of properties and recrystallization behavior of amorphous indomethacin samples prepared by different methods. *Int J Pharm.* 2011; 417: p. 94-100.
78. Patterson J, James M, Forster A, Lancaster R, Butler J, Rades T. The influence of thermal and mechanical preparative techniques on the amorphous state of four poorly soluble compounds. *J Pharm Sci.* 2005; 94: p. 1998-2012.
79. Bansal S, Kaushal A, Bansal A. Enthalpy relaxation studies of two structurally related amorphous drugs and their binary dispersions. *Drug Dev Ind Pharm.* 2010; 36: p. 1271-1280.
80. Bhattacharaya S, Syrayanarayanan R. Local mobility in amorphous pharmaceuticals - characterization and implications on stability. *J Pharm Sci.* 2009; 98: p. 2935-2953.
81. Zhou D, Zhang G, Law D, Grant D, Schmitt E. Thermodynamics, molecular mobility and crystallization kinetics of amorphous griseofulvin. *Mol Pharm.* 2008; 5: p. 927-936.
82. Bhugra C, Pikal M. Role of thermodynamics, molecular, and kinetic factors in crystallization from the amorphous state. *J Pharm Sci.* 2008; 97: p. 1329-1349.

83. Vyazovkin S, Dranca I. Probing beta relaxation in pharmaceutical relevant glasses by DSC. *Pharm Res.* 2006; 23: p. 422-428.
84. Zhou D, Grant D, Zhang G, Law D, Schmitt E. A calorimetric investigation of thermodynamic and molecular mobility contributions to the physical stability of two pharmaceutical glasses. *J Pharm Sci.* 2007; 96: p. 71-83.
85. Newman A, Reutzel-Edens S, Zografi G. Characterization of the "hygroscopic" properties of active pharmaceutical ingredients. *J Pharm Sci.* 2008; 97: p. 1047-1059.
86. Graeser K, Patterson J, Zeitler J. Correlating thermodynamic and kinetic parameters with amorphous stability. *Eur J Pharm Sci.* 2009; 37: p. 492-498.
87. Zhang F, Aaltonen J, Tian F, Saville D, Rades T. Influence of particle size and preparation methods on the physical and chemical stability of amorphous simvastatin. *Eur J Pharm Biopharm.* 2009; 71: p. 64-70.
88. Ohta M, Buckton G. A study of the differences between two amorphous spray-dried samples of cefditoren pivoxil which exhibited different physical stabilities. *Int J Pharm.* 2005; 289: p. 31-38.
89. Konno H, Handa T, Alonzo D, Taylor L. Effect of polymer type on the dissolution profile of amorphous solid dispersions containing felodipine. *Eur J Pharm Biopharm.* 2008; 70: p. 493-499.
90. Vasanthavada M, Tong W, Joshi Y, Kislalioglu M. Phase behavior of amorphous molecular dispersions II: Role of hydrogen bonding in solid solubility and phase separation kinetics. *Pharm Res.* 2005; 22: p. 440-448.
91. Newman A, Knipp G, Zografi G. Assessing the performance of amorphous solid dispersions. *J Pharm Sci.* 2012; 101: p. 1355-1377.
92. Janssens S, Van den Mooter G. Review: Physical chemistry of solid dispersions. *J Pharm Pharmacol.* 2009; 61: p. 1571-1586.
93. Dhirendra K, Lewis S, Udupa N, Atin K. Solid dispersion: A review. *Pak J Pharm Sci.* 2009; 22: p. 234-246.
94. Habib M, Venkataram S, Hussain M. *Pharmaceutical Solid Dispersion Technology.* 1st ed. Habib M, editor. Lancaster: Technomics Publishing Company; 2001.

95. Shah N, Sandhu H, Choi D, Kalb O, Page S, Wyttenbach N. Structured Development Approach for Amorphous Systems. In Miller D, editor. *Formulating Poorly Water Soluble Drugs*. New York: Springer; 2012. p. 267-310.
96. DiNunzio J, Zhang F, Martin C, McGinity J. Melt Extrusion. In Miller D, editor. *Formulating Poorly Water Soluble Drugs*. New York: Springer; 2012. p. 311-362.
97. Mollen M. Historical Overview. In Ghebre-Sellassie I, Martin C, editors. *Pharmaceutical Extrusion Technology, Drugs and the Pharmaceutical Sciences*. New York: Marcel Dekker; 2003. p. 1-18.
98. Rauwendaal C. *Polymer Extrusion*. 4th ed. Cincinnati: Hanser Gardner Publications; 2001.
99. McGinity J, Koleng J, Repka M, Zhang F. Hot melt extrusion. In *Encyclopedia of Pharmaceutical Technology*. New York: Marcel Dekker; 2000. p. 203-226.
100. Bruin S, Van Zuilichem D, Stolp W. A review of fundamental and engineering aspects of extrusion in biopolymers in a single-screw extruder. *J Food Process Eng*. 1978; 2: p. 1-37.
101. Kruder G. Extrusion. In *Encyclopedia of Polymer Science and Engineering*. New York: John Wiley & Sons, Inc.; 1985. p. 571-631.
102. Kolter K, Nalawade S, Rottman N. Hot-Melt Extrusion with BASF Pharma Polymers. *Extrusion Compendium*. 2010.
103. Breitenbach J, Wiesner B. The use of polymers in pharmaceutical melt extrusion. *ExAct*. 2008: p. 8-11.
104. Breitenbach J. Melt extrusion: from process to drug delivery technology. *Eur J Pharm Biopharm*. 2002; 54: p. 107-117.
105. McGinity J, Zhang F, Repka M, Koleng J. Hot-melt extrusion as a pharmaceutical process. *Am Pharm Rev*. 2001; 4: p. 25-36.
106. McGinity J, Zhang F. Melt-extruded controlled release dosage forms. In *Pharmaceutical Extrusion Technology, Drugs and the Pharmaceutical Sciences*. New York: Marcel Dekker; 2003. p. 1-18.

107. Foster A, Hempenstall J, Rades T. Characterization of glass solutions of poorly water-soluble drugs produced by melt extrusion with hydrophilic amorphous polymers. *J Pharm Pharmacol*. 2001; 53: p. 303-315.
108. Forster A, Hempenstall J, Tucker I, Rades T. Selection of excipients for melt extrusion with two poorly water-soluble drugs by solubility parameter calculation and thermal analysis. *Int J Pharm*. 2001; 226: p. 147-161.
109. Patterson J, James M, Forster A, Rades T. Melt extrusion and spray drying of carbamazepine and dipyrindamole with polyvinylpyrrolidone/vinylacetate copolymers. *Drug Dev Ind Pharm*. 2008; 34: p. 95-106.
110. Martin C. Guidelines for operation of Leistritz twin-screw extruder. American Leistritz Corporation. 2001.
111. Luker K. Single-screw extrusion and screw design. In Ghebre-Sellassie I, Martin C, editors. *Pharmaceutical Extrusion Technology, Drugs and the Pharmaceutical Sciences*. New York: Marcel Dekker; 2003. p. 39-68.
112. Steiner R. Extruder Design. In Ghebre-Sellassie I, Martin C, editors. *Pharmaceutical Extrusion Technology, Drugs and the Pharmaceutical Sciences*. New York: Marcel Dekker; 2003. p. 19-37.
113. Thiele W. Twin-screw extrusion and screw design. In Ghebre-Sellassie I, Martin C, editors. *Pharmaceutical Extrusion Technology, Drugs and the Pharmaceutical Sciences*. New York: Marcel Dekker; 2003. p. 19-37.
114. Dreiblatt A. Process design. In Ghebre-Sellassie I, Martin C, editors. *Pharmaceutical Extrusion Technology, Drugs and the Pharmaceutical Sciences*. New York: Marcel Dekker; 2003. p. 153-169.
115. White J. Intermeshing co-rotating twin-screw extrusion. In *Twin Screw Extrusion*. Munich: Carl Hanser Verlag; 1991. p. 195-270.
116. Wildi R, Maier C. Understanding compounding. In *Twin Screw Extrusion*. Munich: Carl Hanser Verlag; 1998.
117. Case C. Melt pelletization. In Ghebre-Sellassie I, Martin C, editors. *Pharmaceutical Extrusion Technology, Drugs and the Pharmaceutical Sciences*. New York: Marcel Dekker; 2003. p. 171-181.

118. Ghebremeskel A, Vemavarapu C, Lodaya M. Use of surfactants as plasticizers in preparing solid dispersions of poorly soluble API: Selection of polymer-surfactant combinations using solubility parameter and testing the processability. *Int J Pharm.* 2007; 328: p. 119-129.
119. Chartoff R, Menczel J, Dillman S. Dynamic mechanical analysis (DMA). In Menczel J, Prime R, editors. *Thermal Analysis of Polymers*. Hoboken: John Wiley & Sons, Inc.; 2009. p. 387-495.
120. Zhu Y, Shah N, Malick A, Infeld M, McGinity J. Solid-state plasticization of an acrylic polymer with chlorpheniramine maleate and triethyl citrate. *Int J Pharm.* 2003; 241: p. 301-310.
121. DiNunzio J, Brough C, Miller D, Williams III R, McGinity J. Applications of Kinetisol dispersing for the production of plasticizer free amorphous solid dispersions. *Eur J Pharm Sci.* 2010; 40: p. 179-187.
122. Miller D, DiNunzio J, Yang W, McGinity J, Williams III R. Targeted intestinal delivery of supersaturated itraconazole for improved oral absorption. *Pharm Res.* 2008; 25: p. 1450-1459.
123. Konno H, Taylor L. Ability of different polymers to inhibit the crystallization of amorphous felodipine in the presence of moisture. *Pharm Res.* 2007; 25: p. 969-978.
124. Vasanthavada M, Tong W, Joshi Y, Kislalioglu M. Phase behavior of amorphous molecular dispersions I: Determination of the degree and mechanism of solid solubility. *Pharm Res.* 2004; 21: p. 1598-1606.
125. Curatolo W, Nightingale J, Herbig S. Utility of hydroxypropylmethylcellulose acetate succinate (HPMCAS) for initiation and maintenance of drug supersaturation in the GI milieu. *Pharm Res.* 2009; 26: p. 1419-1431.
126. Wu T, Sun Y, Li N, de Villiers M, Yu L. Inhibiting surface crystallization of amorphous indomethacin by nanocoating. *Langmuir.* 2007; 23: p. 5148-5153.
127. Taylor L, Zografi G. Spectroscopic characterization of interactions between PVP and indomethacin in amorphous molecular dispersions. *Pharm Res.* 1997; 14: p. 1691-1698.
128. Miyazaki T, Yoshioka S, Aso Y, Kojima S. Ability of polyvinylpyrrolidone and polyacrylic acid to inhibit the crystallization of amorphous acetaminophen. *J Pharm Sci.* 2004; 93: p. 2710-2717.

129. Matsumoto T, Zografi G. Physical properties of solid dispersions of indomethacin with poly(vinylpyrrolidone) and poly(vinylpyrrolidone-co-vinyl acetate) in relation to indomethacin crystallization. *Pharm Res.* 1999; 16: p. 1722-1728.
130. Babcock W, Friesen D, Nightingale A, Shanker R, inventors; Pharmaceutical Solid Dispersions. Europe patent 1027886A2. 2000.
131. Fitzpatrick S, McCabe J, Petts C, Booth S. Effect of moisture on polyvinylpyrrolidone in accelerated stability testing. *Int J Pharm.* 2002; 246: p. 143-151.
132. Hancock B, Shamblin S, Zografi G. Molecular mobility of amorphous pharmaceutical solids below their glass transition temperatures. *Pharm Res.* 1995; 12: p. 799-806.
133. Hancock B, Zografi G. The relationship between the glass transition temperature and the water content of amorphous pharmaceutical solids. *Pharm Res.* 1994; 11: p. 471-477.
134. Rumondor A, Marsac P. Phase behavior of poly(vinylpyrrolidone) containing amorphous solid dispersions in the presence of moisture. *Mol Pharm.* 2009; 6: p. 1492-1505.
135. Marsac P, Konno H. Recrystallization of nifedipine and felodipine from amorphous molecular-level solid dispersions containing poly(vinylpyrrolidone) and sorbed water. *Pharm Res.* 2008; 25: p. 647-656.
136. Rumondor A, Stanford L. Effects of polymer type and storage relative humidity on the kinetics of felodipine crystallization from amorphous solid dispersions. *Pharm Res.* 2009; 26: p. 2599-2606.
137. Andronis V, Zografi G. Crystal nucleation and growth of indomethacin polymorphs from the amorphous state. *J Non-Cryst Solids.* 2000; 271: p. 236-248.
138. Warren D, Benameur H, Porter C, Pouton C. Using polymeric precipitation inhibitors to improve the absorption of poorly water-soluble drugs: A mechanistic basis for utility. *J Drug Target.* 2010; 18: p. 704-731.
139. Brouwers J, Brewster M, Augustijns P. Supersaturating drug delivery systems: the answer to solubility-limited oral bioavailability? *J Pharm Sci.* 2009; 98: p. 2549-2572.

140. Handbook of Pharmaceutical Excipients. 5th ed. Grayslake: Pharmaceutical Press and American Pharmacists Association; 2006.
141. Porter S, Ridgway K. An evaluation of the properties of enteric coating polymers: measurement of glass transition temperature. *J Pharm Pharmacol*. 1983; 35: p. 341-344.
142. Overhoff K, Moreno A, Miller D, Johnston K, Williams R. Solid dispersions of itraconazole and enteric polymers made by ultra-rapid freezing. *Int J Pharm*. 2007; 336: p. 122-132.
143. O'Donnell K, Williams III R. Optimizing the Formulation of Poorly Water-Soluble Drugs. In Miller D, editor. *Formulating Poorly Water Soluble Drugs*. New York: Springer; 2012. p. 27-93.
144. Gilis P, De Conde V, Vandecruys R, inventors; Beads having a core coated with an antifungal and a polymer. United States patent 5633015. 1997.
145. Jaruratanasirikul S, Kleepkaew A. Influence of an acidic beverage (Coca-Cola) on the absorption of itraconazole. *Eur J Clin Pharmacol*. 1997; 52: p. 235-237.
146. Six K, Leuner C, Dressman J, Verreck G, Peeters J, Blaton N, et al. Thermal properties of hot-stage extrudates of itraconazole and Eudragit E100. *J Therm Anal Calorim*. 2002; 68: p. 591-601.
147. Six K, Verreck G, Peeters J, Brewster M, Van den Mooter G. Increased physical stability and improved dissolution properties of itraconazole, a class II drug, by solid dispersions that combine fast- and slow-dissolving polymers. *J Pharm Sci*. 2004; 93: p. 124-131.
148. Six K, Daems T, de Hoon J, van Hecken A, Depre M, Bouche M, et al. Clinical study of solid dispersions of itraconazole prepared by hot-stage extrusion. *Eur J Pharm Sci*. 2005; 24: p. 179-186.
149. Miller D, DiNunzio J, Yang W, McGinity J, Williams III R. Enhanced in vivo absorption of itraconazole via stabilization of supersaturation following acidic-to-neutral pH transition. *Drug Dev Ind Pharm*. 2008; 34: p. 890-902.
150. Badawi A, El-Nabarawi M, El-Setouhy D, Alsammit S. Characterization and stability testing of itraconazole solid dispersions containing crystallization inhibitors. *Am J Drug Discov Dev*. 2011; 1: p. 144-159.

151. Janssen Pharmaceuticals Inc. [Package Insert].; 2003 [cited 2013 June. Available from: <http://www.janssenpharmaceuticalsinc.com/assets/sporanox.pdf>.
152. Welling P. Effects of food on drug absorption. *Annu Rev Nutr.* 1996; 16: p. 383-415.
153. Fleisher D, Li C, Zhou Y, Pao L, Karim A. Drug, meal and formulation interactions influencing drug absorption after oral administration clinical implications. *Clin Pharmacokinet.* 1999; 36: p. 233-254.
154. Gu C, Li H, Levons J, Lentz K, Gandhi R, Raghavan K. Predicting effect of food on extent of drug absorption based on physicochemical properties. *Pharm Res.* 2007; 24: p. 1118-1130.
155. Charman W, Porter C, Mithani S, Dressman J. Physicochemical and physiological mechanisms for the effects of food on drug absorption: the role of lipids and pH. *J Pharm Sci.* 1997; 86: p. 269-282.
156. Custodio J, Wu C, Benet L. Predicting drug disposition, absorption/elimination/transporter interplay and the role of food on drug absorption. *Adv Drug Deliv Rev.* 2008; 60: p. 717-733.
157. Hofmann A, Mysels K. Bile salts as biological surfactants. *Colloid Surface.* 1987; 30: p. 145-173.
158. Dressman J, Vertzoni M, Goumas K, Reppas C. Estimating drug solubility in the gastrointestinal tract. *Adv Drug Deliv Rev.* 2007; 59: p. 591-602.
159. Lee V, Yang J. Oral drug delivery. In Hillery A, Lloyd A, Swarbrick J, editors. *Drug Delivery and Targeting for Pharmacists and Pharmaceutical Scientists.* London: Taylor & Francis; 2001.
160. Klein C, Chiu Y, Awni W, Zhu T, Heuser R, Doan T. The tablet formulation of lopinavir/ritonavir provides similar bioavailability to the soft-gelatin capsule formulation with less pharmacokinetic variability and diminished food effect. *J Acquir Immune Defic Syndr.* 2007; 44: p. 401-410.
161. Lewis R. University of Houston College of Pharmacy, The University of Texas M.D. Anderson Cancer Center. [Online]. [cited 2013 June. Available from: [http://www.aspergillus.org.uk/secure/articles/itraconRLewis/Itra\\_PK\\_revise d.pdf](http://www.aspergillus.org.uk/secure/articles/itraconRLewis/Itra_PK_revise d.pdf).

162. Hall S, Thummel K, Watkins P, Lown K, Benet L, Paine M, et al. Molecular and physical mechanisms of first-pass metabolism. *Drug Metab Dispos.* 1999; 27: p. 161-166.
163. Gubbin P, McConnell S, Penzak S. Antifungal agents. In Piscetelli S, Rodvold K, editors. *Drug Interactions in Infectious Disease*. Totowa, NJ: Human Press; 2001. p. 185-217.
164. Lown K, Kolars J, Thummel K, Barnett J, Kunze K, Wrighton S, et al. Interpatient heterogeneity in expression of CYP3A4 and CYP3A5 in small bowel. Lack of prediction by the erythromycin breath test. *Drug Metab Dispos.* 1994; 22: p. 947-955.
165. Poirier J, Cheymol G. Optimisation of itraconazole therapy using target drug concentrations. *Clin Pharmacokinet.* 1998; 35: p. 461-473.
166. Heykants J, van Peer A, van de Velde V, van Rooy R, Meuldermans W, Lavrijsen K, et al. The clinical pharmacokinetics of itraconazole: an overview. *Mycoses.* 1989: p. 67-87.
167. Stevens D. Intraconazole in cyclodextrin solution. *Pharmacotherapy.* 1999; 19: p. 603-611.
168. Bair H, Akinay A, Menczel J, Prime RB, Jaffe M. Thermomechanical analysis (TMA) and thermodilatometry (TD). In Menczel J, Prime RB, editors. *Thermal Analysis of Polymers*. Hoboken, NJ: John Wiley & Sons, Inc.; 2009. p. 319-385.
169. Chokski R, Sandhu H, Iyer R, Shah N, Malick A, Zia H. Characterization of physico-mechanical properties of indomethacin and polymers to assess their suitability for hot-melt extrusion process as a means to manufacture solid dispersion/solution. *J Pharm Sci.* 2005; 94: p. 2463-2474.
170. Greenhalgh D, Williams A, Timmins P, York P. Solubility parameters as predictors of miscibility in solid dispersions. *J Pharm Sci.* 1999; 88: p. 1182-1190.
171. U.S. Food and Drug Administration. [Online].; 2013 [cited 2013 June. Available from:  
[http://www.accessdata.fda.gov/scripts/cder/dissolution/dsp\\_SearchResults\\_Dissolutions.cfm?PrintAll=1](http://www.accessdata.fda.gov/scripts/cder/dissolution/dsp_SearchResults_Dissolutions.cfm?PrintAll=1).
172. Guzman H, Tawa M. Combined use of crystalline salt forms and precipitation inhibitors to improve oral absorption of celecoxib from solid oral formulations. *J Pharm Sci.* 2007; 96: p. 2686-2702.

173. DiNunzio J, Brough C. Fusion production of solid dispersions containing a heat sensitive active ingredient by hot melt extrusion and Kinetisol dispersing. *Eur J Pharm Biopharm.* 2010; 74: p. 340-351.
174. DiNunzio J, Hughey J, Brough C, Miller D, Williams III R, McGinity J. Production of advanced solid dispersions for enhanced bioavailability of itraconazole using Kinetisol dispersing. *Drug Dev Ind Pharm.* 2010; 36: p. 1064-1078.
175. Zografi G. States of water associated with solids. *Drug Dev Ind Pharm.* 1988; 14: p. 1905-1926.
176. Taylor L, Langkilde F, Zografi G. Fourier transform raman spectroscopic study of the interaction of water vapor with amorphous systems. *J Pharm Sci.* 2001; 90: p. 888-901.
177. Joo Woo S, Han Woo S, Han Soo H, Kim K. Absorption and stability of phthalic acid on a colloidal silver surface: surface-enhanced Raman scattering study. *J Raman Spectrosc.* 2000; 31: p. 145-150.
178. Nyquist R. Infrared studies of ketones: Parameters affecting the induced carbonyl stretching vibration by solute/solvent interactions. *Appl Spectrosc.* 1990; 44: p. 433-438.
179. Mehuys E, Remon J, Vervaet C. Production of enteric capsules by means of hot-melt extrusion. *Eur J Pharm Sci.* 2005; 24: p. 207-212.
180. Rumondor A, Taylor L. Effect of polymer hygroscopicity on the phase behavior of amorphous solid dispersions in the presence of moisture. *Mol Pharm.* 2010; 7: p. 477-490.
181. Dieckmann Y, Mertoglu M, Dobrawa R, Csihony S, Dieleman C, Knieriem T, et al., inventors; Use of block copolymers based on vylactams and vinyl acetate as solubilizers. U.S. patent 8211469. 2012.
182. Six K, Verreck G, Peeters J, Binnemans K, Berghmans H, Augustijns P, et al. Investigation of thermal properties of glassy itraconazole: identification of a monotropic mesophase. *Thermochim Acta.* 2001; 376: p. 175-181.
183. Debenedetti P, Stillinger F. Supercooled liquids and the glass transition. *Nat.* 2001; 410: p. 259-267.
184. Angell C. Formation of glass from liquids and biopolymers. *Sci.* 1995; 267: p. 1924-1935.

185. Angell C. Liquid fragility and the glass transition in water and aqueous solutions. *Chem Rev.* 2002; 102: p. 2627-2650.
186. Janssens S, De Zeure A, Paudel A, Van Humbeeck J, Rombaut P, Van den Mooter G. Influence of preparation methods on solid state supersaturation of amorphous solid dispersions: a case study with itraconazole and Eudragit E100. *Pharm Res.* 2010; 27: p. 775-785.
187. Bustamante P, Navarro-Lupion J, Escalera B. A new method to determine the partial solubility parameters of polymers from intrinsic viscosity. *Eur J Pharm Sci.* 2005; 24: p. 229-237.
188. Rambali ea. Itraconazole formulation studies of the melt-extrusion process with mixture design. *Drug Dev Ind Pharm.* 2003; 29: p. 641-652.
189. Qian F, Wang J, Hartley R, Tao J, Haddadin R, Mathias N, et al. Solution behavior of PVPVA and HPMCAS-based amorphous solid dispersions and their bioavailability implications. *Pharm Res.* 2012; 29: p. 2766-2776.
190. Babcock W, Crew M, Friesen D, Rabenstein M, Smithey D, Shanker R, inventors; Pharmaceutical compositions containing polymer and drug assemblies. European Patent patent WO03000226. 2003.
191. Craig D. The mechanisms of drug release from solid dispersions in water-soluble polymers. *Int J Pharm.* 2002; 231: p. 131-144.
192. Six K, Murphy J, Weuts I, Craig D, Verreck G, Peeters J, et al. Identification of phase separation in solid dispersions of itraconazole and Eudragit E100 using microthermal analysis. *Pharm Res.* 2003; 20: p. 135-138.
193. Kondo N, Iwao T, Hirai K, Fukuda M, Yamanouchi K, Yokoyama K, et al. Improved oral absorption of enteric coprecipitates of a poorly soluble drug. *J Pharm Sci.* 1994; 83: p. 566-570.
194. Kohri N, Yamayoshi Y, Xin H, Iseki N, Sato N, Todo S, et al. Improving the oral bioavailability of albendazole in rabbits by the solid dispersion technique. *Pharmacol.* 1999; 51: p. 159-164.
195. Van den Mooter G, Verreck G, Brewster M, Peeters J, Weuts I, DeCorte A, et al., inventors; Janssen Pharmaceutica, assignee. Solid Dispersions of a Basic Drug Compound and a Polymer Containing Acidic Groups. patent WO/2005/117834. 2005.

196. Booth J. Deconvoluting amorphous solid dispersion dissolution. In PhysChem Forum 11 Meeting; 2011; Nottingham (presentation).
197. Tiwari R, Tiwari G, Srivastava B, Rai A. Solid Dispersions: An overview to modify bioavailability of poorly water soluble drugs. *Int J Pharm Tech Res.* 2009 October December: p. 1338-1349.
198. Denge M, Walde S, Ittadwar A. Development and characterization of transdermal patches of ondansetron hydrochloride. *Int J Pharm Pharm Sci.* 2012; 4: p. 293-298.
199. Fielden K, Newton J. Extrusion and extruders. In Swarbrick J, Boylan J, editors. *Encyclopedia of Pharmaceutical Technology.* New York: Marcel Dekker; 1992. p. 395-442.